June 2017

Effect of contour bunds on surface runoff and soil erosion in the Bokole watershed, Southwest Ethiopia

Shannon de Roos

Universiteit Utrecht

Supervisors:

Dr. L.P.H. van Beek

Dr. G Sterk

Effect of contour bunds on surface runoff and soil erosion in the Bokole watershed, Southwest Ethiopia

Utrecht University
MSc thesis

Supervisors: Dr. L.P.H. van Beek, Dr. G. Sterk and K. Wolka

Faculty of Geosciences, department of Physical Geography

Abstract

Soil erosion belongs to one of the most severe environmental problems in Ethiopia. Particularly in the highlands, land degradation by soil erosion is a concerning issue, due to steep slopes and high intensity rainfall. This while, according to the FAO, nearly all of the national agricultural and economic activity is derived from the highlands. Soil losses on the cultivated highlands were estimated by Hurni around 42 ton/ha/yr. To improve the economic growth of Ethiopia and reduce the threat of land degradation, several soil and water conservation (SWC) measures have been introduced over the years, one of which are contour bunds. Studies show that contour soil and stone bunds have positive effects on soil loss reduction and yield increase. The majority of this research however, is completed in the northern highlands.

In this study, the focus lies on the effectiveness of contour bunds as a soil water conservation measure in agricultural fields in the Bokole watershed, situated in Southwest Ethiopia. Two experimental fields covered with maize crops were studied during a field work between August and September 2016, but only one of these fields was sufficient for erosion and runoff assessment. Both fields were divided into six adjacent plots with total lengths of around 18 to 20 metres and variating widths of around 6 to 10 metres. Each field contained four plots with soil bunds, dividing the plots into an upper (A) and lower (B) section and two plots served as control plots, containing no bunds. On the control plots sediment concentrations were measured. Erosion was assessed on each plot for field 2 with the Assessment of Current Erosion Damage (ACED) method. An additional field with of 1000 m^2 (20m x 50m) was used to assess erosion on land with contour stone bunds. Runoff and erosion was modelled with the rMMF method. To include the effect of bunds on runoff, an adapted version of the rMMF model was used.

The lower plots (B-plots) of the experimental field were more vulnerable to erosion, due to their steeper slopes in combination with greater plot lengths. In general, the control plots contained the most erosion features, with the exception of plot 2B. It shows that slope steepness plays an important role in land degradation. Overall, longer and wider rills were found on the field with stone bunds compared to the experimental field with soil bunds and the control plots, as these features were older than on the experimental field. Erosion of the two control plots was measured at 8.6 ton/ha for the months June up to August and annual modelled losses were in the region of 37 to 44 ton/ha/yr. Annual runoff on fields without any Soil Water Conservation measures was modelled around 500 to 580 mm. The modelled effect of soil bunds showed a reduction in runoff of 20-30% for the upper plots (A-plots) and around 50% for the B-plots. Erosion was reduced by 63-70%. Rainfall variability proved to have a great influence on erosion, varying from 5 ton/ha/yr for the driest year in the record to more than 91 ton/ha/yr for the wettest year.

SWC measures, such as contour soil bunds can be easily included in the adapted rMMF model. Therefore, a new function to compute soil losses for the adapted rMMF model is desired, so that the adapted model can be used for modelling runoff as well as erosion.

Table of contents

List of figures, graphs and tables

Figures

Graphs

Tables

1. Introduction

Soil erosion belongs to one of the most severe environmental problems in Ethiopia (Dejene, 2003; EPA, 2012; Taddese, 2001,). Because of erosion, organic matter is removed from the soil and soil structures break down, reducing soil fertility and crop productivity (Biratu & Asmamaw, 2016). The main causes for intense erosion in Ethiopia are population increases, limited available productive soils on suitable lands, deforestation and overgrazing. These factors are combined with challenging climatic conditions, such as large spatial and temporal precipitation variability (Taddese, 2001; Gebregziabher, 2015). Furthermore, poverty results in poor crop management, despite the knowledge of farmers about soil erosion on their lands (Kidane & Alemu, 2015; Moges & Holden, 2007). Especially in the Ethiopian highlands, which covers almost half of the country, land degradation by soil erosion is a concerning issue, due to steep slopes and high intensity rainfall in this region (Kidane and Alemu, 2015). Nevertheless, the highlands have a population of around 88% of the national total, contain 95% of the cropped lands and more than 90% of the national economic activity (FAO, 1986).

Drought induced famine in the early seventies generated the first nationwide linkage between land degradation and famine and around this time, it became publicly known that the Ethiopian highlands endured annual losses of about one billion tonnes of top soils (Dejene, 2003; FAO, 1986). Awareness of soil erosion grew and in 1981 the Soil Conservation Research Project (SCRP) was initiated by the Ministry of Agriculture and the University of Bern (Dejene, 2003). In a publication by Hurni et al. (1988), estimated soil losses on Ethiopian cultivated highlands were at 42 ton/ha/yr. A report by the Food and Agriculture Organization (FAO) in 1986 pointed out that half of the Ethiopian highlands, approximately 27 million hectares, were significantly eroded, of which a quarter was severely eroded and 2 million hectares had already reached a point of no return.

Despite the severe soil losses, agriculture is an important factor to the accelerating economic growth of the Ethiopian highlands (Alemayehu, 2006; UNCT, 2001). Improved farming practices by small- holder farmers have shown to significantly increase their productivity. As water erosion and soil water losses by runoff and evaporation are the main cause of land degradation in the Ethiopian highlands, efforts by the government have been taken for soil and water conservation (SWC) measures (Gebreegziabher et al., 2009; Wolka et al., 2017). The main purpose of the SCRP is therefore to provide data on soil erosion and to assess the effectivity of SWC projects (Bezuayehu et al., 2006). Studies about implemented SWC structures in the Ethiopian highlands have shown positive results (Amare et al., 2014; Gebreegziabher et al., 2009; Teshome et al., 2013). SWC structures function as barriers for sediment and surface runoff and reduce the length and gradient of slopes, and therefore reduce soil erosion by water (Wolka et al., 2017). Physical SWC techniques that are widely in practice in the Ethiopian highlands, are contour stone bunds and contour soil bunds (figure 1-1), (Gebremichael et al., 2005; Nyssen et al., 2007).

Sediment and water becomes trapped and accumulates behind these bunds, preventing the loss of soil particles, fertilizer and organic matter and increasing infiltration of surface water (Vancampenhout et al., 2006; Wolka et al., 2017). Gebremichael et al. (2005) and Nyssen et al. (2007) observed a reduction of sediment losses by stone bunds of 68% of the highlands in northern Ethiopia. Meshesha et al. (2012) found soil erosion reduction by stone bunds in the order of 13% and 64% in central Ethiopia. Studied sediment yield reduction by soil bunds are in the range between 47% and 84% (Adimassu et al., 2014; Wolka et al., 2017). Research about the effect of contour bunds on crop yield showed varying results. Vancampenhout et al. (2006) observed a yield increase of 7% in the Tigray highlands in North Ethiopia and in the same region Nyssen et al. (2007) observed comparable average increases of 4%, 8% and 11%, depending on different crop types. However, Alemayehu et al. (2006) found an increase in grain yield of 56 to 75% in north Shoa, Amhara region and Herweg & Ludi (1999) found no increase at all in crop yield by contour bunds.

A few limitations are recognized by the use of contour bunds. First of all, a small part of usable land is lost due to placement of the bunds (Hengsdijk et al., 2005; Herweg & Ludi, 1999). An observed downside effect of stone bunds is the formation of soil fertility gradients (Wolka et al., 2017). A soil fertility gradient is created when at the foot of the bund erosion takes place and the sediment accumulates directly behind the next bund (Vancampenhout et al., 2006). The less fertile subsoil becomes exposed at the upside of the hillslope and the most fertile conditions are at the downside, directly above the bund. A limitation of using soil bunds is the blocking effect of accumulated fertile soil in the drainage ditch, causing waterlogging and loss of the soil by flushing (Herweg and Ludi, 1999). Furthermore, fertile sediments in the ditches are removed to raise bunds during maintenance in following years. On the other hand, contour bunds require low maintenance and soil bunds can be combined with vegetation cover on top of the bunds, which further reduces soil loss (Amare et al., 2014; Herweg & Ludi, 1999; Meshesha et al., 2012).

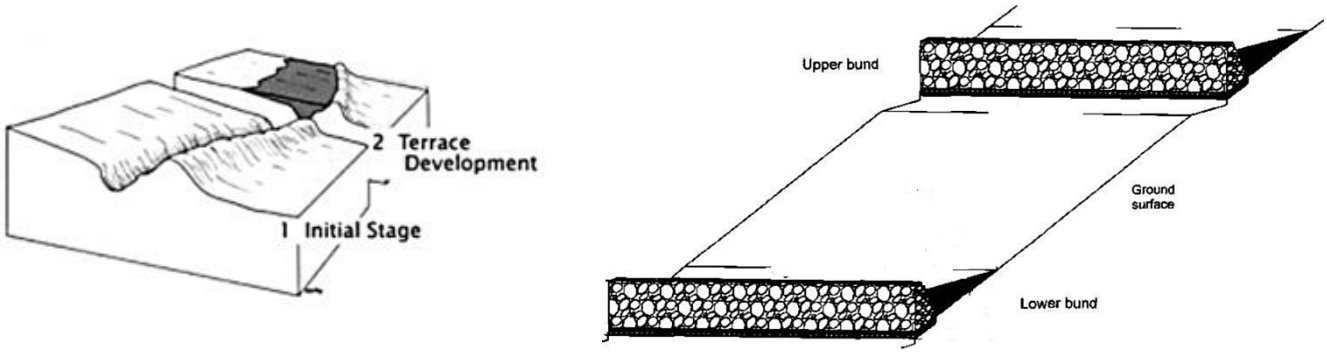

Figure 1-1. Left: sketch of soil bund on hillslope with empty channel (1) and with subsequent channel infilling (2), from: Haile et al., 2006. Right: sketch of stone bunds on hillslope, from Gebremichael et al., 2005.

The majority of the research about the effect of contour soil and stone bunds in the Ethiopian highlands was conducted in northern regions (Gebremichael et al., 2005; Nyssen et al., 2007; Teshome et al., 2013 Vancampenhout et al., 2006). Wolka et al. (2011, 2016) was the first to study the effects of contour bunds on perceived crop yields in the Bokole watershed, situated in the Southwest Ethiopian highlands. Here, soil bunds were newly introduced in the year 2000, with help from the World Food Program (WFP), whereas stone bunds were already in use for several decades. Surveys about perceived crop yield indicated a fast increase (within a year) for 75% of the households in the upper watershed, where mainly soil bunds are in use (Wolka et al., 2017). 19% of the surveyed households in the upper watershed experienced crop yield increases within two years. In the lower watershed, containing mostly stone bunds, crop yields improved within one year for about 48% and within two years for 45% of the respondents. It was discussed that the lack of a channel and the porosity of newly built stone bunds makes them less efficient barriers against runoff, compared to newly built soil bunds. After a while the pores in stone bunds will become filled with sediment and as a consequence, the amount of retained water and sediment will increase (Wolka et al., 2017).

Although the study showed positive results towards the effect of stone bunds and soil bunds on crop yield, Wolka et al. (2017) found no notable differences between the measured soil properties of fields with contour bunds and fields without contour bunds. It was suggested that the relative young age of the contour bunds (< 10 years) could be the reason. The intensity of other land management practices by individual farmers could also play a factor. The crop productions therefore did not increase due to better soil properties, but most likely due to increased available moisture conditions (Wolka et al., 2017). Further research is required to gain more knowledge about the effect of stone and soil bunds in this area. So far, the quantitative effect of contour bunds on surface runoff and soil loss had not yet been studied for this region.

Research objective

The objective is to assess the effectiveness of contour bunds as a soil water conservation measure in agricultural fields in the Bokole watershed, Southwest Ethiopia.

This will be addressed through the following sub-objectives:

1. To determine the current erosion damage on fields with contour bunds
    a. To assess soil loss and runoff on control plots, without SWC measures
    b. To assess soil loss on land with stone bunds
    c. To assess soil loss on plots with soil bunds

2. To quantify the effects of contour soil bunds as a SWC measure, using the rMMF model
    a. To comprehend overland water and sediment transport under natural and interfered conditions
    b. To comprehend the effect of rainfall variability on erosion

To quantify erosion on land with stone bunds, a field of 1000 m^2 with three rows of contour stone bunds was visually assessed during fieldwork. To quantify erosion on land with soil bunds, two separate experimental fields were selected, each containing six adjacent plots, of which four contained soil contour bunds and two served as control plots, without bunds. The plots were generally around 20 meters in length and 5 to 11 meters in width. At the time of fieldwork (August-September 2016), both fields were cultivated and covered with maize. The yield of maize on both fields has been assessed for each plot in a separate, but related MSc research, carried out by Mrs Imke Erven.

To assess the effect of annual variability in rainfall on erosion, for fields with soil bunds, erosion was modelled for the field 2 with the rMMF method. As soil bunds capture the surface water in the channel downslope of an area, there is no inflow of runoff from this section into the following downslope section. An adapted version of the rMMF method, in this study referred to as the rMMF-HS method, was used to include this effect on runoff by soil bunds. Both models were analysed under uncalibrated conditions. After the model analysis, two input parameters were calibrated to obtain the optimal runoff coefficient, so that runoff and erosion could be modelled for each month of the year 2016. These results were validated and compared to the runoff coefficients and soil losses measured during fieldwork. A sensitivity analysis was done to study the effect of separate parameters and to estimate the reliability of the model outcomes.

2. Site description

2.1 Area description

The Bokole watershed is situated near Gessa town, the centre of Loma district, which is about 500 km southwest of the capital, Addis Ababa (Wolka et al., 2017). Its geographic location is between 6°55'N-7°01'N latitude and 37°15'E-37°19'E longitude (figure 2-1). The watershed drains into the Gibe III hydroelectric power plant reservoir on the Omo river. The total area of the watershed is around 54 km^2 and the elevation varies from 1160 to 2400 meter above sea level, with an undulating topography. The Bokole watershed has a population of 11,798 people, of which 3832 reside in the upper watershed (above 2200 m) and 7936 in the lower watershed (Wolka et al., 2011).

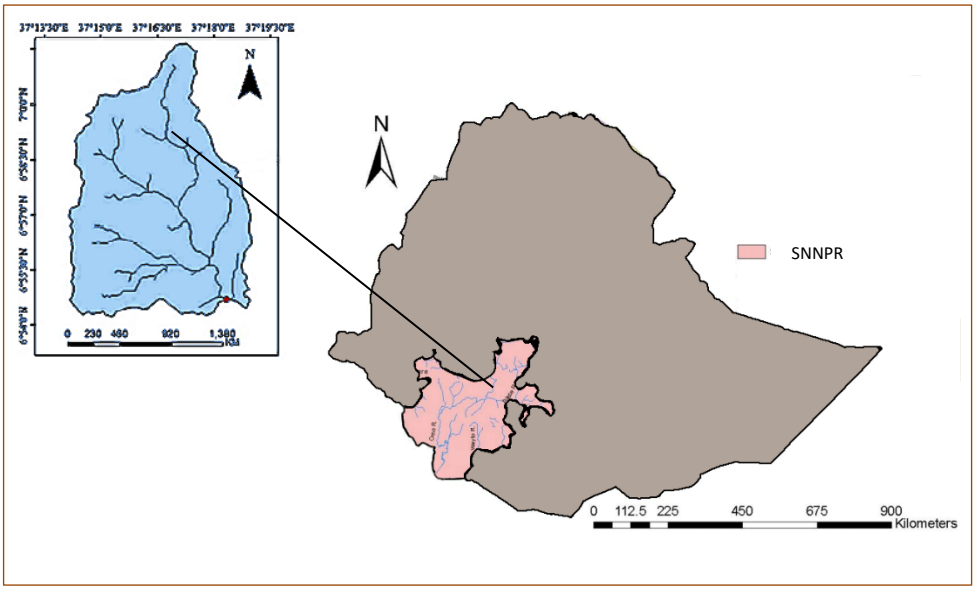

Figure 2-1. Geographic location of the Bokole watershed in Ethiopia, created from: Wolka et al., 2017 and Bossio et al.,2012. The region in which the study area is situated, is the Southern Nations, Nationalities and People Region (SNNPR).

Climatic conditions in Ethiopia are influenced by the geographic location and altitude (Alemayehu, 2006). There is a significant variability of rainfall over the country, where the highest rainfall rates are found at middle and high altitudes (above 1500m), with the exception of western lowlands. In addition, rainfall at higher altitudes is generally less erratic compared to the lowlands. Loma district has a relatively stable rainy season, generally starting in April/May and ending in September. According to Wolka et al. (2017) in the lower watershed, average annual rainfall is between 1400 mm and 1600 mm. In the upper watershed, average rainfall of 1746 mm was measured (Wolka et al., 2017). The upper watershed has a mean minimum temperature of 12.2°C and a mean maximum temperature of 21.9°C.

Graph 1 presents the monthly rainfall and minimum and maximum temperatures from the Gessa weather station during the years 2005 to 2016. Gessa is located approximately six kilometres from the experimental fields, situated in the upper watershed. Gessa has an altitude of 2200 m and the study area has an altitude between 1720 m and 1800 m (Wolka et al., 2017). Graph 2-1 shows typical climatic trends of the upper Bokole watershed, with an average annual rainfall of 1875 mm, a minimum temperature of 12.0 °C and a maximum temperature of 22.0 °C. According to IRENA (2008-2010), wind speeds in the region vary between 1.0 m/s and 3.0 m/s.

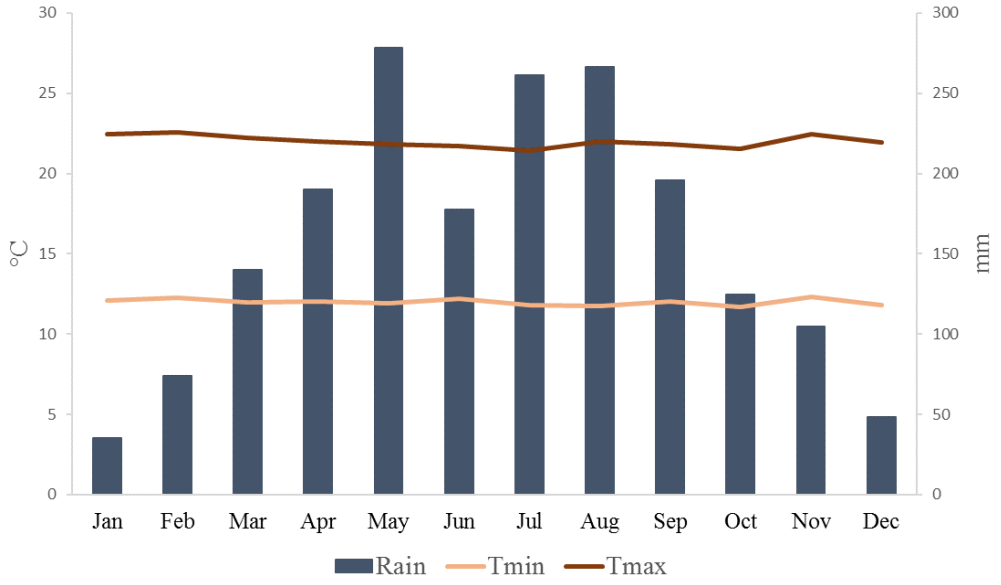

Graph 2-1. Monthly averages of rainfall, minimum temperature and maximum temperature from the Gessa weather station, gained from a record of 12 years, from 2005-2016.

As can be seen in table 2-1, which presents monthly standard deviations of the rainfall between the years 2005 up to 2016, there is a high variability of rainfall, especially during the rainy season. The small standard deviations of the minimum and maximum temperatures show that monthly and yearly temperatures are very constant.

Table 2-1. Standard deviation of monthly and yearly rainfall and temperature, from the past 17 years in Gessa.

	Jan	*Feb*	*Mar*	*Apr*	*May*	*Jun*	*Jul*	*Aug*	*Sep*	*Oct*	*Nov*	*Dec*	*Year*
Rainfall	42.2	48.0	77.3	88.0	163.9	40.4	105.8	98.2	65.6	41.0	60.1	49.7	434.7
Tmin	0.7	0.6	0.6	0.7	0.6	0.6	0.5	0.6	1.2	0.5	1.5	0.4	0.6
Tmax	1.2	1.1	1.0	0.9	0.6	0.3	0.5	1.8	1.2	0.4	2.3	0.3	0.8

Concerning soil types in the Bokole watershed, orthic Acrisol is most common, but dystric Nitosols do also cover parts of the area (Wolka et al., 2017). In the rural parts of the watershed the economic activity consists of agriculture combined with crop production and livestock keeping. Crop species that are widely cultivated in both the upper and lower watershed are maize, sorghum,

teff and haricot bean. In the upper watershed barley, wheat, pea, enset and bean are additionally harvested, while in the lower watershed sweet potato and cassava are grown. In 2016 only maize was cultivated on the experimental fields.

2.2 Experimental setting

The field data was collected during fieldwork in August and September 2016, using two experimental fields (F1 & F2) on which maize was cultivated. The maize on the two fields were in different growth stages during fieldwork, as the second field was sown 20 days before field 1. In F1, the maize reached its maximum growth in August, and in F2, the maize was already matured and almost ready to be harvested during fieldwork. Each field was divided into six adjacent plots, with total lengths of around 18 to 20 metres and variating widths of around 6 to 10 metres, where widths generally increased downslope. Four of these plots had three channel-bund systems: one upslope, one approximately in the middle of the plot, dividing the plot in section A and B, and one downslope, marking the end of the plot (figure 2-2). Two of the plots served as control plots, where no type of contour bund was present. For field 2 this was plot 3 and plot 5 (CP3, CP5). The control plots contained an emplacement downslope, to measure the amount of runoff and sediment. Sediment and runoff were kept in this plot by raised metal sheets on the borders, creating a boundary from their neighbouring plots, and were collected in jerrycans buried in the soil right below the plots (figure 2-3).

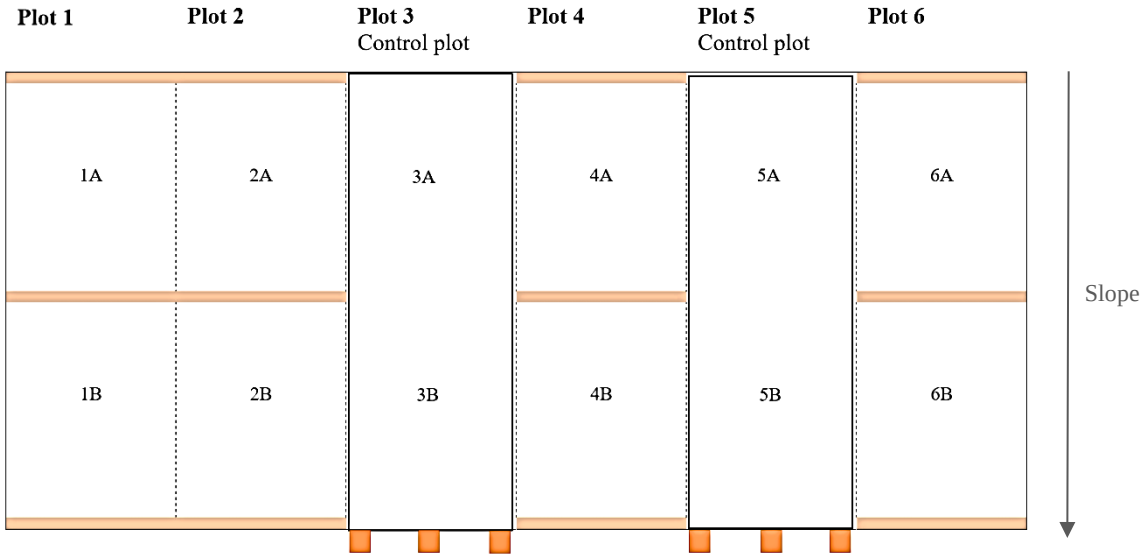

Figure 2-2. Schematic overview of the experimental setting of field 2 (F2). The brown bars indicate the positions of the bunds. Downslope of the control plots CP3 and CP5, orange squares represent the positions of the jerrycans, which collect runoff and sediment.

These jerrycans were placed at three or more locations for one plot, with volumes of 20 litres and 25 litres. Multiple jerry cans were often placed at one location, so that if the first jerry can was filled, the runoff could flow over into the second jerrycan, situated right behind the first one (figure 2-3). Unfortunately, this system with jerrycans appeared to be insufficient to use for runoff quantification, as it could not capture the full amount of runoff during larger rainfall events (Appendix 9.2.3), therefore the jerrycans were only used for sediment collection. It should be noted that field 1 is not used for runoff and erosion modelling, as soil losses in this field could not be measured and sediment concentrations proved to be insufficient. Measured vegetation parameters of field 1 were often used to calibrate parameters of field 2.

Figure 2-3. Runoff collection jerrycans, downslope of the control plots.

Apart from the two experimental fields, an additional field was used to assess erosion features on a field with stone bunds. This field has been used for the growth of haricot bean, but this crop was already cultivated in April or March. During the fieldwork period, weeds of approximately 20 cm in height covered the area. It considered a total area of 1000 m^2 and it was situated approximately 100 m Southwest from field 2. The farmer added an additional SWC measure, an artificial rill, to control the direction of the surface runoff (figure 2-4). The field is divided into three sections based on variation in slope, where the stone bunds mark a boundary for each section (figure 2-4).

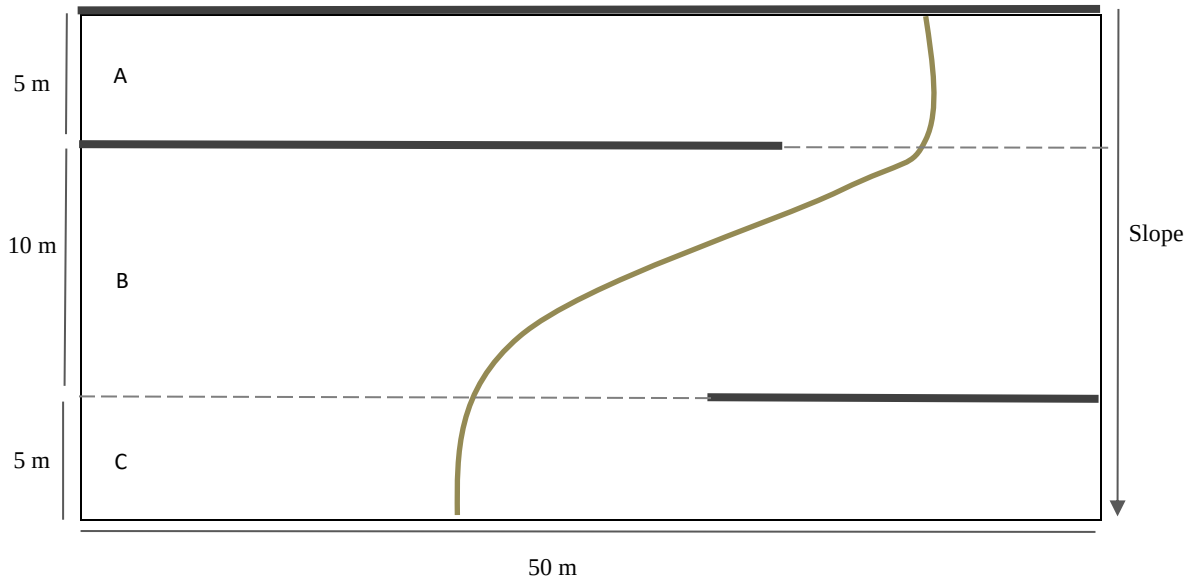

Figure 2-4. Schematic overview of field with stone bunds. Grey lines indicate positions of contour stone bunds. Green line indicates the position of the control ditch, an additional SWC measure created by the farmer.

3. Methods

3.1 Model description

3.1.1 The revised Morgan, Morgan and Finney model

The revised Morgan, Morgan and Finney (rMMF) model is an empirical method to calculate soil erosion on field- sized areas on hillslopes (Morgan, 2005). It considers soil erosion from detachment of soil particles by raindrop impact and transport by runoff. The original Morgan, Morgan and Finney model ignored the ability of rainfall to transport sediment downslope and runoff to erode soil particles (Morgan, 2001). In the revised model, soil detachment by runoff is included. The model is subdivided into two phases; a water phase and a sediment phase.

Water phase

In the water phase, inputs for splash erosion and sediment entrainment by runoff are obtained by using equations to calculate the runoff and the rainfall energy that results from both leaf drainage and throughfall (Morgan, 2005, 2008).

First, rainfall (R; mm) is converted into effective rainfall (ER; mm), resulting in the total amount of rainfall that is not intercepted by vegetation. The percentage of rainfall interception by vegetation (A) is presented as a fraction between 0 and 1:

$$ER = R(1 - A) \quad (1)$$

The effective rainfall is separated into two components; the leaf drainage (LD) and direct throughfall (DT). The leaf drainage is the amount of effective rainfall that is first intercepted by the canopy cover (CC), a fraction between 0 and 1. The rain subsequently reaches the ground via stem flow or by dripping from leaves (Tefera et al., 2006):

$$LD = ER * CC \quad (2)$$

The remaining part of the effective rainfall reaches the ground directly as direct throughfall:

$$DT = ER - LD \quad (3)$$

The kinetic energy (KE; J m^{-2}) resulting from the leaf drainage is dependent upon the height of the plant canopy (PH; m) in the following manner:

$$KE(LD) = [LD(15.8 * PH^{0.5})] - 5.87 \quad (4)$$

The kinetic energy from the direct throughfall is calculated as a function of rainfall intensity (I; mm h^{-1}), which is a value indicating the erosivity of rainfall and is dependent of climatic regions. For the Ethiopian highlands the equation of Wischmeier and Smith (1958) is a suitable equation to calculate the kinetic energy from throughfall (Tefera et al., 2006):

$$KE(DT) = DT(11.9 + 8.7logI) \quad 5$$

The total kinetic energy (KE; J m^{-2}) of effective rainfall is the summation of equation 4 and 5:

$$KE = KE(LD) + KE(DT) \quad 6$$

The equation for calculating surface runoff (Q; mm) is based on the assumption that runoff occurs when the soil moisture storage capacity (S_c; mm) is exceeded by the daily rainfall (Morgan, 2001):

$$Q = Rexp(-\frac{S_c}{R_0}) \quad 7$$

Where R is the mean monthly rainfall (mm) and R_0 is the mean rain per rain day (mm), calculated by dividing the average monthly rainfall (R) with the total rainy days per month (R_n). The soil moisture storage capacity (S_c; mm) is computed with an equation whereby the soil moisture at field capacity (SM; %w w^{-1}), dry bulk density of the soil (BD; Mg m^{-3}), effective hydrological depth of the soil (EHD; m) and the ratio of actual evapotranspiration over potential evapotranspiration (E_t /E_0) have to be known. The EHD replaces the effective rooting depth and is the soil depth within which the moisture storage capacity controls runoff generation (Morgan, 2001):

$$S_c = 1000SM * BD * EHD\left(\frac{E_t}{E_0}\right)^{0.5} \quad 8$$

Sediment phase

In the sediment phase, two equations are used to calculate the total sediment detachment (SD; kg m^{-2}). First, the sediment detachment by raindrop impact (F; kg m^{-2}) is calculated, which is a function of the total kinetic energy (KE; J m^{-2}) and the erodibility of the soil, which is described by the soil detachability index (K; g J^{-1}). K is determined by the weight of soil that is detached from the soil mass, per unit of rainfall energy (Tefera et al., 2006):

$$F = K * KE * 10^{-3} \quad 9$$

The second equation computes the sediment detachment by runoff (H; kg m^{-2}):

$$H = ZQ^{1.5}sinS(1 - GC) * 10^{-3} \quad 10$$

Where S is the slope steepness angle (°) and GC is the ground cover fraction, a factor between 0 and 1. Sediment detachment by runoff is only possible if the soil is not fully protected by ground cover. Z is a value representing soil resistance. It is calculated by the following equation:

$$Z = \frac{1}{0.5COH} \quad 11$$

Where COH is the soil surface cohesion (kPa).
Hence, the total sediment detachment (SD; kg m^{-2}) is calculated as followed:

$$SD = H + F \quad (12)$$

An additional equation estimates the transport capacity (TC; kg m^{-2}) of overland flow, by using a crop cover management factor (C). This factor is a combination of the C and P factors in the Universal Soil Loss Equation (USLE) (Morgan, 2005):

$$TC = CQ^2 sinS * 10^{-3} \quad (13)$$

The final estimation of soil erosion is made by comparing the total sediment detachment with the transport capacity, where the lowest value is taken as the erosion rate. A schematic representation of the model can be seen in figure 3-1.

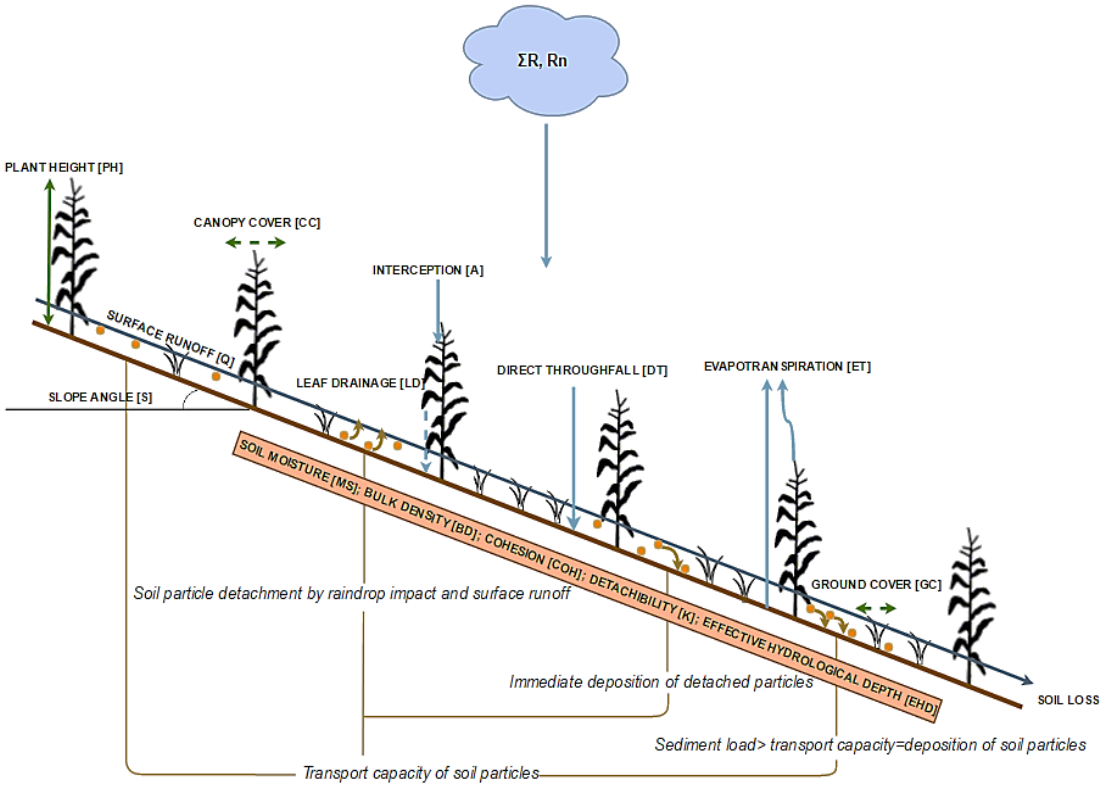

Figure 3-1. Schematic overview of the rMMF model, including all input parameters (inspired from Morgan, 2008)

3.1.2 Hillslope sections; Adapted rMMF model

At the department of Physical Geography of the University of Utrecht, a new version of the rMMF model is in development by G. Sterk, where the modelled hillslope can be divided into several sections, based on differences in input parameters, such as slope and soil and vegetation parameters (Hudek et al., 2014). The only input variables that are assumed to remain equal over all sections are the rainfall and number of rain days. Surface runoff and soil loss are calculated for each section. In the newest adaption, the effect of re-infiltration is incorporated, as a fraction of runoff that is lost in a particular section. The first section begins at the top of the hillslope and the sections increase in downslope direction. For the first section, runoff is calculated for that section only, but from the second section on, runoff of the previous upslope section that is not re-infiltrated, is added to the runoff that is generated in the current section. To describe these variations, the rMMF equations are adjusted.

Water phase

Surface runoff of the first section is converted from mm into a volume per meter width (Hudek et al., 2014). The new surface runoff is now dependent on slope length (L_i; m):

$$Q_1' = 10^{-3} * Q_1 * L_1 \qquad 14$$

Where Q_1' is the runoff volume in m^2 and Q_1 is the surface runoff in mm of the most upslope section, as calculated with equation 7. For the next section, surface runoff of the previous section is added to surface runoff generated on the section itself. The general equation for all the other sections therefore becomes:

$$Q_i' = 10^{-3} * Q_i * L_i + Q_{i-1}' \qquad 15$$

Where Q_i' is the new runoff in m^2 for section i, $i = 1 \ldots . n$ indicates the specific section from the total n number of sections.

A boundary condition (Q_0'; m^2) can be set at zero, in case there is no inflow of surface runoff from the previous section.

Re-infiltration is an important factor for erosion and runoff modelling, when SWC measures are involved, as these methods improve re-infiltration of water. Therefore, an additional variable is introduced, here referred to as RI, which accounts for the amount of runoff that is infiltrated in a given section. Hence, the new equation for surface runoff now becomes:

$$Q_i'' = (10^{-3} * Q_i * L_i + Q_{i-1}')(1 - RI_i) \qquad 16$$

Where Q_i'' is the new runoff in m^2 for each section where re-infiltration is included.

Sediment phase

In the original rMMF model, the surface runoff in mm is used to calculate the transport capacity. As the transport capacity and the amount of detached sediment are dependent on the amount of surface runoff available, unrealistic outcomes can occur by using Q in mm. For example, in the uppermost section, surface runoff in mm can already be quite high, whereas the actual volume is still low, as there is none or little accumulation. This problem can be prevented by using the surface runoff from equation 16. This leads to a new equation for TC:

$$TC' = CQ_i''^2 sinS * L_i \quad 17$$

Where TC' is the transport capacity in Kg m^{-1}. Equation 17 cannot be used for the sediment detachment function (eq. 10), as it is later added to the function of splash erosion (eq 9), which is in Kg m^{-2}. Therefore, for equation 10, Q_i'' is converted into mm again:

$$Q^{cum} = 10^3 * \frac{Q_i''}{\Sigma L_i} \quad 18$$

Where Q^{cum} is in mm and ΣL_i is the cumulative slope length. Equation 12 is then converted into Kg m^{-1} for each section, by multiplying it with ΣL_i.

A sediment transport deficit (ST_i^{def}) is calculated, where the incoming sediment from the above sections is subtracted from the transport capacity:

$$ST_i^{def} = TC_i'' - ST_{i-1} \quad 19$$

A boundary condition called ST_0 can be set at zero, meaning that there is no sediment from upslope entering the given section.

(ST_i^{def}) contains a set of conditions:

- If $ST_i^{def} < 0 \rightarrow ST_i = TC_i'$ deposition
- If $ST_i^{def} = 0 \rightarrow ST_i = TC_i'$ only transport; no loss or deposition
- If $ST_i^{def} > 0 \rightarrow ST_i$ depends on total detachment of the section:
  - If $(F_i + H_i)L_i \geq TC_i' \rightarrow ST_i = TC_i'$ detachment exceeds TC
  - If $(F_i + H_i)L_i < TC_i' \rightarrow ST_i = ST_{i-1} + (F_i + H_i)L_i$ TC exceeds detachment

At last, the soil loss calculated at the final section is divided by the total cumulative length of the hillslope, to transform it into kg m^{-2} again.

For the convenience of this study, there will be referred to this adapted version of the rMMF model as the rMMF-HS model. A schematic overview of the rMMF-HS model can be seen in figure 3-2.

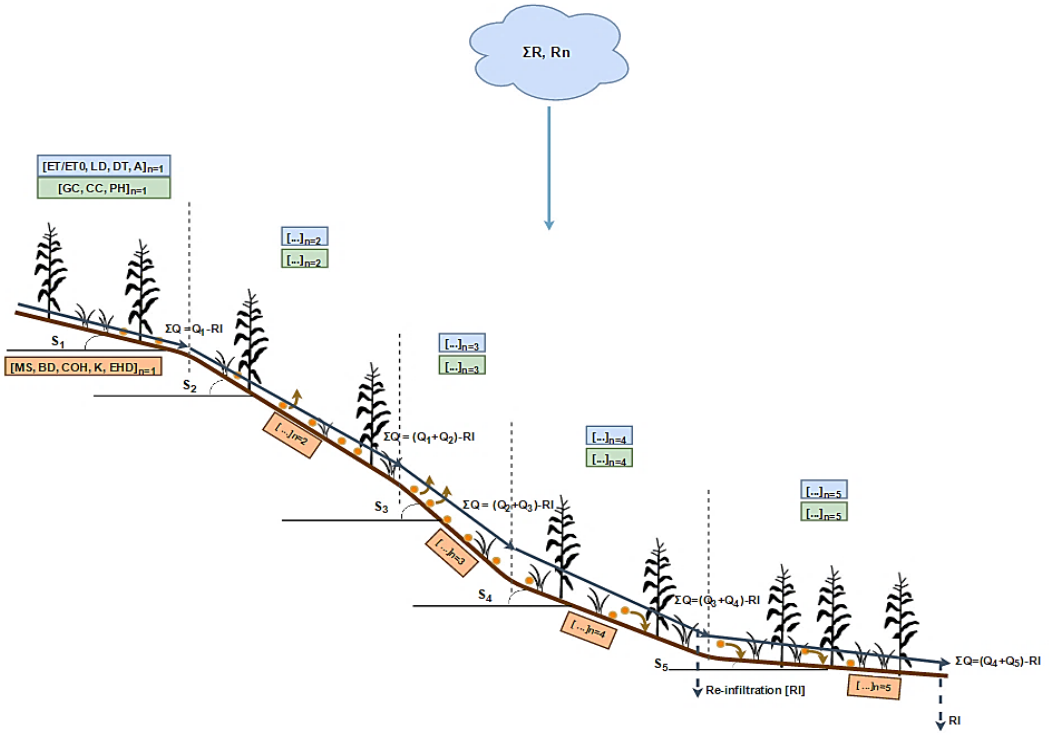

Figure 3-2. Schematic overview of the rMMF-HS model, where the slope is divided into multiple sections.

In this study, each channel and contour bund marks a boundary between sections on the hillslope, in which re-infiltration of surface water takes place, included in the model by RI=1 (figure 3-3). Additionally, a plot can be further divided into sections, dependent on variations in slope steepness. The performance of both models were first analysed, before parameter calibration was done.

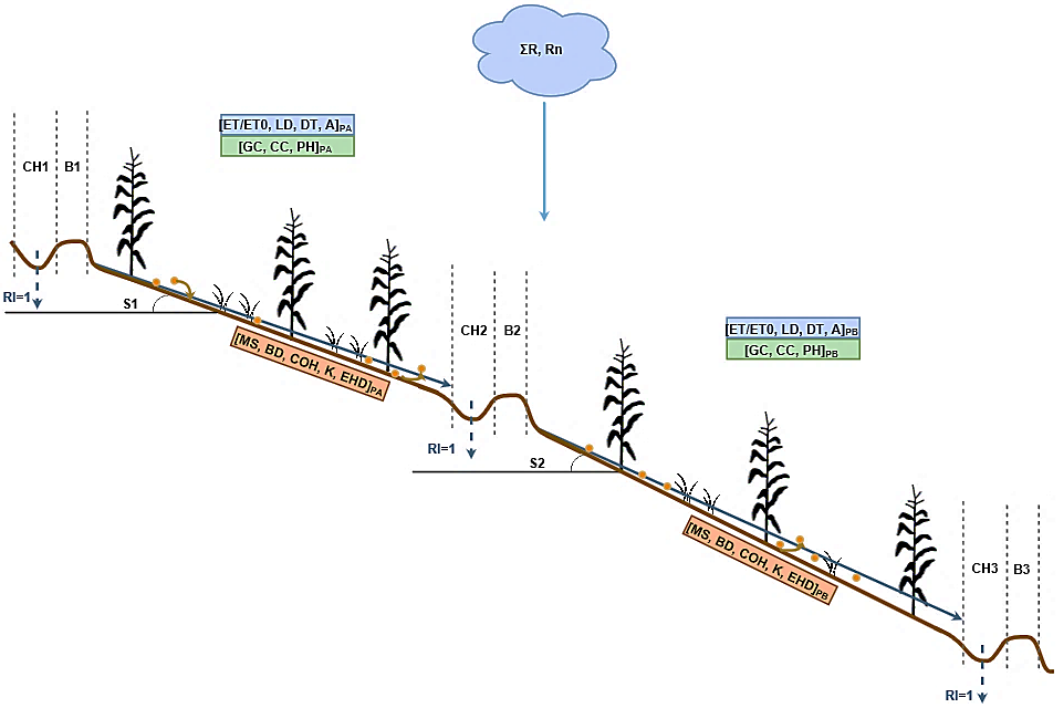

Figure 3-3. Schematic overview of a hillslope from a plot with channel-bund system and how this is incorporated in the rMMF-HS model. The upper section is referred to as section A and the lower section as section B. CH means channel and B is bund. The dotted lines indicate the boundaries of the sections.

3.2 Data acquisition

3.2.1 list of required data

The models were used on a monthly basis, as fieldwork was done for two months during the growing season of the maize. Some of the input variables required for the rMMF and rMMF-HS models change over time, because they are related to meteorological data and vegetation characteristics. For these variables, monthly values were derived by combining the measurements of fieldwork with literature. Table 3-1 shows how the data was collected during fieldwork. This will be explained more extensively in the following sections.

Table 3-1. List of data required for the adjusted rMMF model and collection method.

SOURCE	DATA	COLLECTION METHOD
Meteorological data	Rainfall (mm)	Meteo-station Gessa
	Number of rain days (Rn)	Meteo-station Gessa
	temperature (°C)	Meteo-station Gessa
Field measurements	A (-)	Relationship de Jong & Jetten (2007), Beer-Lambert law
	CC (0-1)	Greencroptool, Photoshop, Raes et al.(2010)
	GC (0-1)	Estimation in field, Descheemaker et al. (2006)
	PH (m)	Measurement tape, Lukeba et al. (2013)
	S (°)	Inclinometer
	BD (Mg m^{-2})	Laboratory
	COH (kPa)	Torvane
	Visual erosion assessment	ACED
	Sediment concentrations	Collected in field
Separate study	E_t/E_0 (-)	Aquacrop; Makkink
Literature	K (g J^{-1})	Laboratory, Morgan (2008)
	EHD (m)	Morgan (2008), calibrated
	C (-)	Morgan (2008), calibrated
	I (mm h^{-1})	Morgan (2008); 25

3.2.2 Meteorological data

Meteorological data of 12 subsequent years was gathered from the weather station located in Gessa town, at an elevation of 2200m (Wolka et al., 2017). This is a station from the National Meteorological Survey (NMS) and contains daily temperature and rainfall data which was used to determine input variables ET/ET_0, R and R_0. The rainfall and temperature records contained gaps for varying months. For the temperature, averages between 2005 and 2016 of maximum and minimum temperature of the coinciding day of the year, were taken to fill the gaps. To create

complete records for rainfall, the most average month was re-used to fill the missing month of the year. For 2016, the climate data for the months April to September was complete, which means that for the other months, months of previous years were used.

3.2.3 ET/ETo

In a separate study, held by I.W.F. Erven, the ratio of actual evapotranspiration over potential evapotranspiration was calculated with AquaCrop. AquaCrop requires reference evapotranspiration (ET_r) to calculate the ratio of actual evapotranspiration (ET) over the maximum evapotranspiration (ET_0) (Raes, 2010, 2011). The most common relation to calculate the reference evapotranspiration, is the Penman-Monteith equation. However, this method requires a substantial amount of meteorological data, such as radiation, relative humidity and wind speed, which could not be measured for this study area. Instead, the Makkink- equation was used to calculate the reference evapotranspiration (ET_r). The Makking- equation is simplified from the empirical Priestley-Taylor equation and requires only temperature and incoming shortwave radiation at the earth's surface as input parameters (Hendriks, 2010).

$$E_{MK} = C_{MK} * \frac{1000}{\rho\,\lambda} * \frac{\Delta}{\Delta + \gamma} * S_t \qquad 20$$

Where E_{MK} is the Makkink reference evapotranspiration (ET_{mk}=ET_r), C_{MK} is the Makkink coefficient, dependent on climatic conditions. Ogolo (2014) found monthly coefficients for different tropical conditions in Nigeria. The coefficients from this study are used from the region with the most similar tropical climate, and adjusted according to temperature and rain differences of the Bokole watershed. ρ is the water density, equal to 1000 g cm^{-3}, λ is the psychrometric constant with a value of 0.067 kPa°C^{-1} , λ is the latent heat of vaporization and is equal to 2.45 MJ kg^{-1}, Δ is the gradient of saturation vapour pressure, calculated as followed:

$$\Delta = \frac{4098\left(0.61 \exp\frac{17.27T}{237.3 + T}\right)}{(237.3 + T)^2} \qquad 21$$

Where T is the air temperature in °C.
S_t is the incoming shortwave radiation at the earth's surface (MJ m^{-2} day^{-1}). It can be calculated as followed:

$$S_t = \left(a_s + b_s * \frac{n}{N}\right) S_0 \qquad 22$$

Where $a_s + b_s$ is a fraction of incident shortwave radiation (S_0; MJ m^{-1} day^{-1}) on clear days which is equal to 0.25 + 0.50, n is the number of bright sunshine hours a day and N is the maximum number of hours of sunshine a day. The latter two parameters are derived from online monthly weather data from Addis Ababa (ClimaTemps, 2009). S_0 is a function of latitude and day of the year and can be determined with figure 3-4 (Hendriks, 2010).

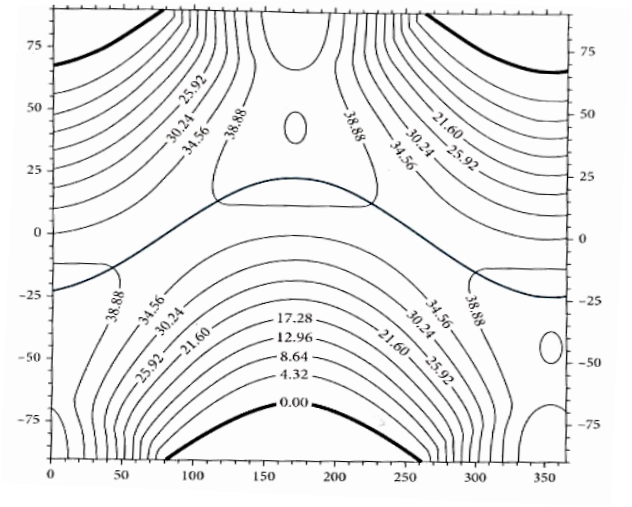

Figure 3-4. Incident shortwave radiation of the sun at the top of the earth's atmosphere (S_0). Vertical axis present the earth's latitude, on the horizontal axis, days of the year are indicated (Hendriks, 2010).

AquaCrop calculates the potential evapotranspiration (ET_0) and actual evapotranspiration (ET), with the dual crop coefficient approach (Allen, 2000; Raes et al., 2010). By multiplying the reference evapotranspiration (ET_r) with the crop coefficient (K_{cb}) and the soil coefficient (K_e), potential crop transpiration and soil evaporation are computed, if there is sufficient soil moisture available:

$$ET_0 = (K_e + K_{cb}) * ET_r \qquad 23$$

Both coefficients are related to canopy cover (CC), where K_{cb} is proportional related to the canopy cover and K_e is proportional related to the soil area not shaded by the canopy cover.
Actual evaporation rates for the soil are dependent on the amount of water in the soil that can be extracted by soil evaporation, whereas the actual transpiration depends on the amount of water that is available in the root zone (Raes et al., 2010).
Evapotranspiration is therefore dependent on the canopy cover, effect of rainfall on the soil moisture conditions and reference evapotranspiration. AquaCrop computes daily ET/ET_0 ratios, these were averaged for each month before it was used in the rMMF model.

3.2.4 Rainfall interception by vegetation

Rainfall interception was calculated by using a relationship between interception and canopy cover, described by de Jong and Jetten (2007):

$$I = C_p S_{max} * (1 - e^{-\frac{kP}{S_{max}}}) \qquad 24$$

Where I (mm) is the cumulative interception loss, C_p is the overall canopy cover fraction, S_{max} (mm) is the canopy storage capacity, k is a correction factor for canopy openness and P (mm) is

the cumulative rainfall since the start of the event. The correction factor (k) can be approached by the following relationship:

$$k = 0.065 * LAI \quad (25)$$

Differences in vegetation types causes variating canopy storage capacity (Smax), due to differences in plant architecture and leaf area. De Jong and Jetten found a general empirical relationship between broadleaved plants and canopy storage capacity:

$$Smax = 0.282 * LAI \quad (26)$$

Where LAI is the leaf area index, which is derived from the canopy cover by using the Beer-Lambert law that is rewritten (Pekin and Macfarlane, 2009; Law &Warning, 1994). It is used as followed:

$$LAI = -\frac{Ln(1 - CC)}{k} \quad (27)$$

the extinction coefficient (k) is a value ranging between 0.53 and 0.67. In this study, the standard mean of 0.62 is used (Vose et al., 1995).

Interception was also measured roughly in the field, placing six cups randomly on the ground, of which one was placed on a part of the field without maize, serving as a control cup. After a rainfall event, the depth of water in the cups was measured and compared to the depth of water in the control cup. The ratio of the difference between the cups and the control cup was assumed as the interception by maize plants. However, this measurement was only done once, after the senescence and therefore no monthly values were available. Furthermore, stem flow is not incorporated with this method. During the model calibration process, the effect of difference in interception values is analysed, where results are compared to the Morgan interception value for maize.

3.2.5 Field measurements

Parameters for the rMMF model that were collected on the experimental fields were the vegetation parameters ground cover (GC),canopy cover (CC) and plant height (PH), the slope steepness (S) and the cohesion of the soil (COH). Additionally, visual erosion assessment was done twice in the experimental fields and on the stone bund field.

Vegetation parameters

For the canopy cover, pictures were taken vertically towards the ground, the second week of August and again on the first of October, where the second measurement is assumed to be representative for the month September. for each subplot, four to seven pictures were selected. The percentage of canopy cover was calculated from these pictures with the Greencroptool, which uses the algorithm of Liu & Pattey (2010) to compute the green vegetation gap fraction. For pictures that contained a lot of green ground cover or more matured maize that reflects a yellow colour from the leaves, the Greencroptool could not be used. Instead, Photoshop 2017 was used to

calculate canopy cover percentages. The maize leaves in the pictures were delineated and given a white colour, and the remaining of the picture was coloured black. The percentage of white indicated the fraction of canopy cover (figure 3-5). The final canopy cover for each subplot resulted from the averages from these percentages. In appendix 9.3, all the canopy cover percentages can be found.

Ground cover was estimated directly in the field, by marking out an area of 1 x 1 meter in the centre of each subplot (A and B) (figure 3-6). This area was assumed to be representative for the whole subplot. Pictures were taken as well, to review estimations and compare these with estimations for other plots and over time.

The plant height was measured in August, where a row of maize plants, approximately in the centre of each subplot were selected and measured alternately. This resulted in an amount of plant heights ranging from 5 to 17, dependent on the width of a subplot. From these values, the average was taken and assumed as the maximum plant height, as the maize on both fields was already matured in August.

The parameters PH, CC and GC are dependent on the maize cycle growth and therefore vary over time. Fieldwork in August and the first of October provided values for most parameters for the end of the growth cycle. To obtain monthly values for CC and PH for the complete growth cycle, literature was consulted, so that monthly values could be derived from the field measurements. As ground cover does not follow a specific growth cycle, literature could not be applied directly. Therefore, a combination of field measurements, rainfall patterns and literature was combined to estimate monthly values for this parameter.

Maize densities were measured on the first of October during the maize yield measurements, where the amount of maize plants in an area of 2x2 m in the centre of each subplot were counted and assumed as representative for the whole plot.

Figure 3-5. Canopy cover calculation in Photoshop 2017, %white is canopy cover.

Figure 3-6. Ground cover measurement

Slope steepness

Slope steepness was measured for each subplot with an inclinometer. For the plots with bunds, the channel-bund system functioned as a boundary between A and B sections. For the control plots, a division into sections was made according to the change in slope. All slope measurements were done twice, by two different persons, to verify the accuracy of the instrument and user.

Soil parameters

The soil cohesion was measured with the 14.10 pocket vane tester (Eijkelkamp, Giesbeek, the Netherlands). It was measured twice during fieldwork, both times in August, where it was applied on each subplot between 3 and 15 times. The amount of measurements depended on the size of the plot and the spread of the results from the instrument. Averages for each subplot were taken from these measurements.

In a separate study that was held during the same period by I.W.F. Erven (2017) on the same experimental fields, soil moisture contents at field capacity were measured, with the Frequency-Domain Reflectrometer (FDR), ThetaProbe ML3 with HH2 moisture meter (Delta-T Devices, Cambridge, England). The FDR measures the soil moisture content from changes in signal frequencies, because of to the dielectric properties of the soil (Robock et al., 2000).

3.2.6 Assessment of Current Erosion Damage (ACED)

A field method was used to visually quantify the amount of soil erosion for the experimental fields with soil bunds and stone bunds. With the Assessment of Current Erosion Damage (ACED), created by Herweg (1996), soil losses can be estimated by measuring rills and gullies. It is a rough, simple method, which only requires the length, width and depth of the erosion features to calculate the amount of soil loss by runoff. By summing the soil losses of all the features, soil erosion per field can be determined. This method is only suitable for study areas where intense rainfall is not evenly distributed throughout the year, but occurs during single events or periods. For the Bokole watershed, where intense rainfall occurs only during several months of the year, this method is applicable.

Several distinctions were made during the erosion assessment with ACED. The first distinction being the presence of contour bunds, where erosion features on all plots of both experimental fields were monitored. Locations of erosion features were mapped, to find out which parts of the plots contribute to surface runoff and soil erosion. Variation in slope steepness was also considered. Rills in the field were classified by difference in length, depth and width. Because features were not very long, but irregular due to the stony nature of the soil, widths and depths were measured approximately every 20 cm and from these measurements, an average was used for computing the soil loss. When two or more rills merged to form a larger rill or gully, this rill-system was subdivided into two separate rills and the rill from the junction.

3.2.7 Laboratory

Soil texture and bulk density

Soil samples of each subplot were taken in the field, using a cylinder with a volume of 385 cm^3. Samples were taken at the centre of the subplot for the first 20 cm of the soil. The dry bulk density was calculated in a laboratory, by dividing the weight of dry soil by the total volume of the soil sample (Mouazen et al., 2002). The weight of dry soil resulted from drying the samples in the oven for 24 hours at 105℃ (Rose, 2004; Vereecken et al. 1989). Additionally, soil samples were taken to determine the soil texture for the soil detachability value (K). The soil was sieved with a 2mm sieve, of which 50 gr was weighed and used for textural analysis. The determination of the soil was made in the laboratory with the hydrometer method. The hydrometer method separates the three components of a soil, namely; sand, clay and silt, by their difference in particle size (Beretta et al., 2014). Equations that were used to calculate the percentage of clay and sand can be found in Appendix 9.1. When the percentages of clay, sand and silt were known, the USDA soil classification was used to determine the soil type. When the soil types were known K-values were derived according to the guide values of Morgan (2005).

Sediment concentrations

Samples for sediment concentrations were taken from the jerrycans downslope of the control plots in the fields. After a rainfall event, the water in the jerrycans was stirred, so that the sediment became evenly distributed. In a suspended state, samples were taken from the jerrycans, by filling one litre bottles. These bottles were taken to the laboratory, where each bottle was filtered (figure 3-7). Multiple filter papers were often needed to empty one bottle and for these samples, filters were collected in paper bags. After drying some days to weeks in the air, the filter papers with sediment were oven dried for 24 hours at 80 °C and weighed. Each filter paper that was used was weighed beforehand, so that the weight of the filter papers could be subtracted from the total weight of each sample. Furthermore, empty paper bags were put in the oven, to measure the weight loss of moisture from the bags, which were subtracted from the total weight as well. Sediment concentrations were then derived in g/L.

Figure. 3-7. Filtering of sediment of 1L bottles. Samples were taken from the jerrycans below the control plots.

3.2.8 Literature

The input parameters EHD and C could not be obtained directly in the field. For these parameters, relevant literature was used for calibration purposes.

The effective hydrological depth (EHD), is a function of plant cover, which affects the root depth and root density, and the effective soil depth, in case of shallow or crusted soils (Morgan, 2001). The values from Morgan (2001, 2008), for bare soils and for maize, which are 0.05 m and 0.12 m respectively, were used as initial EHD values. However, soil depths and maximum rooting depths were measured in the field and these were used to calibrate the EHD parameters during the rainy season.

As previously stated, the crop cover management factor (C), is a combined factor of the crop factor (C) and control practices (P) factors of the USLE equation. The crop cover management factor was altered during the calibration process, where the P-factor was set at 1 for the control plots, as there were no control practices for these two plots. Monthly C-values were calibrated and compared with literature references of rMMF C-values for maize and the USLE C-factors for maize.

3.2.9 Sensitivity analysis

With an average sensitivity analysis (ALS), that is proposed by Nearing et al. (1989), the relative effect of variations between parameter values on the model outcome can be compared (Morgan and Duzant, 2008). The ALS approach expresses the relative normalized change in output over the relative normalized change in input. This is done by dividing the model outputs and the input parameters by their means, as can be seen in equation 28:

$$ALS = \frac{\left[\frac{O_2 - O_1}{\bar{O}}\right]}{\left[\frac{I_2 - I_1}{\bar{I}}\right]} \qquad 28$$

O_1 and O_2 are the model output values, where $\bar{O}$ is the mean of O_1 and O_2. I_1 and I_2 are the input values of a specific parameter with a chosen range, where $\bar{I}$ is the mean of these two input values (Morgan, 2005). When the sensitivity of the model by a specific parameter is analysed, the other parameters remain constant. This method is used, as it is suitable for comparing parameter values of different orders of magnitude (Morgan, 2008). The chosen range for this study is ±10%, as extreme ranges may cause unrealistic parameter values.

3.2.10 rainfall variability

To analyse the effect of dry and wet years in the study fields, the rainfall record, comprising the last 12 years of the Gessa weather station, is used to obtain monthly input variables for Rainfall, number of rain days and the evaporation ratios. Using the rMMF and rMMF-HS model, the effect of variability in rainfall on the processes of runoff and erosion, for fields with and without soil bunds will be assessed.

4. Results

4.1 Rainfall and evaporation characteristics

The Gessa weather station could only provide rainfall and temperature records from 2016 for the months April to September. For the missing months, the most average complete months between the years 2005 and 2015 were used (graph 4-1). The annual rainfall of 2016 is 1886 mm and the total number of rain days is 130. From the record minus the year 2016, the average annual rainfall is computed at 1897mm. This is similar to the average annual rainfall of 1746 mm stated by Wolka et al. (2017), of the upper watershed in the Bokole region.

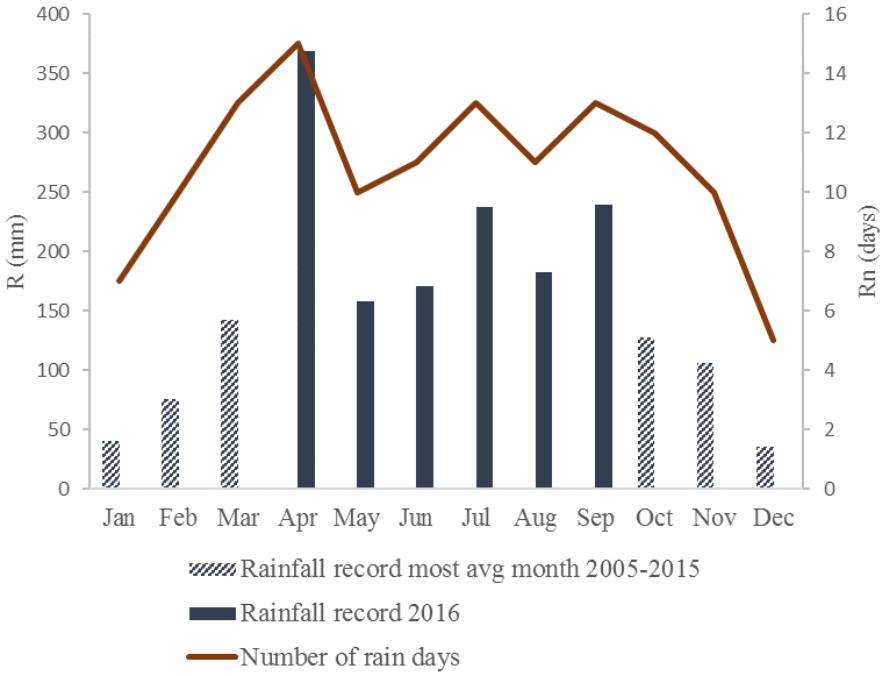

Graph 4-1. Rainfall in 2016 for the study area. From April to September, record data from Gessa station is used, for the remaining months, the months of the record between 2005 to 2015, the most average months are used.

Figure 4-1 presents the monthly rainfall and number of rain days for driest, wettest, and most average years of the rainfall record. The driest year, 2006, in this record has a total rainfall of 1355 mm and the most rain fell in 2014, with a total of 2615 mm. The rainfall of 2008 is the most similar to the annual average of the record, with 1962 mm. Note that for 2006, monthly rainfall volumes are significantly lower compared to the other years, whereas the number of rain days is similar to 2006 and 2008.

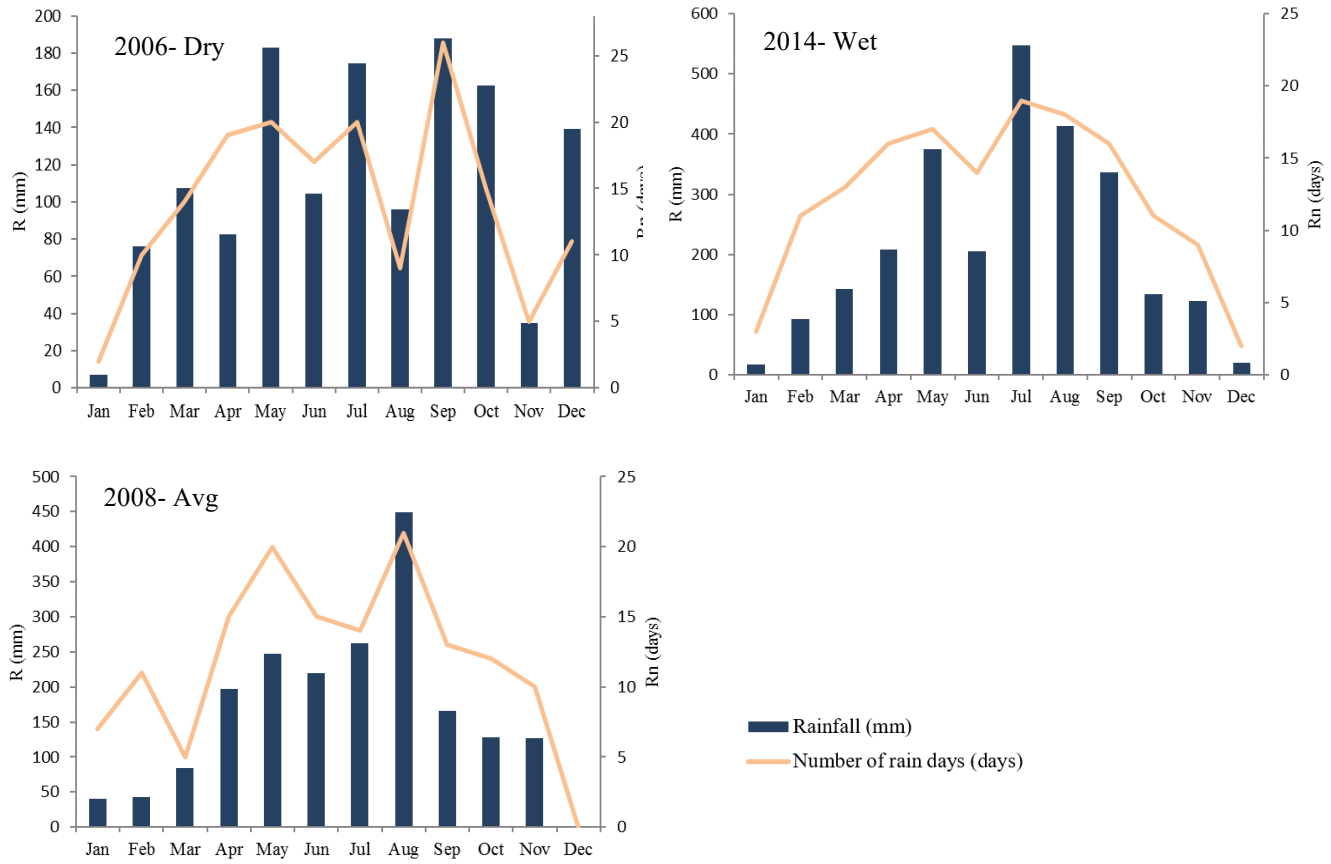

Figure 4-1. Monthly rainfall and number of rain days for the driest, wettest and most average year of the rainfall record in Gessa.

Table 4-1 presents the monthly evaporation ratios for the years that were analysed. The annual averages show that evaporation does not vary as much as rainfall. The year 2006 generally contains slightly lower evaporation ratios due to lower rainfall amounts. This difference is more pronounced for the months during the dry season (November-April).

Table 4-1. Monthly ET/ET_0 values for the years 2006, 2008, 2014 and 2016

	Jan	*Feb*	*Mar*	*Apr*	*May*	*Jun*	*Jul*	*Aug*	*Sep*	*Oct*	*Nov*	*Dec*	*Avg*
2016	0.60	0.57	0.80	0.90	0.85	0.86	0.96	0.85	0.90	0.64	0.79	0.43	0.76
2006	0.08	0.46	0.62	0.63	0.88	0.81	0.97	0.75	0.97	0.73	0.48	0.75	0.68
2008	0.36	0.38	0.30	0.79	0.87	0.99	0.97	0.91	0.97	0.67	0.58	0.07	0.65
2014	0.22	0.70	0.81	0.94	0.97	0.99	0.94	0.99	0.97	0.79	0.59	0.40	0.78

4.2 Plot characteristics

Table 4-2 shows the area, slope and bund characteristics of all the subplots of field 2. The lower plots (B-plots) all have a larger area, mostly due to a longer distance between bund 2 and 3. A clear change in slope is visible, where the B-plots are notably steeper than the A-plots, with the exception of plot 2, where slope 2-A is very similar to slope 2-B. The average slope of field 2 is 3º higher than the average slope of field 1. The height of the bunds directly after the channel are the highest for the upper bunds and lowest for the lower bunds. The downslope height of the bunds are generally higher for the middle bunds, indicating that the transition from the bund to the B-plot is steeper than the transition from bund to the A-plots. The plots geographic locations, measurements and extended bund measurements can be found in appendix 9.2.

Table 4-2. Plot and bund characteristics, field 2.

PLOT	AREA	SLOPE		BUND	UPLSLOPE HEIGHT	DOWNSLOPE HEIGHT	WIDTH [TOP]
	m^2	%	°		*m*	*m*	*m*
1a	26	12	6.2	**1**	0.22	0.45	0.23
1b	48	34	19	**2**	0.19	0.65	0.23
				3	0.02	-	0.43
2a	29	26	14.5	**1**	0.28	0.53	0.35
2b	55	31	16.8	**2**	0.06	0.54	0.38
				3	0.08	-	0.40
3-1	42	15	8.5				
3-2	78	27	15				
3-3	69	23	14				
4a	52	11	6.2	**1**	0.27	0.40	0.35
4b	111	29	16.1	**2**	0.08	0.32	0.34
				3	0.14	-	0.30
5a	37	16	9				
5b	72	32	18.2				
6a	57	13	7.2	**1**	0.21	0.28	0.28
6b	115	29	16	**2**	0.19	0.39	0.30
				3	0.09	-	0.35

The left picture of figure 4-2 shows that channels could be completely filled due to extreme rainfall events. During fieldwork in August channels appeared nearly empty the day after each rainfall event. Complete filling of channels probably occurred after some successive rainfall events and saturated soils.

Figure 4-2. The picture on the left was taken by G. Sterk in July and shows a filled channel with bund. The picture on the right, taken in August, shows an empty channel -bund system.

4.3 Vegetation characteristics

4.3.1 Plant densities

The average plant density of field 2 was 29,167 plants/ha (figure 4-3), which is very small compared to the FAO average maize density of 60,000 plants/ha (Mejía, 2003). Field 1 contained a larger average plant density of 46,042 plants/ha.

Table 4-3. Plant densities of each plot and the average density.

DENSITY	*P1*	*P2*	*P3*	*P4*	*P5*	*P6*	AVG
#plants/m²	3.13	2.50	2.50	3.63	2.75	3	2.92

4.3.2 Plant height

The average maximum plant height of the maize was measured during fieldwork and ranged between 1.5 m and 2 m (table 4-4).

Table 4-4. Average maximum maize height of each subplot, measured in August

PLOT	*1-A*	*1-B*	*2-A*	*2-B*	*3-1*	*3-2*	*3-3*	*4-A*	*4-B*	*5-A*	*5-B*	*6-A*	*6-B*
PH (m)	1.45	1.6	1.76	1.64	1.76	1.66	1.56	1.52	1.55	1.5	1.9	2.03	1.94

The study of Lukeba et al. (2013) was used to estimate the growth of maize from emergence until harvest. In their study, the growth of Zea maize L. of different varieties was simulated for a savanna region of the DR-Congo. The maize variety that was most similar in grow period and maximum plant height to the field measurements, was used to reconstruct the growth of the maize in this study. The height of the maize was read from this graph at 14 different stages spread out over the growth cycle and the ratio of this value over the maximum height was used to calculate the height of the maize for all the plots of field 2 at equal stages. The plant heights for the days in between these converted values were calculated with linear interpolation. The results for each plot are shown in graph 4-2.

The plant growth of maize shows the largest increase during 36 days, where the average plant height of 0.20 m on day 43 reaches to 1.60 m on day 79 of the maize cycle. This vast growth occurred during May and June. On day 90, the maize was at yield state, where maximum plant height is reached. For modelling purposes, monthly averages were used for each subplot.

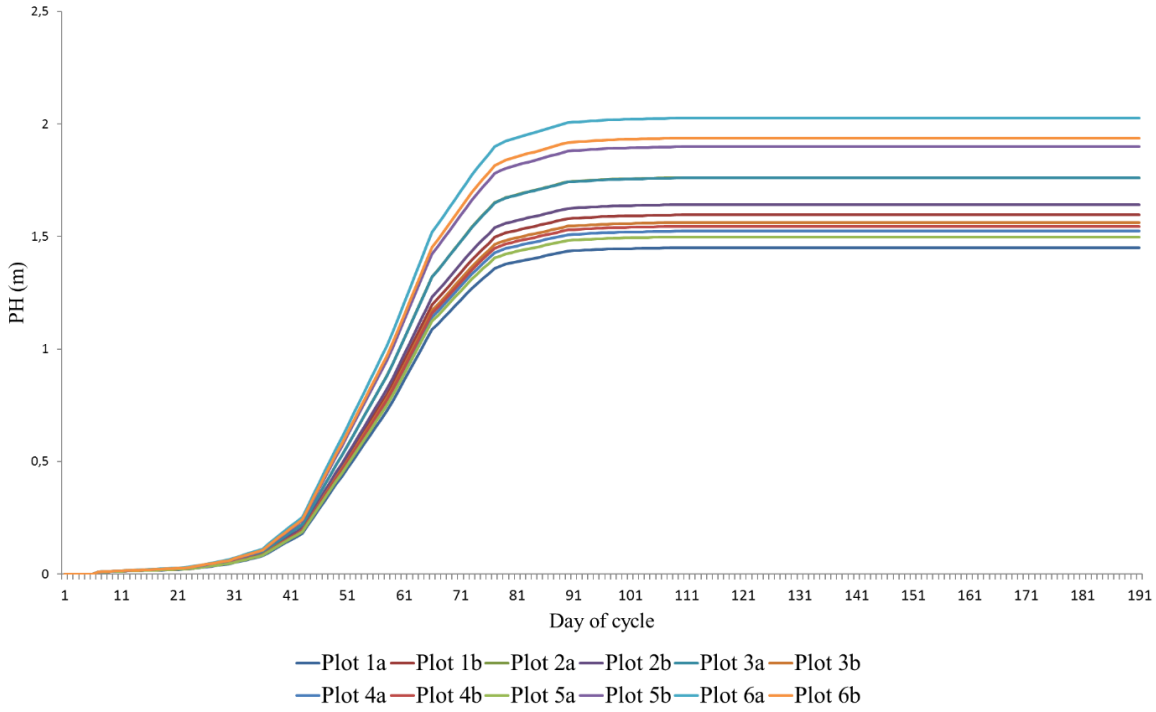

Graph 4-2. Plant height development of maize in field 2, during the maize cycle period of 2016.

4.3.3 Canopy cover

The results of the canopy cover measurements in August and on the first of October can be found in Appendix 9.5. Canopy cover decreased with a total average of 16.5% between August and October, due to maturing of the maize (graph 4-3).

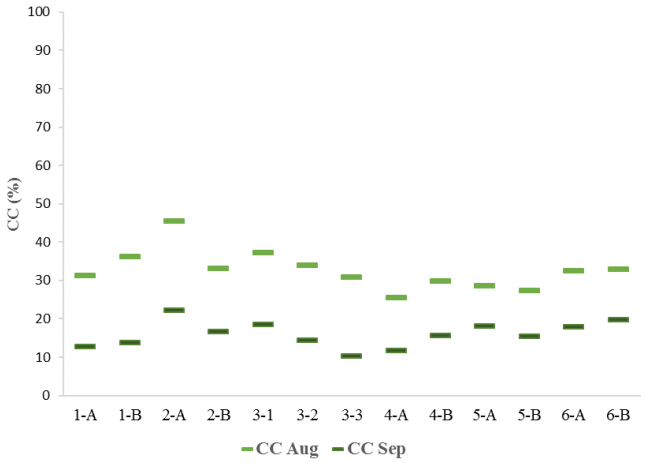

Graph 4-3. Measured canopy cover of August and September 2016 for field 2.

Raes et al. (2010) describes the development of canopy cover during the complete maize cycle, as it is used in the AquaCrop model. It considers three equations, the first calculates the growth until half of the maximum canopy cover is reached, the second equation is used for the maize growth after half of the maximum canopy cover is reached and a third equation calculates the decay, which takes place after senescence of the maize.

Hence, to use the calculation of AquaCrop for canopy cover over time, the maximum canopy cover has to be known first (CC_x). During fieldwork, the maize in field 2 was already in senescence and therefore it was not possible to measure the maximum canopy cover. However, the maize in field 1 did not reach senescence during the measurements in August, so it was still at its canopy cover maximum (CC_x). The maximum canopy cover for field 2 was calculated using the average canopy cover of field 1 during August ($CC_x(F1)$). The difference in maize density and the difference in plant area between F1 and F2 were taken into account as well, as presented by equation 29:

$$Avg\ CC_x(F2) = Avg\ CC_x(F1) * \frac{plant\ density\ F2}{plant\ density\ F1} * \frac{plant\ area\ F2}{plant\ area\ F1} = 47.1 * 0.63 * 1.23 \quad (29)$$

Where $Avg\ CC_x(F2)$ is the average maximum canopy cover for field 2 in %, which was computed at 36.7%.
When the average CC_x of F2 was known, the CC_x of each subplot in F2 could be computed. This was done by calculating the ratio of the average canopy cover of each subplot in F2 in August ($CC_{i_{Aug}}$), to the total average canopy cover of F2 in August ($Avg\ CC_{Aug}$) and multiply that ratio by the $Avg\ CC_x(F2)$ of 36.7%:

$$CC_x\ (P(i)) = \left(\frac{CC_{i_{Aug}}}{Avg\ CC_{Aug}}\right) * 36.7 \quad (30)$$

Where $CC_x\ (P(i))$ is the maximum canopy cover for subplot i= 1a, 1b, …, 6b.

When CC_x was known for each subplot of field 2, the first stage of canopy cover growth could be computed. Equation 31 is valid when CC ≤ CC_x /2:

$$CC = CC_0 e^{tCGC} \quad (31)$$

Where CC_0 is the canopy cover at 90% emergence, CGC is the canopy growth coefficient and t is the time in days or growing degree days (GDD). Values for CC_0 and CGC for maize are 0.02% and 0.0011 respectively (Raes et al., 2012). A growing degree day (GDD) expresses a certain stage or time in heat units instead of number of days. The unit for GDD is ºC day and it is calculated as followed:

$$GDD = T_{avg} - T_{base} \quad (32)$$

Where T_{avg} is the average daily temperature, obtained from the average of the daily maximum and minimum temperature and T_{base} is the base temperature in ºC at below which crop development does not progress (Raes et al., 2012). For maize this equals to 8.0 ºC (Abedinpour et al., 2012; Raes, 2012).

When CC > CCx/2, a new equation must be used which calculates the exponential decay:

$$CC = CCx - 0.25 * \frac{(CC_x)^2}{CC_0} e^{-tCGC} \quad (33)$$

After senescence, the green canopy cover starts to decline. This is indicated with equation 34:

$$CC = CC_x[1 - 0.05 * \left(e^{\frac{CDC}{CC_x}t} - 1\right)] \quad (34)$$

Where CDC is the canopy decline coefficient, a measure for the speed of decline of the green canopy cover once it is triggered (Raes et al., 2010). The measurements of canopy from the first of October were done right before the harvest. Therefore the CDC is calibrated for each plot, to a value that matches the measured final canopy cover. The results of the canopy cover development calculations are shown in graph 4-4. Monthly averages are taken for the model process.

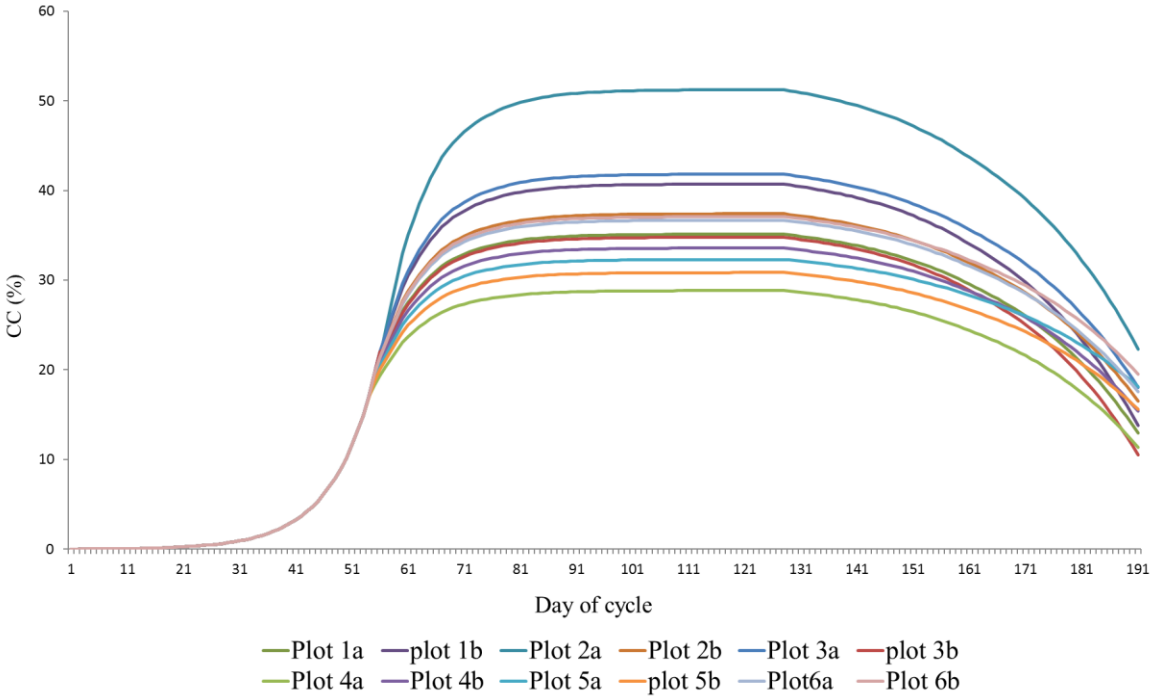

Graph 4-4. Development of canopy cover (%) for each subplot with equations from AquaCrop 2010.

4.3.3 Ground cover

Ground cover was measured twice during fieldwork, during the middle of August and the first of October. Graph 4-5 shows the averages of these measurements. Measured ground cover generally increased from August until October. Exceptions are subplot 2-B, where ground cover remained equal and subplot 4-B, 6-A and 6-B, in which ground cover decreased. Both measurements were taken after the senescence of the maize (Appendix 9.3.1). This means that maize had already began to decay, which could explain the increase in ground cover between the two measurements, as the competition for light and water from the maize decreased.

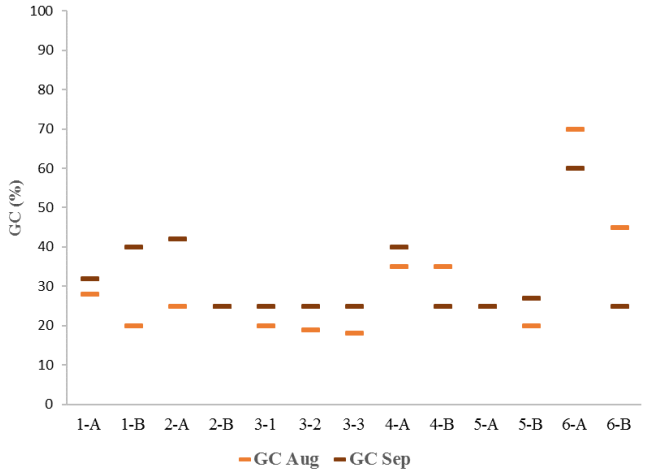

Graph 4-5. Averages of ground cover percentages from field measurements, for August and September

To obtain ground cover data during the maximum canopy cover of maize (June and July) of field 2, the ratio of ground cover in August over the ground cover in October of field 1 was used, as the maize in field 1 was still at maximum canopy cover in August. An average ratio of 0.5 was found, which was used to estimate the ground cover in F2 during June and July.

It was assumed that in March, the ground cover was equal to the ground cover in April, as rainfall started to increase in March causing the growth of weeds, but the ground cover had to regrow in April, due to ploughing of the land.

For April and May, ground cover fractions were estimated, however keeping in mind the fast growth of the canopy cover in these months (graph 4-5). It is assumed that between April and May, ground cover also undergoes a fast growth, due to increase in rainfall. However, as the canopy of the maize increases, it is assumed that the speed of ground cover growth between May and June decreases. Therefore, for April the ground cover is set at 50% of the ground cover of June and July (during CCx) and in May at 80%.

The measurement made on the first of October is used as the monthly ground cover value for September. It is assumed that after the rainy season at the end of September, ground cover decreases at a fast rate. As the average rainfall for the months October and November are relatively equal, ground cover is estimated to decrease only with 10%.

During the dry season, there is in general no vegetation, but as there is still some rainfall during these months, even though it is sporadic, it is assumed that a small part of the weeds are still able to grow. Descheemaeker et al. (2006) stated that during the dry season in the northern Ethiopian highlands, the cover of herbs and grasses are assumed to be 15% of the cover during the rainy season. This percentage was used for estimating the ground cover for the months December, January and February. Graph 4-6 shows the resulting development of ground cover over the months.

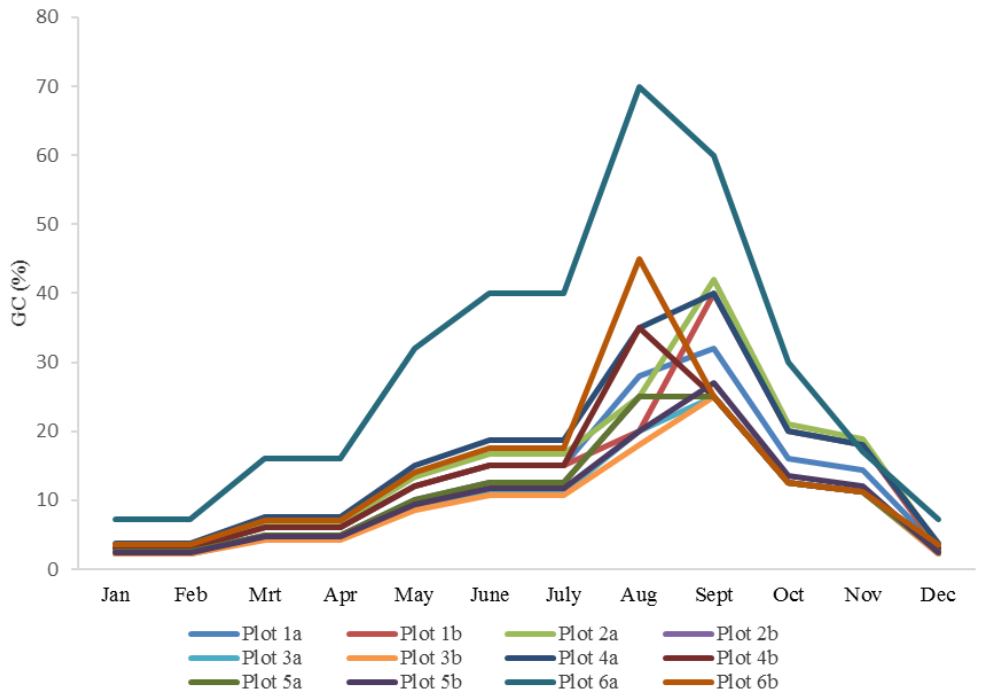

Graph 4-6. Monthly development of ground cover for each subplot.

4.3.4 Interception

The interception fraction was calculated for each rainfall event and subsequently averages of each month were taken, resulting in the values as can be seen in table 4-5.

Table 4-5. Monthly interception values for each subplot.

	PLOT											
	1a	*1b*	*2a*	*2b*	*3a*	*3b*	*4a*	*4b*	*5a*	*5b*	*6a*	*6b*
Apr	0.000	0.000	0.000	0.000	0.000	0.000	0.000	0.000	0.000	0.000	0.000	0.000
May	0.001	0.002	0.002	0.002	0.002	0.001	0.001	0.001	0.001	0.001	0.001	0.001
Jun	0.007	0.010	0.020	0.008	0.011	0.007	0.004	0.006	0.005	0.005	0.008	0.008
Jul	0.007	0.010	0.020	0.008	0.011	0.006	0.004	0.006	0.005	0.005	0.007	0.008
Aug	0.006	0.009	0.018	0.007	0.009	0.006	0.004	0.005	0.005	0.004	0.007	0.007
Sep	0.001	0.003	0.007	0.003	0.004	0.002	0.002	0.003	0.003	0.002	0.003	0.004

The calculated interception values are very low, compared to the advised maize interception values of Morgan (2005, 2008). Interception was also roughly measured in the field once after a rainfall event in September. This resulted in an average interception of 0.27, which is significantly higher and more comparable to the value of Morgan of 0.25. The effect of difference in interception values to the model outcome was analysed in section 4.9.

4.4 Soil characteristics

Small variations between subplots are present for the soil parameters bulk density, soil moisture at field capacity and cohesion. The bulk densities coincide more or less with the Morgan (2005) values for the same soil texture. Soil moisture values are relatively high, compared to advised soil moisture value of 0.2 of loamy soils by Morgan (2005). Cohesion values are also high, compared to the recommended value of 3 kPa for loamy soils (Morgan, 2005). Cohesion is generally lower when the soil is wet, as wetting weakens the soil aggregates (Morgan, 2005). The cohesion was measured on the 23rd of August, around the time some strong rainfall events occurred in the area. The maximum rooting depth was measured for each subplot and contained an average of 0.32 m. The effective rooting depth, the depth where about 70% of the soil water is extracted from the plant roots, is approximately one- half the maximum rooting depth (Evans et al. 1996, Amend, 2005). Visible in table 4-6, is that the effective rooting depth is more or less equal to the measured soil depth. The average soil depth of field 2 is 0.13 m, which is very low compared to the FAO average requirement for maize of 1m to 1.7m (FAO, 2017; Mejía, 2003).

*Table 4-6. Soil characteristics of each subplot. * indicates section 3-2, parameter values are created from the average of 3-1 and 3-3.*

PLOT	BD	SM (FC)	COH	SOIL DEPTH	ROOT DEPTH MAX	SOIL TEXTURE				K
	Mg/m³	*%w/w*	*kPa*	*m*	*m*	*% sand*	*% clay*	*% silt*	*class*	*kPa*
1a	1.149	0.34	12.7	0.12	0.30	54.4	22.4	23.2	S.C. loam	0.1
1b	1.149	0.35	11.5	0.13	0.35	50.4	20.4	29.2	Loam	0.8
2a	1.335	0.35	12.0	0.19	0.29	-	-	-		
2b	1.193	0.32	11.7	0.16	0.35	-	-	-		
3-1	1.111	0.35	10.4	0.14	0.40	46.4	22.4	31.2	Loam	0.8
3-2	1.112*	0.35*	10.7*	0.12*	0.35*	-	-	-		
3-3	1.114	0.34	11.0	0.10	0.29	-	-	-		
4a	1.135	0.33	10.5	0.12	0.40	-	-	-		
4b	1.217	0.32	11.4	0.10	0.35	-	-	-		
5a	1.073	0.36	9.5	0.13	0.23	44.4	26.4	29.2	Loam	0.8
5b	1.073	0.36	9.0	0.09	0.19	46.4	22.4	31.2	Loam	0.8
6a	1.077	0.36	10.1	0.19	0.37	-	-	-		
6b	1.173	0.34	10.4	0.12	0.29	-	-	-		
Avg	1.150	0.34	10.8	0.13	0.32	48.4	22.8	28.8		

The percentages clay, sand and silt, resulting from the soil texture analysis for field 2 can be seen in table 4-6. The soil texture with coinciding detachability is visible in figure 4-3. The results of the soil texture analysis show that around 50% of the soil consists of sand and that clay is the smallest component. According to Morgan (2005), soils with a clay content between 9% and 30% are the most erodible, as clay particles combine with organic matter to form aggregates. Soil analysis held by I.W.F. Erven, showed that the soil samples all had a very low organic matter

content (1-2%), which would increase the erodibility of the soil. Most samples were classified as loam, but plot 1-A was classified as sandy clay loam. Figure 4-3 shows that the K value for loam and most closely situated soil classes, deviates extremely from the K value for sandy clay loam, which is considerably lower, even though the distribution of the three soil components are not that wide. Tesfahunegn et al.(2014) used different k-values for sandy clay loam and clay loam, of 0.3 gm/J and 0.4 gm/J respectively. The effect of different soil detachability values on the model results was evaluated in section 4.9.

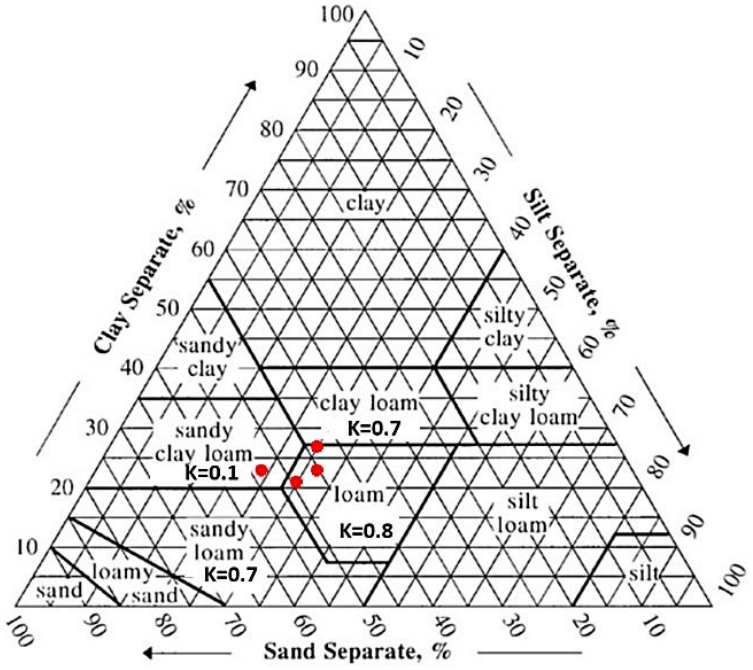

Figure 4-3. Soil texture according to the USDA soil classification, with coinciding soil detachability (K) values for soil types of interest according to Morgan, 2005

4.5 Measured soil losses

4.5.1 Visual erosion assessment with ACED

Field 1 contained no measurable rills during the fieldwork, except for one small feature on a lower plot with bunds. Erosion features such as orientated stone fragments and pathways were an indication of small runoff streams during heavy rain events. These features were not considered as rills, because of their very shallow depth and unclear boundaries. The upper sections of field 1 had an average slope of 9.4º and the lower sections had an average slope of 13.5º.

The visual erosion assessment for field two (F2) was done twice, on August 20 and on August 24. During this period, a total rainfall amount of 92.3 mm had fallen, of which most fell during two larger rainfall events of more than 30 mm.
Appendix 9.4.1 shows the measurements of the erosion features for each subplot and a schematic view of their locations. All rills on F2 were classified as shallow (width <25 cm, depth <15 cm). Erosion features were mostly visible on the lower plots (B-plots). Plot 2 and 5, contained some features on the upper half as well. Close to the metal edges of the control plots, pathways were visible. For every field, small pathways were visible between maize plants as well, some more clear than others. Most erosion features were found on plot 2b, 3b and P5, where 2b and 5b also stand out in slope steepness. Plot 3b has the smallest slope compared to other B-plots, but the total plot has a length of 21 m, which makes it the longest of the six plots. P1b has the steepest slope but contained no measurable erosion features. However, a significant rill on plot 2b was situated nearly on the border between plot 1b. Soil losses between August 20 and August 24 varied between the plots with rills, from 1.8 kg to 12.7 kg, with the exception of plot 4b that showed a soil loss of 36 kg between these dates, which is significantly higher than for the other plots (graph 4-7). Table 4-7 shows the large variations in soil loss between subplots when it is expressed as ton/ha.

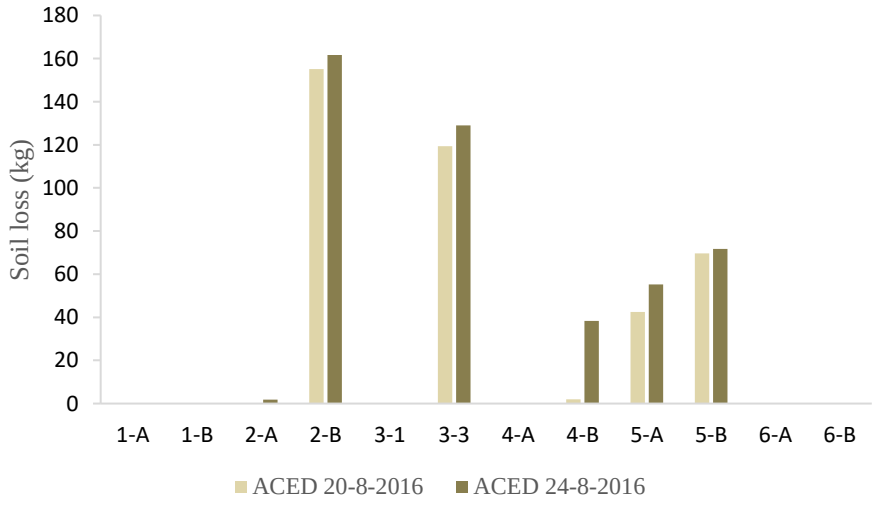

Graph 4-7. Measured soil losses in kg, for each subplot. Measurements were held on August 20 and August 24.

Table 4-7. Soil losses in ton/ha for subplots that contained rills on the 20th of August and the 24th of August and the difference in soil loss between this period.

	2a		2b		3b		4b		5a		5b	
	20-8	*24-8*	*20-8*	*24-8*	*20-8*	*24-8*	*20-8*	*24-8*	*20-8*	*24-8*	*20-8*	*24-8*
ton/ha	0.00	0.60	28.20	29.40	17.00	18.40	0.20	3.50	11.50	14.90	9.70	10.00
Δton/ha	0.60		1.20		1.39		3.30		3.40		0.30	

Visual erosion assessment on the field with stone bunds was done on the 16th of August and again ten days later on the 26th. This field was abandoned approximately around the end of April or early May, due to the final harvest of the crops. The amount of rainfall that fell in May is around 160 mm. The last significant rainfall event in April took place on the 24th, with an amount of 39.7 mm. The amount of rainfall that fell between the two assessments is almost equal to the amount of rainfall between the two assessments of field 2, but with an addition of 6.7 mm that fell on the 25th of August.
This field contained shallow rills and shallow wide rills (15<w<200cm, d<15cm) and one artificial deep rill (w<50 cm, 15<d<100 cm). Appendix 9.6.2 shows the position of the rills. This field was divided into three sections with varying slope, section A, had a slope of 17º, section B had a slope of 14º and the most downslope section, section C, had an estimated slope of 2º. The lengths of section A, B and C, are 5 m, 10 m and 5 m respectively and all widths were equal to the width of the field, which is 50 m (figure 2-4).

Apendix 9.4.2 shows that the positions of the features stayed relatively constant during the two assessments. In section A, small incisions were clearly visible, with lengths of 1 m or 2 m. Section B showed longer and wider rills that mostly extended from the artificial rill, of which one even extended through the lower bund to section C. This rill had a measured length of 17 m. A similar feature was visible in section A, where a smaller rill extended through the middle bund.

On the assessment on the 26th of August, a new rill was found in each section, all with lengths of several meters and of which the longest was situated in section C, containing a length of 6 m.

Table 4-8 shows the erosion of each section and of the total area, of both assessments. Visible is that erosion is the most significant on section B and that the soil losses between the two measurements are comparable for each section and to the total area. It also shows greater soil losses than field 2, between the two assessments, yet rainfall was approximately equal. The period of origin of soil losses of the first measurement cannot be exactly determined. It was expected that the crops after the harvested around the end of April or early May, no agricultural activity took place.

Table 4-8. Soil losses in ton/ha assessed on the field with stone bunds on the 16th of August and the 26th of August.

	SOIL LOSS STONE BUND FIELD		
	16-08-16	26-8-2016	Δ
	ton/ha	*ton/ha*	*ton/ha*
Section A	15.3	20.5	5.2
Section B	31.3	35.5	4.3
Section C	15.7	22.2	6.4
Total area	23.4	28.4	5.1

4.5.2 Sediment concentrations

Sediment concentrations were measured on 24 different days on field 2, between 26 May and 24 August, all of which can be found in appendix 9.7. The sediment concentrations show a large variation, as can be seen in graph 4-3 and table 4-9, with values ranging between 0.68 g/L and 26.14 g/L and an average sediment concentration of 6.47 g/L. Sediment concentrations cannot be directly linked to a certain rainfall event, as rainfall was not recorded locally on the field and differences in rainfall between the study field and Gessa can exist due to the distance of 6 km and difference in elevation of around 450 m. Graph 4-8 shows that the highest sediment concentrations were measured between the end of June and the end of July. Between this time, four rainfall events were recorded in Gessa with a depth of 40 mm or higher.

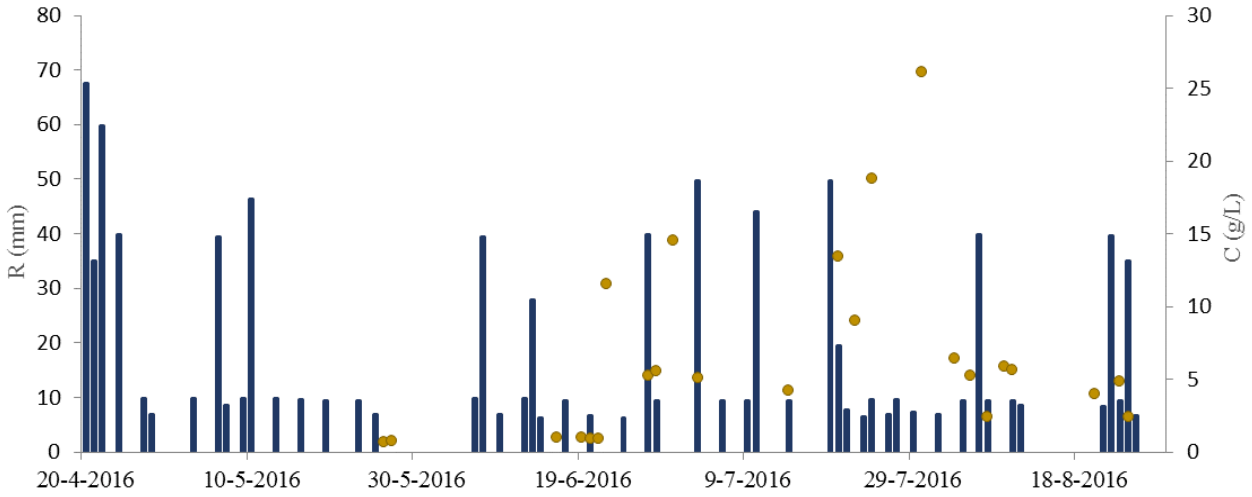

Graph 3-8. Daily rainfall (blue bars) in mm and sediment concentrations (yellow dots) in g/L, that were measured from the end of March until the end of August.

Table 4-9. Range of sediment concentrations in g/L and the number of measurements that fell in this range (count). The average value and standard deviation is noted as well.

Count	*6*	*3*	*8*	*1*	*1*	*5*	*Avg*	*STDev*
C (g/L)	0 - 2	2 - 4	4 - 6	6 - 8	8 - 10	>10	6.5	6.2

4.6 Initial EHD and C-factor values

4.6.1 Effective hydrological depth

Table 4-10 shows the initial values for each month, which were derived from Morgan, (2001). For the months December, January and February, vegetation was rare and therefore the value of 0.05 for bare soils was used. The maize cycle started in April and lasted until September, hence the EHD value for maize crops of 0.12 was used for this period. For the months March, October and September, no crops covered the fields. However, as the rainfall during these months exceeded 100 mm, weeds were expected to grow. The values for Morgan could not be directly used, but had to be estimated to lie between 0.05 and 0.12. For March, EHD depths were most likely to increase, due to the effect of rooting depths of the weeds. An estimated value of 0.09 was chosen for this month. For October and November, EHD values decreased as the maize had already been harvested, although weeds were still present. Estimated values of 0.09 for October and 0.08 for November were chosen.

Table 4-10. Monthly initial EHD values, minimum and maximum values derived from Morgan (2001)

	Jan	**Feb**	**Mar**	**Apr**	**May**	**Jun**	**Jul**	**Aug**	**Sep**	**Oct**	**Nov**	**Dec**
EHD	0.05	0.05	0.09	0.12	0.12	0.12	0.12	0.12	0.12	0.09	0.08	0.05

4.6.2 C-factor

Morgan (2005, 2008) advises a C-factor for maize of 0.2, which was used as initial values for the months April to September. Bare soils have a C-factor of 1.0, but as it was expected that the 3% of weeds that were assumed to remain during the dry months, would prevent the C-factor of becoming 1.0. That is why a value of 0.95 was used for the months December. January and February. For March, October and November, the effect of weeds had to be estimated once more. Table 4-11 shows the initial values for each month.

Table 4-11. Monthly initial C-factor values, minimum and maximum values derived from Morgan (2001)

	Jan	**Feb**	**Mar**	**Apr**	**May**	**Jun**	**Jul**	**Aug**	**Sep**	**Oct**	**Nov**	**Dec**
C-FACTOR	0.95	0.95	0.7	0.2	0.2	0.2	0.2	0.2	0.2	0.5	0.7	0.95

4.6 Model analysis of rMMF and rMMF-HS

4.6.1 Runoff

The modelled runoff of the rMMF is compared to the modelled runoff of the rMMF-HS model, for control plot 3 (CP3) and control plot 5 (CP5) under uncalibrated conditions. As the rMMF model is not able to include slope sections, the total runoff for each plot is the result of the averaged runoff of the sections that together make up the plot. The ratio of the section length to the total plot length was used for this averaging. Graph 4-9 presents the monthly runoff of both models.

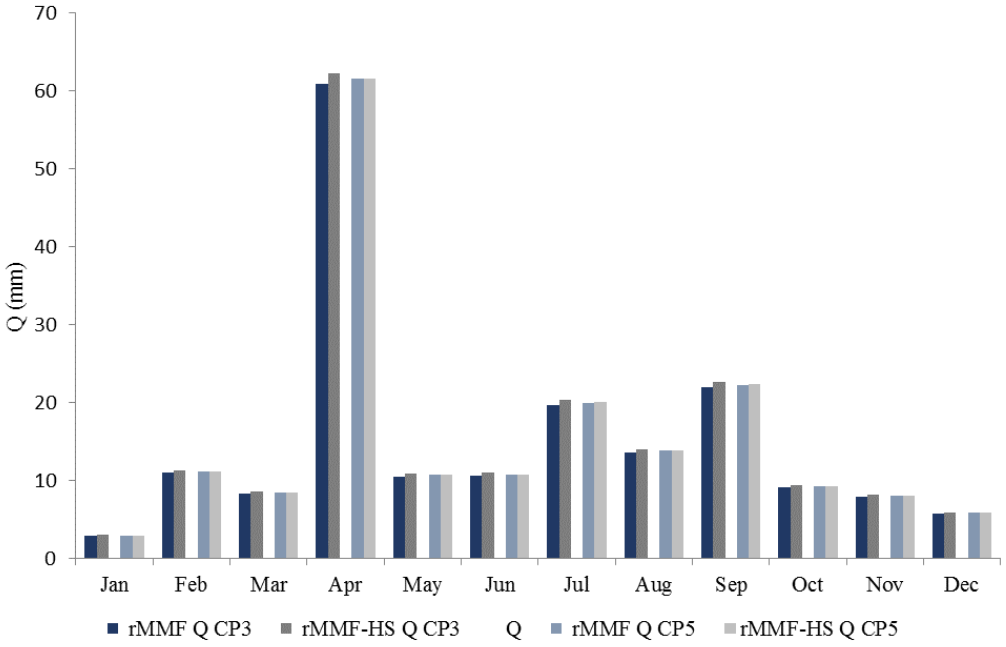

Graph 4-9. Monthly modelled runoff for control plot 3 and control plot 5, comparing the rMMF and the rMMF-HS model results.

The runoff pattern follows the pattern of the monthly rainfall, with a peak in April. The different models show almost equal values. CP3 shows slightly higher values for the rMMF-HS model, an average of 2.7%, while CP5 shows no notable difference between the two models. The main cause for this disparity between model results for CP3 are the parameters MS and BD, which are not equal for each section. Because the rMMF-HS model computes over the length, taking into account the runoff of the previous section, while the rMMF model averages over all the sections, depending on their length, this change in MS is not included in the same way for both models. Also, CP3 is the only plot that is divided into three sections instead of two, which may emphasize this deviation. This problem is not visible with CP5, as the soil moisture for sections A and B are equal.

When the model is used for a yearly calculation with monthly averaged parameters, the runoff shows no notable difference to the sum of the monthly runoff values. The only averaged parameters that are used for calculating runoff and could therefore create a difference between monthly and yearly modelling, are EHD and ET/ET_0. SM and BD are soil constants and are therefore equal to the input parameters for annual modelling.

Figure 4-4 presents the total annual runoff in m^2 of the rMMF-HS model over the hillslope length of CP3 and CP5. The slope, and therefore the variation in slope over the transect, is not included in the runoff equation, resulting in a linear accumulation of runoff over the slope length. The runoff volumes in mm remain equal over each hillslope section, because there is no re-infiltration of water.

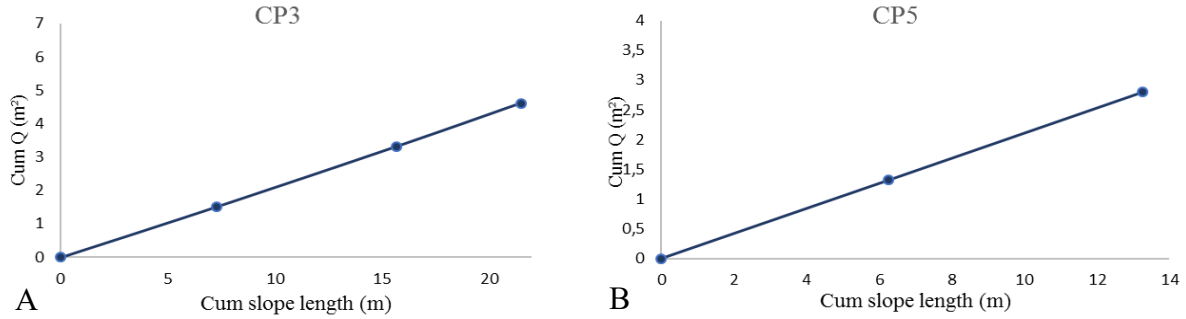

Figure 4-4. Cumulative annual runoff of control plot 3 and control plot 5 over the hillslope section.

The rMMF and rMMF-HS method show almost equal results for modelled runoff and because the effect of the bunds on runoff and runon can be incorporated in the rMMF-HS model, this model is used to calculate the new runoff on plots with bunds.

4.6.2 Bunds in rMMF-HS model

Three assumptions were made when the channel- bund system was included in the rMMF-HS model:

1. All surface runoff generated during a rainfall event can be captured by the downslope channel, i.e. RI=1 for the channel sections.
2. For no-bund situations, no re-infiltration takes place, meaning that RI=0 for every other section.
3. The bunds do not generate runoff, which is included in the model by EHD values of 0.5 m for the bund sections.

Figure 4-5 shows the effect of the bunds for plots 1, 2, 4 and 6 over the slope length. Annual runoff volumes are used in these graphs. The runoff accumulation without bunds, is not exactly linear, especially for plot 2, due to changes in parameters MS and BD over the section. Section A and B are clearly distinguishable due to the re-infiltration in the channel section. There is a significant larger decrease in runoff for section B, because the accumulated runoff in a no-bund situation is much higher further downslope. Figure 4-5 clearly shows that the relative effect of the bunds is dependent on their position on the hillslope. Variations in the relative decrease between plots are caused by differences in length, where relative decreases in B-sections increase when the upslope length is greater. That is why the B-section of P4 shows a larger reduction in runoff than the B-sections of other plots.

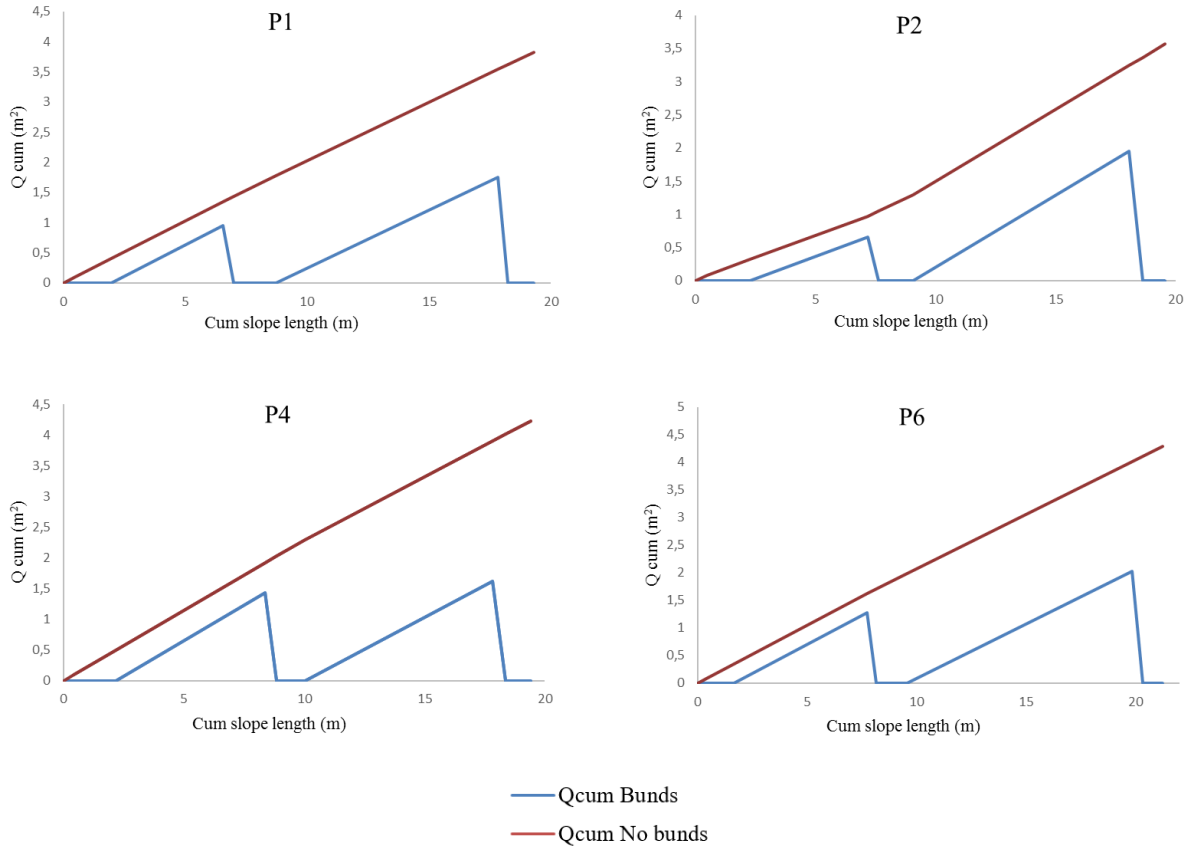

Figure 4-5. Accumulation of runoff (annually) with and without bunds over the hillslope, for all the plots with bunds.

Furthermore, monthly variations in the B-sections of the plots are recognised. This is caused by variations in the parameters MS and BD between section A and B. For plot 1, 4 and 6, this effect is not larger than 0.8%, but for plot 2, there is a maximum monthly variation of 6.5%. For the A-sections, this problem is not recognized, as parameters MS and BD do not change until the second channel- bund system.

4.6.3 Soil loss

In graph 4-10 the rMMF and rMMF-HS model outcomes for soil loss are presented for control plots CP3 and CP5. Monthly soil losses computed by the rMMF and rMMF-HS both show that soil losses peak in April, with a contribution of 60% to the total erosion of 2016. It can be seen that most erosion occurs between April and September.

The graph further shows that the monthly soil losses are greater for the rMMF model than for the rMMF-HS model, where soil losses of the rMMF-HS model are almost insignificant. Monthly erosion modelling over hillslope sections with the rMMF-HS method proved to be insufficient. Therefore, the rMMF model was used for modelling soil losses.

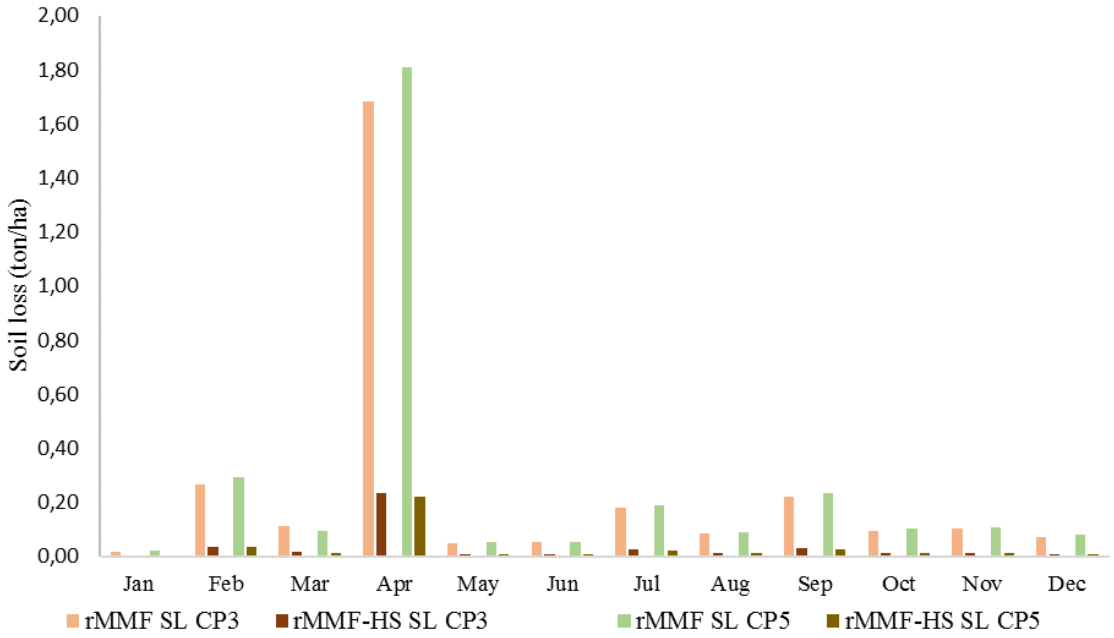

Graph 4-10. Monthly modelled soil loss for control plot 3 and control plot 5, comparing the rMMF and the rMMF-HS model results.

4.7 Parameter calibration and validation

4.7.1 Surface runoff and soil loss of control plots

The runoff coefficient (Q_c) during fieldwork for the control plots was determined with combined measurements of the visual erosion assessment and the sediment concentrations. As it was not clear from which of the two control plots the sediment concentrations were taken, the area and soil losses of plot 3 and 5 (both upper and lower sections) were taken together as one.

Hoeing on field 2 took place until approximately the end of May, therefore the soil losses that were measured with the visual erosion assessment on the 20th of August were assumed to have occurred over a time span of 85 days, starting on the 26th of May. The 26th of May is chosen, as there are no sediment concentration records before this time. In the first period, between May 26 and August 20, a soil loss of 7.8 ton/ha was measured on plot 3 and 5 combined. During the second period, between August 20 and August 26, a soil loss of 0.8 ton/ha was measured. Combined, this results in a soil loss of 8.6 ton/ha, for the months June, July and August.

Table 4-12 shows how the runoff coefficient was derived. First, the soil losses from the ACED method on the control plots P3 and P5 were converted to grams and divided by the average sediment concentration of the first period (May 26 - August 20), obtaining the average amount of runoff in litres. The runoff was converted into mm, using the combined area of CP3 and CP5, and divided by the amount of rainfall of the same period.

As was shown in section 4.5.2, the sediment concentrations have a large variation, especially for the first period. Sediment concentrations between 4-6 g/L were most common, but there are also peaks for the lowest and highest range. Because of this large variation, an additional runoff coefficient was calculated, by using the average of the values measured in the most common range (4-6 g/L), which is equal to 5.2 g/L. This coincides with a runoff coefficient of 0.31 for the months June, July and August (table 4-12).

Table 4-12. Used variables for calculating the runoff coefficient (Qc. For Q in mm, the combined area of CP3 and CP5 is used, as the ACED values are also for both control plots combined.

	C *g/L*	ACED *g*	VOLUME *L*	Q *mm*	R *mm*	Qc *0-1*
25/5-20/8	6.87	231471	33693	115	492	0.23
20/8-24/8	3.74	24490	6546	22.3	92.3	0.24
25/5-20/8	5.21	231471	44428	151	492	0.31

Comparing the runoff coefficients to relevant studies held in various parts of the Ethiopian highlands in table 4-13, it shows that a runoff coefficient of 0.24 for the two events in August and the average runoff coefficient of 0.23, is corresponding with the literature. The larger runoff coefficient of 0.31, calculated from the average sediment concentration of 5.2 g/L falls within the range of Qc values from literature as well. Due to uncertainties of the sediment concentration measurements and the large variation presented by literature, calibration will be done twice. First with the runoff coefficient of 0.23, calculated as an average for the months June, July and August and again for these months with a Qc of 0.31.

Table 4-13. Runoff coefficients during the rainy season from different studies and different parts of Ethiopia. The factors slope, rainfall and vegetation cover are noted as well.

	LOCATION	SLOPE *(%)*	ANNUAL RAINFALL *(mm)*	VEGETATION COVER *(%)*	RUNOFF COEFFICIENT *(%)*
Descheemaeker et al. 2006	Tigray (North)	35	700	40-70	22 2-56
Alemayu et al. 2013	Upper Blue Nile basin (NW)	15-25	1532	76	28
Adimassu & Haile 2011	Central Highlands	10	525	?	31 23-42

4.7.2 EHD calibration and modelled runoff in rMMF-HS

EHD depths were first altered in the rMMF-HS model, where for June, July and August a value of 0.068 resulted in an average runoff coefficient of 0.23. Lower EHD values for maize are presumable, because of the low maize density in the fields. The value of 0.068 was used for the months May to September. The maize in April was still very small for all plots (CC=0.01, PH=0.04 m), so a slightly lower value of 0.066 was used for this month. Values for the months March, October and September had to be altered as well, in accordance with the maximum depths during

maize growth. Monthly calibrated EHD values with resulting runoff coefficients can be seen in table 4-14. The annual average Qc of this calibration is 0.20.

Tabel 4-14 Monthly EHD values and modelled runoff coefficient in the rMMF-HS model for the first calibration. Qc values presented are from CP3. Differences between CP3 and CP5 are 0% to 1%, CP5 has the same annual average of 20%.

	Jan	*Feb*	*Mar*	*Apr*	*May*	*Jun*	*Jul*	*Aug*	*Sep*	*Oct*	*Nov*	*Dec*	*Avg*
EHD (cm)	5.0	5.0	6.5	6.6	6.8	6.8	6.8	6.8	6.8	6.5	6.0	5.0	6.2
Qc (%)	8.0	15.0	13.0	38.0	22.0	21.0	25.0	23.0	26.0	15.0	15.0	17.0	20.0

An average runoff coefficient for the months June, July and August of 0.31 coincides with a maximum EHD value of 0.055 m. The difference between the EHD values during the dry months and during the rainy season is significantly smaller for this calibration, with an increase of only 0.5 cm. Table 4-15 shows that the average annual runoff coefficient for the second calibration coincides with 0.25, a 5% difference from the previous calibration.

Tabel 4-15 Monthly EHD values and modelled runoff coefficient in the rMMF-HS model, for the second calibration. Qc values presented are from CP3. Differences between CP3 and CP5 are 0% to 1%, CP5 has the same annual average of 25%.

	Jan	*Feb*	*Mar*	*Apr*	*May*	*Jun*	*Jul*	*Aug*	*Sep*	*Oct*	*Nov*	*Dec*	*Avg*
EHD (cm)	5.0	5.0	5.2	5.3	5.5	5.5	5.5	5.5	5.5	5.3	5.2	5.0	5.3
Qc (%)	8.0	15.0	20.0	46.0	29.0	28.0	32.0	31.0	34.0	21.0	19.0	17.0	25.0

Graph 4-11 shows the resulting runoff for the first (avg Qc of 0.20) and second (avg Qc of 0.25) calibration in the rMMF-HS model. Averages of both control plots are used. Modelled runoff for the second calibration is 20% larger. Annual runoff volumes for CP3 and CP5 are 447 mm and 444 mm respectively for the first calibration, against 573 mm and 569 mm respectively for the second calibration.

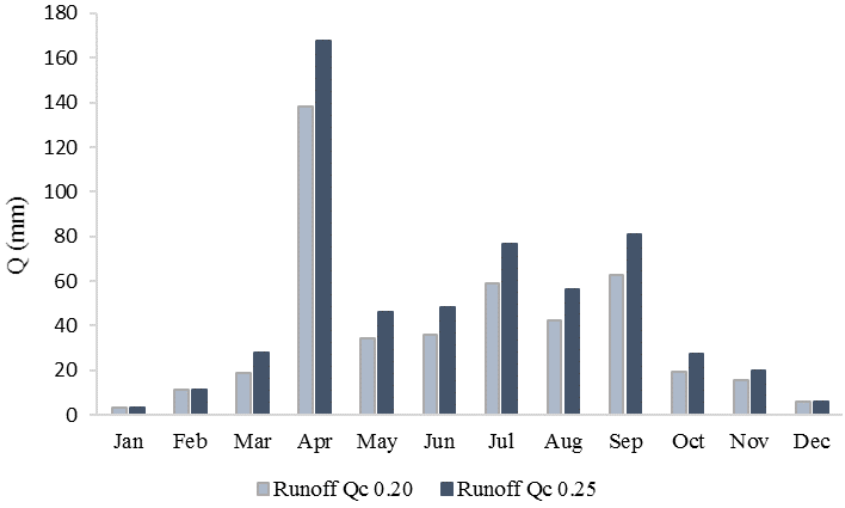

Graph 4-11. Monthly runoff volumes of the control plots in rMMF-HS, for both calibrations (avg Qc 0.20 and 0.25)

4.7.3 C-factor calibration and modelled soil loss in rMMF

The C-factor in the rMMF method is a combination of the USLE C- and P-factors and for the control plots, P is equal to 1, as there are no control practices for these plots. Therefore, the C-factor for the rMMF method should be the same value as the C-factor of the USLE equation. In Morgan (2005), presented USLE C-factors for maize vary between 0.20 and 0.90, depending on the productivity and tillage. In the study area, measured maize densities were low compared to FAO records (Raes et al., 2010). A higher C-factor than 0.20 for this study area is therefore not unlikely.

Model calibrations for the soil losses were done in the rMMF model, with the calibrated EHD values from the rMMF-HS model. During the months of maize growth, a factor of 0.40 was found for the first calibration with an annual Qc of 0.20. For the months June, July and August, this resulted in a soil loss of 5.7 ton/ha for CP3 and 6.2 ton/ha for CP5. This is close to the estimated soil loss for CP3 and CP5 of 8.6 ton/ha for the same period (section 4.7.1). For April, the initial value was increased with 0.10, as the effect of maize is still very small, and for October the C-factor was increased with 0.10 as well, to make it a better fit between the values for September and November. The values for the other months remain equal to the uncalibrated ones.

For the second calibration, with an average annual Qc of 0.25, a C-factor of 0.30 during maize growth was found. This resulted in soil losses of 7.4 ton/ha for CP3 for June-August and 8.1 ton/ha for CP5. These values are very close to the ACED measurement of 8.6 ton/ha. April was given a C-factor of 0.40. For the other months, the uncalibrated values were used.

Apart from the monthly C-factors, Figure 4-6 shows the monthly soil losses that were modelled with the rMMF model for both calibrations (Qc:0.20 & Qc:0.25). For the first calibration, annual soil losses for CP3 were modelled at 32.8 ton/ha and 35.6 ton/ha for CP5. For the second calibration, soil losses were 40.6 ton/ha for CP3 and 44.1 ton/ha for CP5.

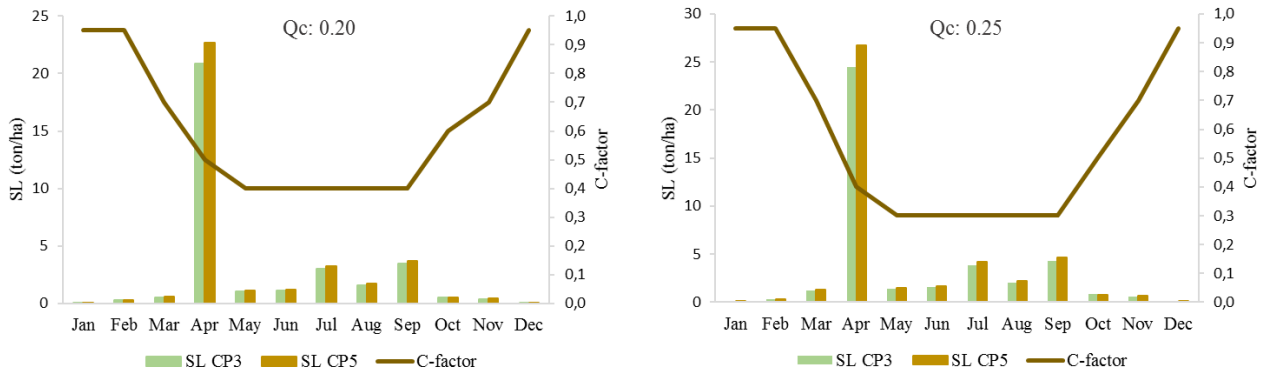

Figure 4-6. Soil losses for the first calibration, where an annual Qc of 0.20 was modelled and for the second calibration, where an annual average Qc of 0.25. Soil losses were modelled with the rMMF model. The C-factor for both calibrations is also presented.

4.8 The effect of bunds

4.8.1 Reduction in runoff

Graph 4-12 presents the new reduction of runoff by bunds, modelled in the rMMF-HS model under calibrated conditions (avg Qc: 0.20). The monthly averages of the relative decrease in runoff for each subplot was used as a scaling factor for the runoff in the rMMF model. Percentages for the second calibration (avg Qc: 0.25) are almost equal and can be found in appendix 9.6.2. Actual runoff values with and without bunds, predicted with the rMMF-HS model can be found in appendix 9.6.1, for the first calibration and in 9.6.2 for the second calibration.

Figure 4-5 already showed that the lower sections have a larger reduction in runoff. In the upper sections, runoff reductions are between 21% and 30%, depending on the length of the section, and on the lower sections, runoff is reduced by 44% to 58%.

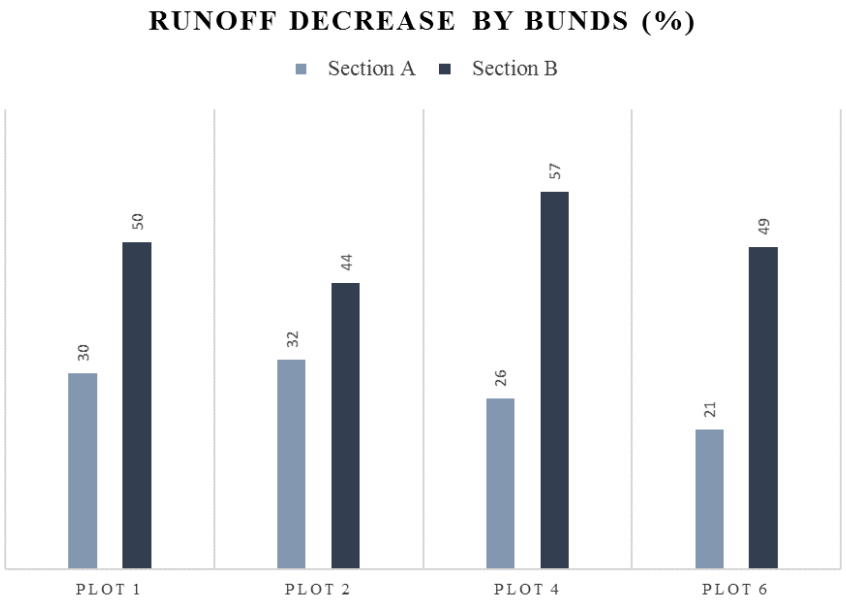

Graph 4-12. Relative decrease in runoff by bunds. The calibrated EHD and C-factor parameters of the first calibration (Qc: 0.20) was used. For the second calibration (Qc: 0.25), relative reduction was almost equal for each plot and section.

4.8.2 Reduction in soil loss

For each plot, the soil loss was modelled in the rMMF model without bunds and again with the scaling factor for runoff, to include the effect of the bunds. Table 4-16 shows the resulting modelled decrease by the channel-bund system for each plot. The placement of the channel-bund system caused an annual decrease in soil loss of 65% to 73%. Monthly values are available in appendix 9.6.

Table 4-16. Effect of soil loss by bunds for each plot and for both calibrations.

	Avg Qc: 0.20			Avg Qc: 0.25		
	NB (ton/ha)	*B* (ton/ha)	*Decrease* (%)	*NB* (ton/ha)	*B* (ton/ha)	*Decrease* (%)
P1	34.2	10.0	70.7	42.6	12.6	70.4
P2	36.7	12.9	64.8	46.4	16.2	65.2
P4	30.2	8.2	73.0	37.6	10.1	73.0
P6	30.8	10.5	66.0	38.7	13.1	66.0

To be able to apply the reduction in runoff by soil bunds in the conventional rMMF model directly, the USLE control practice factor (P-factor) was predicted for each plot. The runoff in the rMMF model was reset, removing the scaling factor from the rMMF-HS model, and the C-factors were multiplied with a factor until the same reduction in soil loss as in table 4-16 was derived. Combining the USLE P-factor with the USLE C-factor, results in the final rMMF C-factor for maize with bunds. Table 4-17 shows the resulting P-factors with bunds. For both calibrations, the same average P-factor of 0.32 was found. Table 4-17 also shows the modelled rMMF C-factors during the months of maize cover for fields with soil bunds (May- September).

Table 4-17. Modelled USLE P-factors and rMMF C-factors for fields with bunds. rMMF C-factors are during the months of maximum maize cover. Values were derived in the rMMF model.

	Qc: 0.20		Qc: 0.25	
	USLE P-factor	*rMMF C-factor*	*USLE P-factor*	*rMMF C-factor*
P1	0.29	0.12	0.29	0.09
P2	0.38	0.15	0.38	0.11
P4	0.27	0.11	0.27	0.08
P6	0.34	0.14	0.34	0.10
Avg	0.32	0.13	0.32	0.10

4.9 Model sensitivity analysis

The effect of parameter values on the model output between plots have already been recognized. The parameters SM, BD and S showed to be the main causes for these differences. Graph 4-13 presents the averaged outcome of all plots of the sensitivity analysis, as differences between the plots were very small. Annual model outputs were used for the ALS analysis.

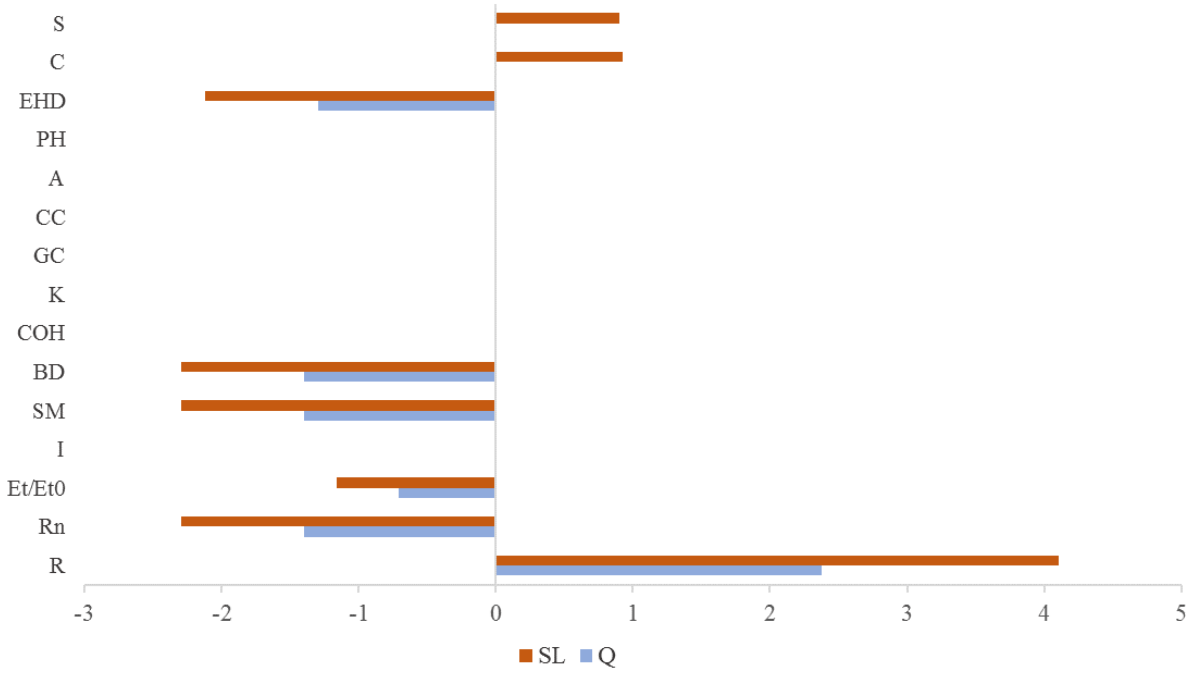

Graph 4-13. Results of sensitivity analysis for the rMMF model.

As could be expected, the vegetation parameters do not influence the model outcome. This is because the transport capacity was always significantly smaller than the sediment detachment rate, with as a result that the transport capacity will remain the limiting factor in each scenario. It can be clearly seen which parameters contribute to the runoff and transport capacity calculation. Soil loss and runoff both are the most sensitive to rainfall. EHD and number of rainy days, come second and show similar results, influencing the model output severely as well (ALS>1.0). Soil loss and runoff are equally sensitive to the parameters SM and BD, as they are multiplied in the soil moisture storage capacity (S_c) equation (eq. 8). The soil loss is moderately sensitive to the slope and C-factor (1.0 >ALS ≥ 0.5). Runoff is moderately sensitive to evaporation, whereas the soil loss shows a larger sensitivity to evaporation.

4.10 Effect of rainfall variability

The sensitivity analysis showed that the amount of rainfall and number of rain days have a significant influence on the modelled erosion in the rMMF- model. From the rainfall record from Gessa, the climatic parameters R, Rn and ET/ET_0 from the driest (2006), wettest (2014) and most average (2008) year, are used in the model, with EHD and C-factor values from the first calibration, to analyse the change in runoff and erosion for extremes and evaluate the accuracy of the P-factor when it is applied to other years.

In the driest year, annual soil losses are modelled below 5 ton/ha, while in 2014, the average annual soil loss for the control plots reaches to 90 ton/ha. Annual runoff for 2014 exceeds 730mm, whereas for 2006, runoff remains below 130 mm. For the year 2008, the most average year, annual runoff for the control plots is below 430 mm, which is comparable, but slightly less than was modelled for 2016. Annual soil losses in 2008 are therefore slightly lower as well compared to 2016, with an average of 30 ton/ha for CP3 and CP5.

The peak of July in 2014 and August for 2008, visible in figure 4-7, can be explained by higher rainfall, whereas the peak in 2006 for December is mainly caused by the low number of rainy days, indicating relatively more intense rainfall events (section 4.1). This is also the reason why the total erosion in 2008 is lower than 2016, while the rainfall in 2008 just exceeded the rainfall of 2016 with 76 mm.

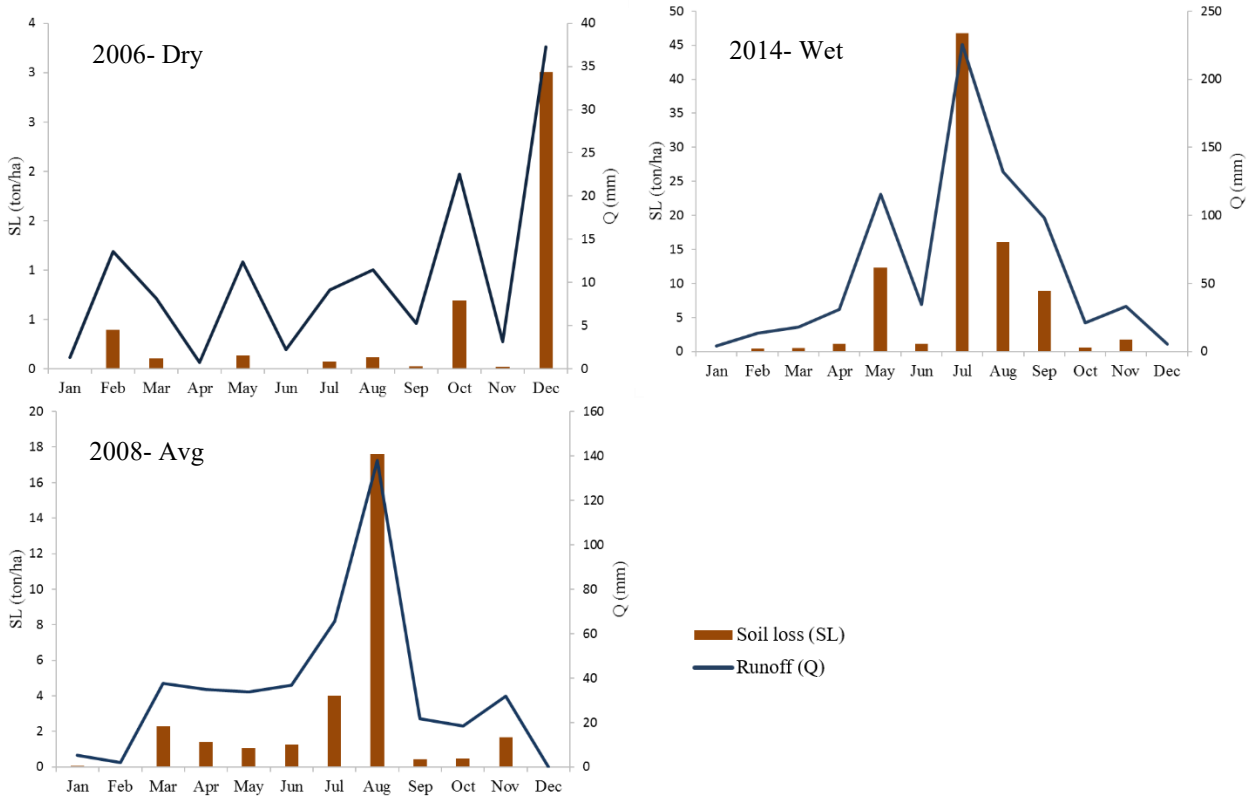

Figure 4-7. Monthly runoff and soil losses for the driest, wettest and most average year.

Figure 4-8 shows annual runoff values for plot 4 with bunds for the years 2006, 2008, 2014 and 2016, modelled with the rMMF-HS model. The difference in runoff between 2006 and 2014 is around 600 mm for all plots in case of no bunds and when the effect of bunds are included, the difference in runoff between these years ranges between 300 mm and 500 mm for the A-sections and is around 300 mm for the B-sections.

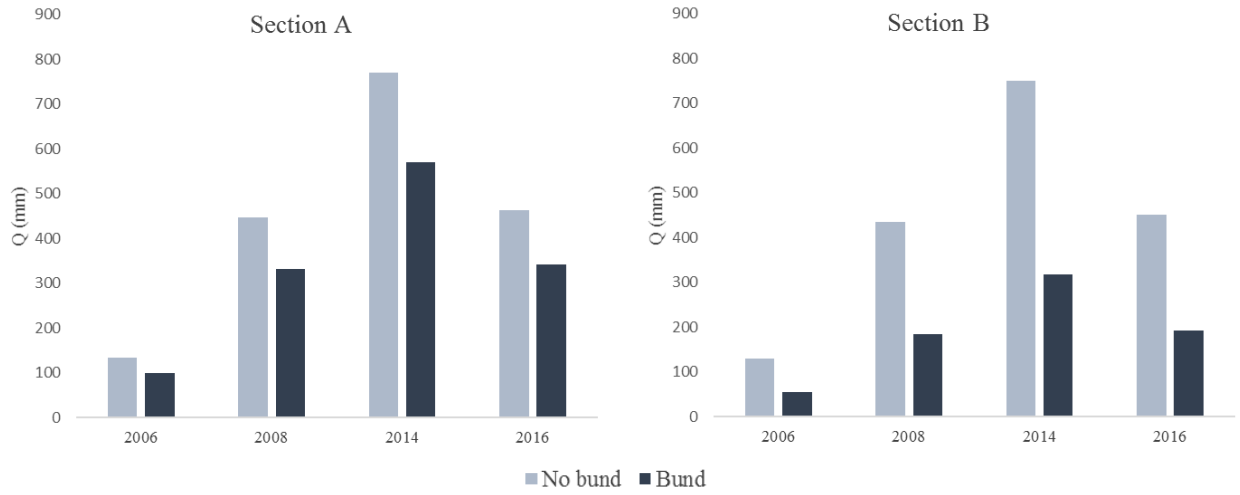

Figure 4-8. Annual runoff values (P4) for all of the modelled years, with and without the effect of the contour soil bunds.

The P-factors of the plots were multiplied with the C-factors in the rMMF model, to simulate the effect of bunds for each plot, and the decrease was computed for the three alternative years. Table 4-18 shows the annual soil losses with and without the new C-factors for bunds and the reduction in soil loss in percentage. Reductions for each plot for different years are almost equal. Slight variations occur for plot 1 and 2. For plot 1, differences occur because during high rainfall, section 1 can be limited by the sediment detachment rate instead of transport capacity, which results in a lower decrease, as the P-factor, and therefore the reduction by bunds, is not included in these months. This causes a maximum difference of 1.1%. For plot 2, differences occur due to the effect of larger variations in parameters MS and BD, which causes a maximum difference in decrease of 0.8%.

Table 4-18. Annual soil losses modelled in the rMMF model, with and without the new C-factors for bunds, for the driest, wettest and most average year and decrease, compared to 2016.

	2006			2014			2008			2016		
	NB Ton/ha	*B* Ton/ha	*Decrease* %	*NB* Ton/ha	*B* Ton/ha	*Decrease* %	*NB* Ton/ha	*B* Ton/ha	*Decrease* %	*NB* Ton/ha	*B* Ton/ha	*Decrease* %
P1	4.5	1.3	71.0	88.1	26.5	69.9	30.3	8.8	71.0	34.2	10.0	70.7
P2	4.8	1.7	64.2	97.4	34.1	65.0	32.2	11.4	64.6	36.7	12.9	64.8
P4	4.1	1.1	73.0	79.4	21.5	73.0	26.7	7.2	73.0	30.2	8.2	73.0
P6	4.0	1.4	66.0	81.4	27.7	66.0	27.1	9.2	66.0	30.8	10.5	66.0

5. Discussion

5.1 Field measurements

5.1.1 Experimental setting

Section 4.2 showed characteristics of the channel-bund system and appendix 9.2.3 showed the channel and jerrycan measurements. The channels could capture 10 to 35 times more runoff than the jerrycans. Apart from the fact that these channels contain a significantly larger volume, due to the middle bunds, the channels have to capture runoff from only half the area that the jerrycans have to collect. Although the filled channels were presumably the result of some successive rainfall events and the jerrycans were emptied each day, the jerrycans of the control plots were most likely not able to capture all the runoff from larger events. It should also be noted that over the months of the rainy season, new jerrycans were added, as experience showed that they kept overflowing, and that maximum volumes only applied from the 10th of August.

It should also be noted that the effect of the channel-soil bund system in this study was assumed to be 100%. In order to realize this in the field, bund maintenance is important. It often occurred that people (unintentionally) stepped on a bund, reducing its height, or rodents making their home into a bund, by digging small holes and channels.

5.1.2 Soil characteristics

According to Hurni et al., in 1988, between 40% and 70% of this region in the Ethiopian highlands had soil depths of 1.3 m and between 6% and 11% had soil depths of 0.1 m. His study also stated that soil depths in the Ethiopian highlands were originally more than 0.5 m deep and rooting depths exceeded 1 m. The soil depths and rooting depths found in this study were significantly lower, showing the severity of land degradation in this area.

Although most soil samples from the subplots were classified as loam, the soil moisture at field capacity, bulk density and cohesion values are all higher compared to the advised Morgan (2005, 2008) soil parameter values for loam. All soil parameters showed a larger resemblance to the soil type clay loam, but as can be seen in figure 4-3, these soil types are situated in a close range and deviations could be the result of a standard uncertainty between the USDA soil texture classification and field measurements. Concerning the K-value, there is not a significant difference between clay loam and loam.

5.1.3 Erosion and runoff assessment

In some subplots, no rills were found. This, of course does not necessarily mean that no erosion took place in those plots during fieldwork, as there were often small erosion features found. With the ACED method however, the erosion could not be determined, as it was not severe enough to form rills. Small plots represent large areas, which may not be realistic. Longer slopes can result in accumulation of runoff and erosion and therefore large erosion features can be created, which is not the case on small plots. This can be the reason why plot 3 showed the most erosion features. The ACED method contains an error of 15% to 30% (Herweg et al., 1996), where the error can

further decrease with increasing vegetation cover. It shows that visual erosion assessment with ACED is difficult to use as a reference for soil losses in the field and should mainly be used as a guideline to assess the actual field erosion.

Runoff coefficients remain difficult to determine, as is shown by literature and the large variations in measured sediment concentrations. Additionally, varying sediment concentrations are not only the result of the amount of runoff during an event, but also by the intensity of the rain. This brings another uncertainty to use sediment concentrations as a factor to determine the amount of runoff. Defersa & Melesse (2012) found an additional factor that influences the amount of sediment concentrations. Their study, held in a watershed in East Ethiopia, showed that sediment concentrations were generally lower with higher antecedent moisture contents of soils. The measured sediment concentrations of their study were a little under 20 g/L for wet soils, which is significantly higher than what was found in this study. Guzman et al. (2013) studied monthly sediment concentrations in combination with soil loss and runoff in three watersheds in the central Ethiopian highlands. Sediment concentrations in the study of Guzman et al. showed large variations, and averages of 20-30 g/L were found during the months before the rainy season and reduced sediment concentrations of around 10 g/L were found during the rainy season. Sediment concentrations in this study were measured during the rainy season, and shows slightly lower, yet similar sediment concentrations, with a total average of 6.5 g/L. Another study by Guzman et al. (2016) showed how sediment concentrations for close rainfall events contain large variations, as was observed with the sediment concentration measurements of this study.

5.2 Model

5.2.1 rMMF-HS performance

The rMMF-HS model was used for monthly runoff and to model the effect on runoff by bunds.
The model showed that the magnitude of the effect of the bund is dependent on the distance the bund is placed from the start of the hillslope and the amount of bunds required to capture all runoff, as after each bund, the runoff accumulation starts from zero again and therefore the effect is greater for bunds further downslope.
The rMMF-HS model provided consistent results when for the no-bund situation, there was a linear accumulation of runoff, meaning that soil moisture at field capacity and bulk density did not change over the section. This is because equation 16 takes into account the runoff of the previous section, and adds this to the runoff of the next section. With a constant SM and BD this results in a linear accumulation, but as soon as one or both of these parameters change, an inclination is created in the runoff accumulation slope. This inclination is not static. It changes when other parameters for the runoff equation change, such as rainfall, causing a different steepness in accumulation for section B. When the bunds are included in the rMMF-HS model, this causes monthly variation in the relative effects of bunds. Although variations in MS and BD causes inconsistencies in the rMMF-HS model, it is debatable whether a large change in MS and BD over a short length is presumable to occur in nature. In this study, variations caused by this effect were not larger than 2.7 %.

Hudek et al. (2014) used the rMMF-HS model for modelling erosion on a 50 m long hillslope with equal sections of 5 m, which showed good results. The rMMF-HS model in this study proved to be insufficient for modelling soil loss, where monthly values where too low. The rMMF-HS model also showed to be very sensitive to changes in slope length. Increasing the slope length by a few meters can cause an increase in erosion with a factor of 2.

Both the rMMF and rMMF-HS model showed significant differences between annual and monthly erosion modelling. This can be explained by the equation for the transport capacity (equation 13). The runoff creates a significant larger soil loss when the annual runoff is squared at once for calculating the transport capacity and smaller soil losses when runoff of each month is squared and the monthly transport capacities are summed. The rMMF model was originally created for predicting annual soil losses (Morgan, 2001), but monthly modelled soil losses proved to be more accurate with the findings in the field for this study. With a new equation for transport capacity, the rMMF and the rMMF-HS model could be applied on an annual as well as on a monthly basis.

5.2.2 Model results

Calibration with the rMMF-HS model was done twice, with two different runoff coefficients that were estimated from field measurements for the period of June to August. This resulted in an average annual runoff coefficient of 0.20 and 0.25. The maximum EHD depth that was found for the runoff coefficient of 0.25 was close to the advised EHD value of Morgan (2001) for bare soils on steep slopes. Although soil conditions in the study area were very poor, it is expected that there is some significant change in EHD depths between dry season and wet season. However, the soil losses that were modelled for the second calibration (Qc: 0.25), where slightly closer to the measured soil losses of the control plots, during the months June, July and August.

Annual soil losses modelled for this study on cultivated fields are comparable to the 42 ton/ha/yr that was estimated by Hurni et al. (1988). Modelled erosion by Tesfahunegn et al. (2014) in regions with similar slope steepness, mostly exceeded 40 ton/ha/yr, sometimes reaching close to 100 ton/ha/yr or higher. Runoff for these regions was modelled in the range of 200 mm to 380 mm. A study by Amare et al. (2014) in the Northwestern Ethiopian highlands, showed average annual soil losses for fields without SWC measured of 71 ton/ha combined with runoff of 302 mm. In this study, runoff in 2016 was modelled higher than the previous two mentioned studies, while erosion was lower.

The introduction mentioned the studies of Gebremichael et al. (2005), Nyssen et al. (2007) and of Meshesha et al. (2012), where reduction of soil losses by stone bunds were found to be 68% by the first two mentioned publications and 13% to 64% by Meshesha et al.
Adimassu et al. (2014) found an effect of contour soil bunds of 47% in Dendi Wereda, in the central highlands of Ethiopia. This study had a very similar experimental set up, but a slope of only 9% and no channels in front of the bunds. The effect of bunds modelled in this study are comparable to most decreases by bunds found in literature. Amare et al. (2014), found lower

decreases for soil losses by soil bunds, around 35% and reduction in runoff of around 15%. The soil loss reduction of 63% to 70% found in this study, is somewhat higher, but similar compared to findings of other studies. It should be noted that in this study, the channel-bund system was included in the model for each month of 2016, whereas the bunds in the experimental fields were not placed until April that year. Reduction by bunds in 2016 would therefore be lower in reality.

In this study, an average P-factor of 0.32 was found for the USLE method. Gebremichael et al. (2006) found an equal USLE P-factor of 0.32, for stone bunds in northern Ethiopia. If the USLE P-factor that was computed in this study was to be applied to other studies, it should be noted that the effect of the bunds are dependent on their position on the hillslope.

5.2.3 Sensitivity analysis and rainfall variability

The results of the sensitivity analysis were in line with the sensitivity analysis of the rMMF model by Morgan and Duzant (2008). It showed that especially rainfall and soil parameters influence the model output. The EHD value, which was calibrated using field measurements, showed to be of large significance to the model output as well. It shows that correct field measurements are of great importance to strive for optimal model results.

The sensitivity analysis method that was applied, regarded a change of 10% for all parameters. However, certain parameters will have a larger actual influence on the model because they have a larger natural variation than other parameters. For example, in this study the parameter BD varied more between sections than parameter SM, which resulted in a runoff that was more influenced by the changes in BD. More pronounced examples include the variability in rainfall and number of rain days.

When the rainfall and number of rain days of other years from the rainfall record were used, it was assumed that all the other parameters, except for evaporation, remained constant. However in reality, these parameters are strongly correlated and changing one single parameter value, while other parameter values remain constant, is not realistic.

6. Conclusion

This study was conducted in the southwestern highlands of Ethiopia, in the Bokole watershed, a region where agriculture provides the main economic income. This despite the poor soil conditions, with low organic matter content and measured soil depths below 20 cm, very steep slopes and heavy rainfall events during the rainy season. Not surprisingly, erosion is a common threat to local farmers, a problem that is confirmed by the findings of this study.

1. To determine the current erosion damage on fields with contour bunds

To assess soil loss and runoff on control plots, without SWC measures

Sediment concentrations varied strongly, from 0 g/L to 26 g/L, which is most likely the result of difference in rainfall intensity. Most sediment concentrations were found in the range between 4-6 g/L. From the ACED erosion assessment, measured sediment concentrations and literature, it was expected that during the months June to August, on average between 23% and 31% of the rainfall became runoff.

During the months June, July and August, erosion were estimated with the ACED method, where CP3 and CP5 were taken as one plot. Soil losses were measured to be 8.6 ton/ha,.

With the combined use of the sediment concentrations and the ACED erosion assessment, the average runoff coefficient could be computed for the period of June up to August. Because of the larger variety between sediment concentrations, two values were taken to calculate the runoff coefficient. The average of all sediment concentrations, 6.47 g/L, resulted in a runoff coefficient of 0.23 and the average of the middle range in the sediment concentrations, 5.21 g/L, resulted in a runoff coefficient of 0.31. This means that during the months June, July and August, between 136 mm and 183 mm of runoff was generated on the control plots.

To assess soil loss on land with stone bunds

Average erosion on the field with stone bunds was expected to be 23.4 ton/ha during the end of April or early May to half of August. Rainfall during this period was either around 650 mm or 700 mm, depending on start of field abandonment. In a period of ten days, during which 99 mm of rain fell, 5.1 ton/ha of soil loss was estimated.

Overall, longer and wider rills were found on the field with stone bunds compared to the experimental field with soil bunds and the control plots, as these features were older than on the experimental field. During the assessment of the field with stone bunds. it was visible that stone bunds did not block all of the surface water, as the water created erosion features incising through the bunds, indicating poor maintenance of the stone bunds.

To assess soil loss on land with soil bunds

Soil losses on the plots with bunds showed varying results, where plot 1 and plot 6 did not contain measurable erosion features. The lower section of plot 2 contained many features, resulting in a measured soil loss of approximately 30.0 ton/ha for the whole plot. For plot 4, the upper section contained no erosion features, whereas for the lower section, 3.50 ton/ha was measured for the period of June up to August.

Both control plots contained visual erosion features, whereas from the plots with bunds, plot 2B and 4B contained erosion features as well. Overall, B-plots were more vulnerable to erosion, due to their slope steepness in combination with greater plot lengths. In general, the control plots contained the most erosion features, with the exception of plot 2B, which contained the most erosion of all (sub)plots. It shows that slope steepness remains an important factor to erosion. This is emphasized by the fact that field 1 did not contain measurable erosion features and that the average slope of the lower sections of this field was 3º less than for field 2.

2. To quantify the effect of contour soil bunds as a SWC measure, using the rMMF model

To comprehend overland water and sediment transport under natural and interfered conditions

Calibration with the rMMF-HS model was done twice, with the two runoff coefficients that were estimated from field measurements for the period of June to August. This resulted in an average annual runoff coefficient of 0.20 and 0.25. For the first calibration (Avg Qc: 0.20) between 400 mm and 500 mm of runoff was modelled for the control plots. For the second calibration (Avg Qc: 0.25) volumes of over 580 mm were modelled for the control plots. The rMMF model was used to compute monthly soil losses. Both calibrations showed good results, compared to the measured ACED soil losses of 8.6 ton/ha, for the months Jun, July and August. The first calibration showed losses for the control plots between 5.7 ton/ha for CP3 and 6.2 ton/ha for CP5. The second calibration gave slightly better results, with soil losses of 7.5 ton/ha for CP3 and 8.1 ton/ha for CP5 during the same months. Annual losses for the year 2016 were modelled around 36.8 ton/ha/yr and 41.9 ton/ha/yr for the first calibration and 40.5 ton/ha/yr and 44.0 ton/ha/yr for the second calibration.

The model showed that the bund after the first section caused a decrease in runoff between 20% to 30% and that the effect of the second bund for section B is around 50%. The main difference in effect of the bund is caused by its distance towards the uphill beginning of the slope. The parameters MS and BD, caused some minor variations in monthly runoff calibrations.

The model showed that bunds can decrease erosion by 63% to 70%, which coincides with an average USEL P-factor of 0.34. The predicted rMMF C-factor on fields with contour soil bunds during maize growth were between 0.10 and 0.13 for this study area.

To comprehend the effects of rainfall variability on erosion

For the modelled year 2014, containing the most amount of rainfall in the record, soil losses exceeded 91 ton/ha, whereas the driest year from the record, 2006, did not reach 5 ton/ha. Peaks, where high rainfall amounts occur in just one month can often be the cause for more than half of the total annual erosion. Annual runoff between 2006 and 2014, modelled in the rMMF-HS model, showed a difference of around 600 mm for fields without bunds. In case of bunds, the difference in runoff is still predicted between 300 mm and 500 mm. The model results clearly show the effect of the stochastic behaviour of rain and its intensity to runoff and erosion.

Recommendations

It remains difficult to provide a conclusive answer on the effect of bunds on soil losses from the field measurements. To improve knowledge about erosion in the study area and model results, a better system should be set up to assess soil erosion in the field. To capture all the runoff of big events, a larger system is required than the jerrycans that are currently placed, or a smaller area should be enclosed to capture runoff. If runoff and soil losses can be more accurately measured, it would give a better insight of the severity of the erosion in the study area and the effects of measures can be studied more precisely. To further enhance field data, more frequent measures should be taken, preferentially after each rainfall event, where the rainfall intensity can be studied as well. More test plots are desirable, maybe on a larger scale, where gradual variations in soil moisture, bulk density and slope steepness can be studied better in the field.

Farmers should maintain their bunds as much as they can, to make sure the effect of the bunds is at maximum capacity. To capture all runoff, bunds should be placed regularly after several meters, or channels are more likely to flood. Slope steepness remains a large threat to soil conservation, even when SWC measures such as bunds are placed. It is wise to place contour bunds more frequently when slope steepness increases.

An adapted version of the rMMF model, that divides the hillslope in sections was combined with the conventional rMMF model. Unfortunately, the adapted rMMF model could not be used for computing soil losses, because in the transport capacity equation, runoff is squared, causing extreme differences between sections of different length. To include the accumulation of runoff over length, the function might be used when sections of equal lengths are used, however, the best option would be to transform the transport capacity function into a function where the sediment transport is not directly related to the squared runoff.

7. References

Abedinpour, M., Sarangi, A. Rajput, T.B.S., Singh, M., Pathak, H. & Ahmad, T.(2012) Performance evaluation of AquaCrop model for maize crop in a semi-arid environment. Agricultural Water Management, 110, 55-66.

Adimassu, Z., and Haile, N.(2011). Runoff, soil loss and their relationships under different land uses in the central highlands of Ethiopia. *Ethiopian Journal of Applies Sciences & Technology*, 2, p. 39-49.

Adimassu, Z., Mekonnen, K., Yirga, C. & Kessler, A.(2014). Effect of soil bunds on runoff, soil and nutrient losses and crop yield in the central highlands of Ethiopia. *Land Degradation and Development*, 25(6), 554-564.

Alemayehu, M. (2006). *Country pasture/forest resource profiles: Ethiopia*. FAO.

Alemayehu, M., Yohannes, F. & Dubale, P.(2006). Effect of indigenous stone bunding on crop yield at Mesobit-Gedeba, North Shoa, Ethiopia. *Land Degradation and Development*, 17(1), 45-54.

Alemayehu, M., Amede, T., Böhme, M., Peters, K.J.(2013). Collective management on communal grazing lands; its impact on vegetation attributed and soil erosion in the upper Blue Nile basin, northwestern Ethiopia. *Livestock Science*, 157, p. 271-279.

Allen, R.G.(2000). Using the FAO-56 dual crop coefficient method over an irrigated region as part of an evapotranspiration intercomparison study, *Journal of Hydrology*, 229(1-2), 27-41.

Amare, T., Zegeve,. A.D. Yitaferu, B., Steenhuis, T.S.., Hurni H. & Zeleke, G.(2014). Combined effect of soil bund with biological soil and water conservation measures in the northwestern Ethiopian highlands, *Ecohydrology & Hydrobiology*, 14(3), 192-199.

Amend, I.G.(2005). Irrigation guide: crops, *USDA: NRCS*, NJ3-1-NJ3-7, New Jersey.

Asfaw, A., Almekinders, C.J., Struik, P.C. & Blair, M.W.(2013). Farmers‘ common bean variety and seed management in the face of drought and climate instability in southern Ethiopia. *Scientific Research and Essays*, 8(22), 1022-1037.

Beretta, A.N., Silbermann, A.V., Paladino, L., Torres, D., Kassahun, D., Musselli, R. & Lamohte, A.G.(2014). Soil texture analyses using a hydrometer: modification of the Bouyoucos method. *Ciencia e investigacion agraria* 41(2), 263-271.

Biratu, A.A. & Asmamaw, D.K.(2016). Farmers‘ perception of soil erosion and participation in soil and water conservation activities in the Gusha Temela watershed, Arsi, Ethiopia. *International Journal of River Basin Management*, 1-10.

Bossio, D., Erkossa, T., Dile Y., McCartney, M., Killiches, F., Hoff, H.(2012). Water implications of foreign direct investment in Ethiopia's agricultural sector, *Water Alternatives*, 5(2), 223-242.

ClimaTemps.(2009). *Sunshine and daylight hours in Addis Ababa, Ethiopia*, consulted on 6 December 2016, from: http://www.addis-ababa.climatemps.com/sunlight.php

Defersha, M.B. & Melesse, A.M.(2012). Effect of rainfall intensity, slope and antecedent moisture content on sediment concentration and sediment ratio, Catena, 90, 47-52.

Dejene, A.(2003). Integrated natural resources management to enhance food: The community based approach in Ethiopia. *Food and Agriculture Organization (FAO) of the UN*, 16.

Descheemaeker, K., Nyssen, J., Poesen, J., Raes, D., Haile, M., Muys, B. Deckers, S.(2006). Runoff on slopes with restoring vegetation: a case study from the Tigray highlands Ethiopia. *Journal of Hydrology*, 331, p. 219-241.

EPA.(2012). National report of Ethiopia. *The United Nations Conference on Sustainable Development*: Rio, 20.

Evans, R.O., Cassel, D.K. & Sneed, J.(1996). Soil, water and crop characteristics important to irrigation scheduling. *AG-North Carolina Agricultural Extension Service, North Carolina State Univerisity*.

Estefan, G., Sommer, R, Ryan, J.(2013). *Methods of soil, plant and water analysis: A manual for the West Asia and North Africa region.* (third edition), 32-34, Lebanon: ICARDA.

FAO.(1986). Ethiopian highlands reclamation study. *Food and Agriculture Organization (FAO)*.

FAO.(2017). *Crop information; Maize*, consulted on: 3 February 2017, from: http://www.fao.org/land-water/databases-and-software/crop-information/maize/en/

Gebreegziabher, T., Nyssen, J., Govaerts, B., Getnet, F., Behailu, M., Haile, M. & Deckers, J.(2009). Contour furrows for in situ soil and water conservation, Tigray, northern Ethiopia. *Soil and Tillage Research*, 103(2), 257-264.

Gebregziabher, G. Rebelo, L.M. & Langan, S.(2015). Interdependence in rainwater management m*Environment, Development and Sustainability*, 8(2), 1-18.

Gebremichael, D., Nyssen, J., Poesen, J., Deckers, J., Haile M., Govers, G. & Moeyersons, J.(2005). Effectiveness of stone bunds controlling soil erosion on cropland in the Tigray highlands, northern Ethiopia. *Soil Use and Management*, 21(3), 287-297.

Guzman, C.D., Tilahun, S.A., Zegeve, A.D. & Steenhuis, T.S.(2013). Suspended sediment concentration-discharge relationships in the (sub)- humid Ethiopian highlands, Hydrology and Erath System Sciences, 17(3), 1067-1077.

Guzman, C.D., Zimale, F.A., Tebebu, T.Y., Bayabil, H.K., Tilahun, S.A., Yitaferu, B.,… & Steenhuis, T.(2016). Modeling discharge and sediment concentrations after landscape interventions in a humid monsoon climate: the Anjeni watershed in the highlands of Ethiopia, *Hydrological Processes*, 31(6), 1239- 1257.

Haile, M., Herweg, K. & Stilihardt, B.(2006). Sustainable land management: a new approach to soil and water conservation in Ethiopia. *Land Resources Management and Environmental Protection Department, Center for Development and Environment (CDE) and Swiss National Center of Competence in Research (NCCR).*

Hendriks, M.R.(2010). *Introduction to physical hydrology*. Utrecht University: Oxford University press.

Hengsdijk, H., Meijerink, G.W. & Mosugu, M.E.(2005). Modelling the effect of three soils and water conservation practices in Tigray, Ethiopia. *Agriculture, Ecosystems and Environment*, 105(1), 29-40.

Herweg, K.(1996). *Field manual for assessment of current erosion damage*. University of Berne: Soil and Conservation Research Programme and Centre for Development and Environment of Geographica Bernensia, Ethiopia.

Herweg, K. & Ludi, E.(1999). The performance of selected soil and water conservation measures: case studies from Ethiopia and Eritrea. *Catena*, 36(1), 99-114.

Hudek, C., Sterk, G., van Beek, R.L. & de Jong, S.M.(2014). Modelling soil erosion reduction by Mahonia aquifolium on hillslopes in Hungary: The impact of soil stabilization by roots. *Catena*, 122, 159-169.

Hurni, H.(1988). Degradation and conservation of the resources in the Ethiopian highlands. *Mountain Research and Development*, 8(2), 123-130.

IRENA.(2008-2010).*Wind atlases by CENER*, consulted on 2 February 2017, from: http://irena.masdar.ac.ae/#

Kidane, D. & Alemu, B.(2015). The effect of upstream land use practices on soil erosion and sedimentation in the Upper Blue Nile basin, Ethiopia. Research Journal of Agriculture and Environmental Management, 4(2), 55-68.

Law, B.E. and Warning, R.H.(1994). Remote sensing of leaf area index and radiationintercepted by understory vegetation, *Ecological applications*, 4(2),p. 272-279

Lukeba, J.C.L., Vumilia, R.K., Nkongolo K.C.K., Mwabila, M.L., Tsumbu, M. (2013). Growth and leaf area index simulation in maize (Zea mays L.) under small-scale farm conditions in a Sub-Saharan African region. *American Journal of Plant Sciences*, 4, 575-583.

Liu, J. & Pattey, E.(2010). Retrieval of leaf area index from top-of-canopy photography over agricultural crops. *Agricultural and Forest Meteorology*, 150, 1485-1490.

Mejía, D.(2003). *Maize: Post-Harvest Operation organisation: Food and Agriculture Organization of the United Nations (FAO)*, consulted on May 5 2017: http://www.fao.org/fileadmin/user_upload/inpho/docs/Post_Harvest_Compendium_-_MAIZE.pdf

Meshesha, D.T., Tsunekawa, A., Tsubo, M. & Haregeweyn, N.(2012). Dynamics and hotspots of soil erosion and management scenarios of the Central Rift Valley of Ethiopia. *International Journal of Sediment Research*, 27(1), 84-99.

Moges, A. & Holden, N.M.(2007). Farmers' perceptions of soil erosion and soil fertility loss in southern Ethiopia. *Land Degradation and Development*, 18(5), 543-554.

Morgan, R.P.C.(2001). A simple approach to soil loss prediction: a revised Morgan- Morgan-Finney model. *Catena*, 44(4), 305-322.

Morgan, R.P.C. (2005). *Soil Erosion and Conservation*, Oxford: Blackwell Publishing. Third edition.

Morgan, R.P.C. & Duzant, J.H.(2008). Modified MMF (Morgan-Morgan-Finney) model for evaluating effects of crops and vegetation cover on soil erosion, *Earth Surface Processes and Landforms*, 33(1), 90-106.

Mouazen, A.M., Ramon, H., & de Baerdemaekter, J.(2002). SW- Soil and Water: Effects of bulk density and moisture content on selected mechanical properties of sandy loam soil. *Biosystems Engineering*, 83(2), 217-224.

Nyssen, J., Poesen, J., Geremichael, D., Vancampenhout, K., D' aes, M., Yihdego, G.,… & Haregeweyn, N.(2007). Interdisciplinary on-site evaluation of stone bunds to control soil erosion on cropland in northern Ethiopia. *Soil and Tillage Research*, 94(1), 151-163.

Ogolo, E.O.(2014). The comparative analysis of performance evaluation of recalibrated reference evapotranspiration models for different regional climatic conditions in Nigeria. *Ife Journal of Science*, 16(2), 191-210.

Pekin, B and Macfarlane, C.(2009). Measurement of crown cover and leaf area index using digital cover photography and its application to remote sensing, *Remote Sensing*, p.1298-1320.

Raes, D., Stedutro, P., Hsiao, T.C., Fereres, E.(2010). *AquaCrop version 3.1 reference manual chapter 3: calculation procedures*. Rome, Italy: FAO.

Raes, D., Stedutro, P., Hsiao, T.C., Fereres, E.(2012). *AquaCrop version 4.0 reference manual Annex I*. Rome, Italy: FAO.

Robock, A., Vinnikov, K.Y., Srinivasan, G., Entin, J.K., Hollinger, S.E., Speranskaya, N.A., …& Namkhai, A.(2000). The global soil moisture data bank. Bulletin of the American Meteorlogical Society, 81(6), 1281-1299.

Rose, C.W.(2004). *An introduction to the environmental physics of soil, water and watersheds*. United Kingdom: Cambridge University press.

Taddese,G.(2001). Land degradation: a challenge to Ethiopia. *Environmental management*, 27(6), 815-824.

Tefera, B., Sterk, G. & Yaekob, T. (2006). Erosion and sedimentation modelling in Fincha's watershe, western Ethiopia. *Tropical Research Management Papers*, 75, 47-68.

Tesfahunegn, G.B., Tamene L., Vlek, P.L.G.(2014). Soil erosion prediction using the Morgan-Morgan-Finney model in a GIS based environment in northern Ethiopia catchment. *Applied Environmental Soil Science*, Vol. 2014, p. 1-15.

Teshome, A., Rolker, D. & de Graaff, J.(2013). Financial viability of soil and water conservation technologies in northwestern Ethiopian highlands. *Applied Geography*, 37, 139-149.

UNCT. (2001). Contributing towards reducing absolute poverty in Ethiopia: 2002-2004. *United Nations Development Assistance Framework (UNDAF).*

Vancampenhout, K., Nyssen, J., Gebremichael, D., Deckers, J., Poesden, J., Haile, M. & Moeyersons, J.(2006). Stone bunds for soil conservation in the northern Ethiopian highlands: Impacts on soil fertility and crop yield. *Soil and Tillage Research*, 90(1), 1-15.

Vereecken, H., Maes, J., Feyen, J., & Darius, P.(1989). Estimating the soil moisture retention charachteristic from texture, bulk density, and carbon content. *Soil Science*, 148(6), 389-403.

Vose, J.M., Sullivan, N.H., Clinton, B.D. and Bolstad, P.V.(1995). Verical leaf area distribution, ligh transmittance, and application of the Beer-Lamber Law in four mature hardwood stands in the southern Appalachins, *Can. J. For. Res*, 25, p. 1036-1043

Wolka, K., Moges, A., & Yimer, F.(2011). Effects of level soil bunds and stone bunds on soil properties and its implications for crop production: the case of Bokole watershed, Dawuro zone, Southern Ethiopia. *Agricultural Sciences*, 2(3), 257-363.

Wolka, K., Sterk, G., Moges, A.,Yimer, F., de Jong, S.M.(In press). The effect of contour bunds on soil properties and crop production in the Bokole watershed, Dawuro zone, SOuthwest Ethiopia. *Land degradation and development.*

8. Acknowledgements

First, I would like to thank Geert Sterk, for providing the opportunity to make a master thesis such a special experience and for his help during the beginning of the project, steering us into the right direction, and further on the way. I would like to thank Rens van Beek for taking over the task of being our supervisor and for all his advice that improved my thesis. And I want to thank Imke, for her help during the fieldwork; joining me during the endless days of filtering sediment, staying awake until I safely returned from the nightly toilet visits in Ela and especially for her infinite optimism.

In Ethiopia, our supervisor Kebede Wolka supported us for study-related issues, but he was also the person who showed us the day to day life in and around Wondo Genet and introduced us to his lovely family. I would like to thank him for his devotion and hospitality. I would like to thank Asfaw for all the times he accompanied us to Gessa, either to go to the hospital for eye drops or to buy tomatoes on the market and protect us from eagerly interested children. And of course, for his help in the field, working with us and being our translator. A special thanks to his wife, Birre, for making all our meals during our stay in Ela; even though our food preferences must have seem quite strange to everyone, we appreciate every meal that was made for us. And I would like to thank Dubalei, Chondu and Arja for their help and hospitality in the field and for all the muz (bananas) and avocados. The coffee ceremony in the field was also a very nice gesture.
During the work in the laboratory, we could always count on Tizazu, for help and advice, or just for some small-talk when there was no electrical power to work with – which was quite often. And then finally, I would like to thank Alex for driving us safely over the not so safe roads and for the enthusiasm he brings wherever he goes.

For the moral support, I have to thank Imke again. I am happy we encountered this adventure together and I know we will always share some special memories. Also my parents, Marc and Miriam and my sister Alannah, thank you for either comforting or pushing me whenever I needed it.

9. Appendix

9.1 Soil texture determination: hydrometer method

A dissolution of 40gr sodiumhexamethaphosphate and 10gr sodiumcarbonate anhydrous in 1L distilled water was used as an dispersion agent for soil particles. 100ml of this dissolution was added to the soil samples and were mechanically shaken for 3 hours, with a speed of 180 osc/min, to break the aggregates. Then, the mixtures were stirred for five minutes with distilled water and put in cylinders, that were all filled with distilled water to create equal volumes of 1L. The cylinders were shaken vigorously by hand for 30 seconds, to suspend all particles, and placed on a flat surface.

Sand particles deposit after 40 sec:

$$Sand\ (\%\ wt) = 100 - (d_1 + T_1CF - B)\ \frac{100}{50} \qquad 29$$

d_1 is the hydrometer reading value after 40 seconds, T_1CF is the temperature correction factor after 40 seconds (table 8-1) and B is the blank hydrometer reading of only the dispersion agent (ml), as the dispersion agent contains a density of its own.

Clay particles deposit after 2 hours:

$$\%\ clay = (d_2 + T_2CF - B)\ \frac{100}{50} \qquad 30$$

Where d_2 is the hydrometer value for clay and T_2CF is the temperature correction for the temperature after two hours.

Percentage silt particles:

$$\%\ silt = 100\% - (\%sand + \%clay) \qquad 31$$

Table 8-1: Temperature correction factors, derived from ICARDA (Estefan et al. 2013).

T (ºC)	TCF (-)
19	-0.4
20	0
21	0.4
22	0.8
23	1.2
24	1.6
25	2.0

9.2 Field 2 plot characteristics

9.2.1 Plot characteristics

Plot measurements, done in August. Lengths are measured from bund to bund.

	GPS COORDINATES	HEIGHT *m*	ACCURACY *m*	LENGTH *m*	WIDTH *m*	AREA m^2
Plot 1a	37N 0312088 UTM 0771652	1751	7.8	4.6	6.3	26
Plot 1b	37N 0312081 UTM 0771647	1749	8.7	9.1	5.3	47.5
Plot 2a	37N 0312086 UTM 0771643	1750	7.9	4.9	6.1	29.4
Plot 2b	37N 0312077 UTM 0771642	1747	9	9	6.4	55.4
Plot 3a	37N 0312087 UTM 0771636	1750	7.3	21.5	5.8	188.7
Plot 3b	37N 0312077 UTM 0771630	1748	9.3		11.8	
Plot 4a	37N 0312095 UTM 0771625	1750	10.9	6.2	5.8	51.6
Plot 4b	37N 0312092 UTM 0771617	1750	8.4	7.8	17.6	111.2
Plot 5a	37N 0312104 UTM 0771625	1747	8.5	6.25	5.9	36.7
Plot 5b	37N 0312107 UTM 0771620	1743	9.3	7	10.3	71.8
Plot 6a	37N 0312112 UTM 0771638	1746	11.3	6.1	10	57.2
Plot 6b	37N 0312112 UTM 0771623	1739	11.3	10.3	13.6	115.1

9.2.2 bund characteristics

Measurements of the bunds in field 2 in August. Bund 1 is the upper bund, bund 2 is the middle bund, between section A and B, and bund 3 is the lower bund.

		Plot 1	Plot 2	Plot 4	Plot 6
Bund 1	length	6.25	6.10	5.75	10.00
	height downslope	0.45	0.53	0.40	0.28
	height upslope	0.22	0.28	0.27	0.21
	bottom width	1.45	1.80	1.74	1.25
	top width	0.23	0.35	0.35	0.28
	channel depth	0.44	0.51	0.54	0.36
	channel width	0.48	0.49	0.43	0.39
	vegetation	no	no	no	no
	seedlings	yes	no	no	yes
	Note			stony	stony
Bund 2	length	5.20	5.90	10.90	8.75
	height downslope	0.65	0.54	0.32	0.39
	height upslope	0.19	0.06	0.08	0.19
	bottom width	1.75	1.43	1.17	1.4
	top width	0.23	0.34	0.38	0.3
	channel depth	0.36	0.40	0.40	0.34
	channel width	0.42	0.45	0.50	0.42
	vegetation	no	yes	yes	no
	seedlings	yes	no	no	yes
	Note	stony			
Bund 3	length	5.25	6.4	17.6	13.6
	height downslope	-	-	-	-
	height upslope	0.015	0.08	0.14	0.088
	bottom width	1.05	0.95	1.05	0.92
	top width	0.425	0.4	0.3	0.346
	channel depth	0.335	0.33	0.408	0.365
	channel width	0.41	0.55	0.51	0.48
	vegetation	yes (0.3%)	yes (0.3%)	no	no
	seedlings	yes	no	no	yes
	note				

9.2.3 Channel and jerrycan volumes

The volumes of channels were calculated and converted to mm using the area above the channel. The jerrycan volumes of the two control plots were also calculated.

		m^3	L	mm
P1	Channel 2	0.78	782	29.7
	Channel 3	0.71	714	15.0
P2	Channel 2	1.05	1051	35.7
	Channel 3	1.16	1156	20.9
P4	Channel 2	2.21	2209	42.8
	Channel 3	3.69	3692	33.2
P6	Channel 2	1.26	1259	22.0
	Channel 3	2.40	2395	20.8
CP3	Jerrycans	0.23	230	1.2
CP5	Jerrycans	0.15	150	1.4

9.3 Maize cycle parameters

9.3.1 Maize cycle stages of field 2 2016

Stage	SOWING DATE	EMERGENCE	VEGETATIVE STATE	FLOWERING	FULLY FLOWERING	MATURITY	HARVEST
Date	25-3-2016	31-3-2016	23-4-2016	31-5-2016	22-6-2016	31-7-2016	1-10-2016

9.3.2 Canopy Cover gained from Photoshop and the Greencroptool.

Maximum canopy cover (CC_x) for field 1 in August calculated with the greencroptool.

Plot	*Picture*	*Gap frac. (%)*	*CC_x (%)*	*Plot*	*Picture*	*Gap frac. (%)*	*CC_x (%)*	*Plot*	*Picture*	*Gap frac. (%)*	*CC_x (%)*
1a	Average	46.23	53.77	**2a**	Average	40.77	59.24	**3a**	Average	44.14	51.86
	7524	49.4	50.60		7548	39.46	60.54		7585	41.9	58.10
	7526	48.52	51.48		7550	43.1	56.90		7586	61.7	38.30
	7527	49.71	50.29		7551	30.8	69.20		7588	33.32	66.68
	7528	33.6	66.40		7553	49.7	50.30		7590	39.65	60.35
	7529	49.93	50.07						7591	64.12	35.88
1b	Average	52.74	47.26	**2b**	Average	58.96	41.04	**3b**	Average	53.43	46.57
	7534	49.08	50.92		7564	49.27	50.73		7596	65.73	34.27
	7538	55.5	44.50		7565	51.371	48.63		7597	43.53	56.47
	7539	56.17	43.83		7569	68.7	31.30		7599	57.3	42.70
	7541	50.21	49.79		7570	55.51	44.49		7600	61.64	38.36
					7571	68.81	31.19		7601	56.46	43.54
					7572	67.56	32.44		7602	56.6	43.40
					7574	51.5	48.50		7603	49.67	50.33
									7604	46.37	53.63
									7605	44.36	55.64
									7608	48.1	51.90
									7609	58.015	41.99
Plot 4a	Average	47.54	52.46	**Plot 5a**	Average	56.84	43.16	**Plot 6a**	Average	54.55	45.45
	7614	48.14	51.86		7641	57.25	42.75		7673	56.67	43.33
	7616	58.6	41.4		7642	52.66	47.34		7675	56.5	43.5
	7617	48.06	51.94		7643	71.85	28.15		7676	46.78	53.22
	7619	37.8	62.2		7647	48	52		7677	56.96	43.04
	7620	45.08	54.92		7648	49.03	50.97		7678	52.55	47.45
					7649	62.27	37.73		7682	48.53	51.47
									7683	63.86	36.14
Plot 4b	Average	56.22	43.78	**Plot 5b**	Average	59.41	40.59	**Plot 6b**	Average	59.30	40.70
	7625	52.52	47.48		7654	55.93	44.07		7685	44.61	55.39
	7626	53.33	46.67		7655	46.9	53.1		7686	59.31	40.69
	7627	61.47	38.53		7656	57.43	42.57		7687	55.66	44.34
	7629	59.21	40.79		7657	71.07	28.93		7688	61.67	38.33
	7630	60.41	39.59		7658	64.3	35.7		7690	53.6	46.4
	7631	46.71	53.29		7661	59.49	40.51		7691	64.69	35.31
	7632	50.7	49.3		7662	65.63	34.37		7692	65.81	34.19
	7633	60.72	39.28		7666	53.75	46.25		7693	55.94	44.06
	7634	42.27	57.73		7667	60.18	39.82		7694	57.69	42.31
	7637	54.06	45.94						7695	65	35
	7638	65.57	34.43						7697	50.85	49.15
	7639	67.68	32.32						7700	71.85	28.15
									7701	64.25	35.75

Canopy cover field 2 in August, calculated with Photoshop 2017. Percentages in white is equal to canopy cover.

Plot	*Picture*	*%Black*	*%White*	*Plot*	*Picture*	*%Black*	*%White*	*Plot*	*Picture*	*%Black*	*%White*
Plot 1a	Average	68,45	31,12	**Plot 2a**	Average	52,51	45,40	**Plot 3a**	Average	61,90	37,06
	7799	48,27	51,73		7788	31,86	63,86		7776	49,73	50,27
	7800	63,19	36,12		7789	55,5	41,83		7777	71,37	28,63
	7801	70,83	28,71		7790	45,72	52,93		7779	64,59	32,27
	7802	76,25	23,64		7791	66,41	32,25				
	7803	83,71	15,39		7792	63,08	36,12				
Plot 1b	Average	63,80	36,07	**Plot 2b**	Average	65,52	33,14	**Plot 3b**	Average	69,18	30,82
	7805	68,09	31,37		7793	71,08	24,89		7780	73,4	26,60
	7806	73,25	26,75		7794	59,72	40,28		7782	66,24	33,76
	7807	43,7	56,3		7795	54,6	45,4		7783	65,68	34,32
	7808	70,14	29,86		7796	69,24	30,76		7784	61,69	38,31
					7797	65,31	34,69		7785	78,88	21,11
					7798	73,17	22,83				
Plot 4a	Average	75,27	25,55	**Plot 5a**	Average	72,07	28,62	**Plot 6a**	Average	67,49	32,51
	7762	82	18		7742	66,86	33,14		7727	69,15	30,85
	7763	78,21	21,79		7743	73,13	26,87		7728	69,19	30,81
	7764	70,04	29,96		7744	61,93	38,07		7730	73,05	26,95
	7766	73,99	26,01		7745	79,69	20,31		7732	60,67	39,33
	7768	72,1	31,98		7746	78,76	21,24		7734	65,38	34,62
					7747	67,91	32,09				
Plot 4b	Average	71,66	29,76	**Plot 5b**	Average	72,67	27,33	**Plot 6b**	Average	67,15	32,85
	7769	71,59	28,41		7748	75,14	24,86		7735	79,13	20,87
	7770	68,16	31,84		7750	55,37	44,63		7737	74,15	25,85
	7771	74,89	25,11		7752	64,11	35,89		7738	57,94	42,06
	7773	79,92	27,14		7753	86,36	13,64		7739	59,88	40,12
	7774	63,72	36,28		7756	79,69	20,31		7740	64,64	35,36
					7758	75,35	24,65				

Canopy cover field 2 in October, at day of harvest, calculated with Photoshop 2017.

Plot	*Picture*	*%black*	*%white*	*Plot*	*Picture*	*%black*	*%white*	*Plot*	*Picture*	*%black*	*%white*
Plot 1a	Average	87,27	12,73	**Plot 2a**	Average	77,81	22,19	**Plot 3a**	Average	81,55	18,35
	8500	88,88	11,12		8523	84,7	15,3		8549	79,35	20,65
	8501	89,15	10,85		8524	88,7	11,3		8551	78,23	21,77
	8502	83,78	16,22		8525	65,64	34,36		8552	89,37	10,13
					8528	71	29		8554	79,04	20,96
					8529	79,02	20,98		8555	81,74	18,26
Plot 1b	Average	86,28	13,72	**Plot 2b**	Average	83,48	16,52	**Plot 3b**	Average	89,69	10,31
	8511	82,37	17,63		8535	77,31	22,69		8561	83,25	16,75
	8512	91,4	8,6		8539	85,92	14,08		8563	87,5	12,5
	8514	81,04	18,96		8542	74,98	25,02		8565	94,68	5,32
	8515	90,32	9,68		8543	86,08	13,92		8573	90,83	9,17
					8545	93,1	6,9		8582	92,18	7,82

Plot	*Picture*	*%black*	*%white*	*Plot*	*Picture*	*%black*	*%white*	*Plot*	*Picture*	*%black*	*%white*
Plot 4a	Average	88,36	11,65	**Plot 5a**	Average	81,13	18,10	**Plot 6a**	Average	82,15	17,85
	8592	95,87	4,13		8640	98,68	1,32		8682	91,87	8,13
	8593	88,57	11,43		8641	81,31	18,69		8684	91	9
	8596	84,58	15,42		8642	90,7	9,3		8685	78,73	21,27
	8597	84,4	15,6		8647	73,33	25,56		8686	84,07	15,93
	8600	90,72	9,28		8648	78,76	19,91		8687	76,61	23,39
					8650	81,54	17,05		8690	70,61	29,39
Plot 4b	Average	84,47	15,53	**Plot 5b**	Average	84,66	15,34	**Plot 6b**	Average	80,32	19,68
	8607	89,88	10,12		8659	83,35	16,65		8707	73,63	26,37
	8608	79,12	20,88		8660	85,75	14,25		8708	70,71	29,29
	8609	91,41	8,59		8664	87,04	12,96		8710	85,84	14,16
	8614	85,25	14,75		8667	92,64	7,36		8711	84,47	15,53
	8628	83,65	16,35		8670	85,44	14,56		8715	86,94	13,06
	8631	77,49	22,51		8676	73,73	26,27				

Camera specifics

Brand	Canon IXUS 230 HS	
Sensor size	6,16 x 4,62	mm
Sensor horizontal size	6,16	mm
Focal length min	5	mm
Focal length max	40	mm
Camera looking angle	57d5	picture taken at a slant angle of 57.5 degrees
	nadir	picture taken vertically towards the ground

Parameter setup greencroptool

Camera looking direction	down	
Camera looking angle	57d5	
Sensor horizontal size	6,16	mm
Range of angle	5	degrees
Focal length	5	mm

Statistics

Average (CCx F1):	47,16	%
Maize denisty F1	46042	
Maize denisty F2	29167	
Density fraction F2	0,63	
Plant A F1	836	cm2
Plant A F2	1028	cm2
Area Fraction F2	1,23	
CCx F2 average (based on field 1)	36,70	%
CC August average	32,52	%

CC_x field 2

Plot	*Fraction of Avg*	*% CCx*
1a	0,96	35,1
1b	1,11	40,7
2a	1,40	51,2
2b	1,02	37,4
3a	1,14	41,8
3b	0,95	34,8
4a	0,79	28,8
4b	0,92	33,6
5a	0,88	32,3
5b	0,84	30,8
6a	1,00	36,7
6b	1,01	37,1

9.3.3 Leaf area index

Monthly values are shown, calculated from canopy cover growth and the Beer and Lambert law.

	Plot 1a	*Plot 1b*	*Plot 2a*	*Plot 2b*	*Plot 3a*	*Plot 3b*	*Plot 4a*	*Plot 4b*	*Plot 5a*	*Plot 5b*	*Plot 6a*	*Plot 6b*
Apr	0.01	0.01	0.01	0.01	0.01	0.01	0.01	0.01	0.01	0.01	0.01	0.01
May	0.33	0.37	0.45	0.35	0.38	0.33	0.29	0.32	0.31	0.30	0.34	0.35
Jun	0.81	1.02	1.61	0.89	1.07	0.80	0.61	0.75	0.71	0.67	0.86	0.88
Jul	0.83	1.07	1.75	0.92	1.12	0.82	0.63	0.78	0.74	0.69	0.90	0.91
Aug	0.76	0.96	1.52	0.84	1.01	0.74	0.58	0.72	0.68	0.64	0.82	0.84
Sep	0.47	0.56	0.87	0.55	0.63	0.44	0.38	0.48	0.50	0.45	0.55	0.58

9.4 ACED measurement results

9.4.1 Field 2

Date	Plot 2A			Plot 2B			Plot 3B		
20-08-16					L (m)	W (cm)	D (cm)		L (m)	W (cm)	D (cm)
				1	8.8	11.7	5.3	1a	7	13.3	6
				2	4.3	11.0	4.0	1b	1	11	7
				3	3.2	13.7	5.0	2	4	9.5	5.8
				4	2.5	10.5	5.5	3	0.5	5	6.3
	* Not significant			5	2.0	7.3	2.0	4	3	13	4.2
				6	4.8	12.0	4				
24-08-16		L (m)	W (cm)	D (cm)		L (m)	W (cm)	D (cm)		L (m)	W (cm)	D (cm)
	1	0.4	13	3	1	8.8	11.7	5.3	1a	2.1	13.3	6
					2	4.3	9.0	6.5	1b	0.4	11	1.5
					3	3.2	8.7	5	1c	1.2	11.3	5
					4	2.5	8.3	3.50	1d	4.9	12.5	6.5
					5	2.0	12.5	2	2	3	14.5	4.3
					6	4.8	12.3	5	3	2.3	5.0	3.5
					7	1.2	18.0	3	4	6	9.5	4.5
	* Incisions between maize								* Pathways between maize			
	Plot 4B			Plot 5A			Plot 5B		
20-08-16		L (m)	W (cm)	D (cm)		L (m)	W (cm)	D (cm)		L (m)	W (cm)	D (cm)
	1	0.5	17.7	2	1	1.5	10	3	1a	6	3	1.5
					2a	2.5	10	3	1b	1.5	12.5	1.5
					2b	2.5	20	5	2a	4.5	20	5
									2b	2.5	20	2
24-08-16		L (m)	W (cm)	D (cm)		L (m)	W (cm)	D (cm)		L (m)	W (cm)	D (cm)
	1	1.1	18.5	6	1	1.5	10	2	1	0.6	12.50	4.5
	2a	1.8	17.8	5.9	2	2.5	20.0	9	2a	5	20	3.5
	2b	1.5	9.7	1					2b	2	20	6
	2c	0.6	12	1								
	* Pathways common everywhere, more significant downslope.				* Some pathways downslope				* Pathways common			

ACED measurements subplots field 2. Numbered lines are measured rills. Pathways are indicated with yellow. Boundaries of sketches are bunds, except for CP3b and CP5. P3b is plot 3-3.

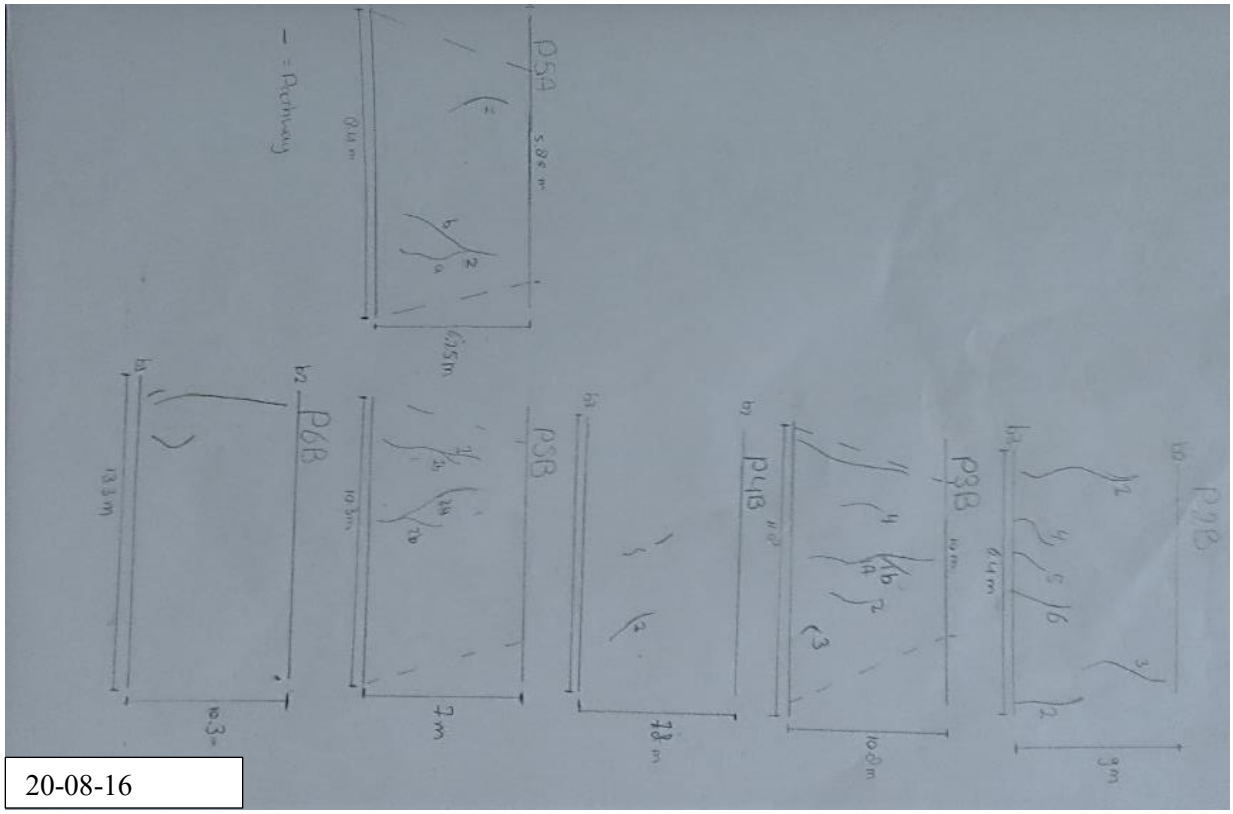

20-08-16

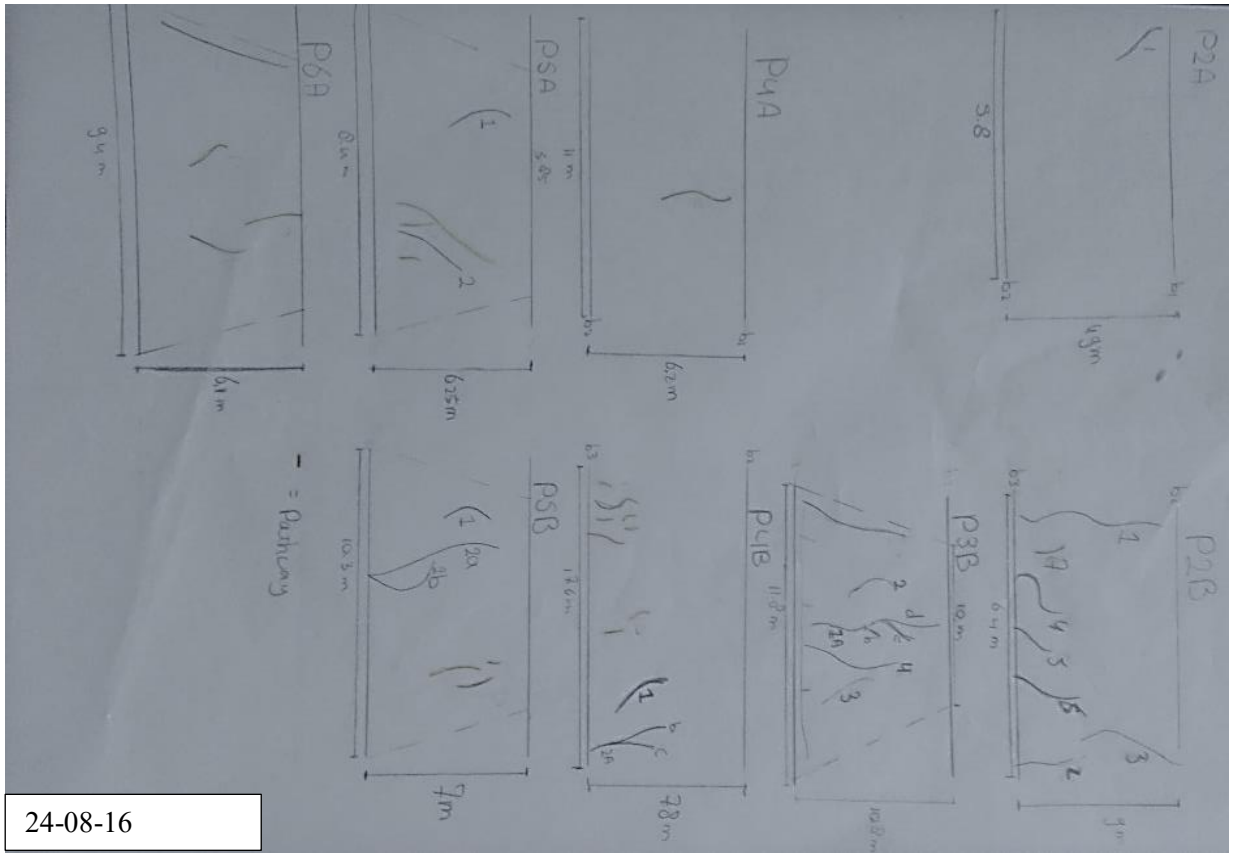

24-08-16

BD	1.150	ton/m3
$1m^3$=	1.150	tonnes
$1m^2$=	0.0001	ha

DATE	PLOT	SOIL LOSS		
		kg	*Δkg*	*kg/m²*
20-8-2016	**1-A**	0.0	0.0	0.0
24-8-2016		0.0	0.0	0.0
20-8-2016	**1-B**	0.0	0.0	0.0
24-8-2016		0.0	0.0	0.0
20-8-2016	**2-A**	0.0	0.0	0.0
24-8-2016		1.8	1.8	0.1
20-8-2016	**2-B**	155.2	0.0	2.8
24-8-2016		161.6	6.4	2.9
20-8-2016	**3-1-2**	0.0	0.0	0.0
24-8-2016		0.0	0.0	0.0
20-8-2016	**3-3**	119.4	0.0	1.7
24-8-2016		129.1	9.7	1.8
20-8-2016	**4-A**	0.0	0.0	0.0
24-8-2016		0.0	0.0	0.0
20-8-2016	**4-B**	2.0	0.0	0.0
24-8-2016		38.3	36.3	0.3
20-8-2016	**5-A**	42.5	0.0	0.0
24-8-2016		55.2	12.6	0.0
20-8-2016	**5-B**	69.6	0.0	1.0
24-8-2016		71.7	2.1	1.0
20-8-2016	**6-A**	0.0	0.0	0.0
24-8-2016		0.0	0.0	0.0
20-8-2016	**6-B**	0.0	0.0	0.0
24-8-2016		0.0	0.0	0.0

Soil losses for CP3 and CP5, used for calculating the runoff coefficient:

20/08

0.23	ton	231471.2 g
7.79	t/ha	
0.030	ha	

20/08-24/08

0.02	ton	24490.2 g
0.82	ton/ha	

20/08 + 24/08

8.62	t/ha

9.4.2 Field with stone bunds

		Length	*Area*		*S*	*(°)*	*%*
	a	5 m	250	m^2	a	17	31
	b	10 m	500	m^2	b	14	26
	c	5 m	250	m^2	c	2	
Total length:	20	m					
Width:	50	m					
Total area:	1000	m^2	0.1	Ha			
Geographic location:	100 m Southeast from field 2						

ACED measurement held on 16-08-16

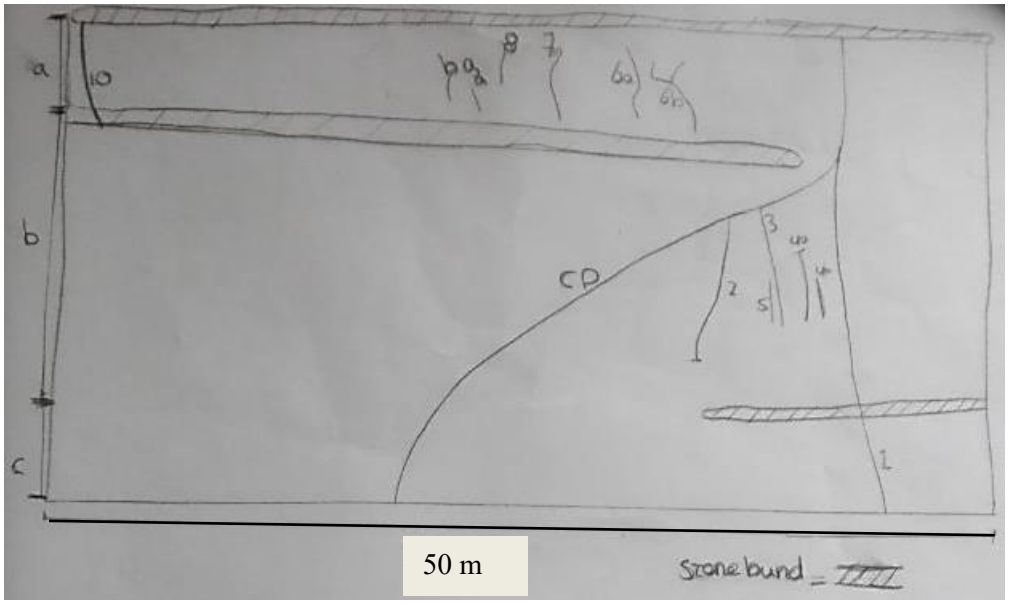

20 m

ACED measurement held on 26-08-16

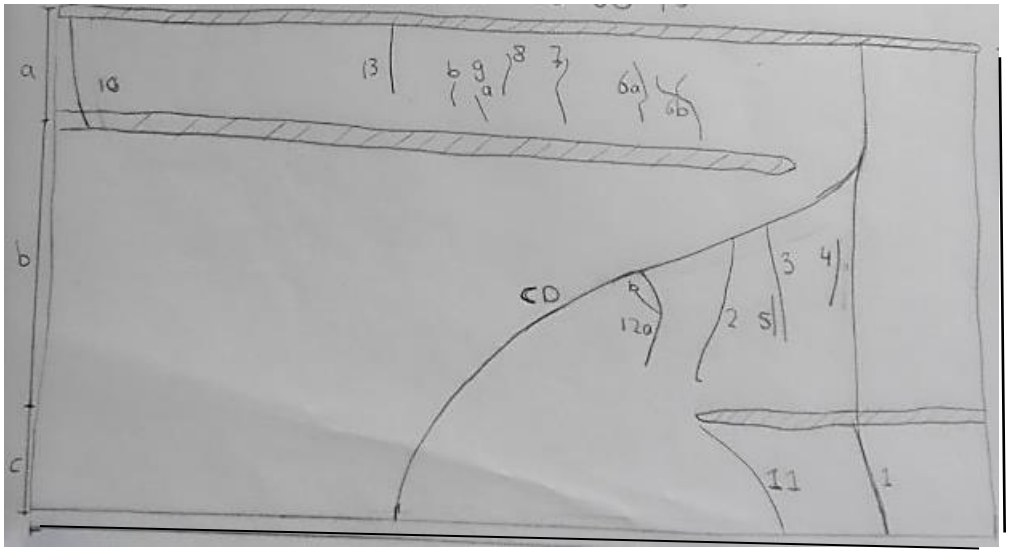

20 m

50 m

Date: 16-08-16			
	L (m)	W (cm)	D (cm)
CD*	25	47	27
1	17	59	10
2	5	38	15
3	5	39	12
4a	2	40	12
4b	2	35	12
5	2	15	10
6a	2	25	17
6b	2	25	15
7	2	18	13
8	1	13	5
9a	1	15	6
9b	1	15	6
10	7	15	12

16-08-16			
a	382.9858	kg	1.5 kg/m2
b	1562.791	kg	3.1 kg/m2
c	393.4683	kg	1.6 kg/m2
1	1180.405		

Date: 26-08-16			
	L (m)	W (cm)	D (cm)
CD*	25	47	27
1	17	52	14
2	5	39	14
3	5	39	12
4a	2	39	12
4b	2	35	12
5			
6a	2	29	14
6b	2	24	12
7	2	28	16
8	1	26	14
9a	1	23	10
9b	1	23	10
10	7	21	8
11	6	32	4
12a	4	20	10
12b	1	24	7
13	2	24	8

26-08-16			
a	513.0	kg	2.1 kg/m2
b	1777.2	kg	3.6 kg/m2
c	554.5	kg	2.2 kg/m2
1	1414.61		

CD*= control ditch

For converting m^3 to tonnes, the same density is used as for field 2.

9.5 Sediment concentrations field 2

Codes used in table

SB small brown bag
LB large brown bag
W newspaper bag
NB no bag

CODE	DATE	V BOTTLE	BAG	ΔW_{BAG}	PW	FW	DW + PW + FW	DW	C
		L		*g*	*g*	*g*	*g*	*g*	*g/L*
9/18/2008	5/26/2016	1	NB	0	0	0.538	1.22	0.68	0.68
9/19/2008	5/27/2016	1	NB	0	0	1.666	2.4	0.73	0.73
10/9/2008	6/16/2016	0.6	NB	0	0	0.512	1.1	0.59	0.98
10/12/2008	6/19/2016	0.6	NB	0	0	0.51	1.09	0.58	0.97
10/13/2008	6/20/2016	0.6	NB	0	0	0.503	1.03	0.53	0.88
10/14/2008	6/21/2016	0.6	NB	0	0	0.541	1.07	0.53	0.88
10/15/2008	6/22/2016	0.6	NB	0	0	0.528	7.44	6.91	11.52
10/20/2008	6/27/2016	0.6	SB	0.53	7.15	1.045	10.82	3.16	5.26
10/21/2008	6/28/2016	0.6	P	0.55	9.28	0.985	13.03	3.32	5.53
10/23/2008	6/30/2016	0.6	SB	0.53	6.95	0.997	18.92	11.50	19.17
10/23/2008	6/30/2016	0.6	SB	0.53	7.301	1.553	19.6	11.28	18.79
10/23/2008	6/30/2016	0.6	NB	0	0	0.526	3.99	3.46	5.77
10/26/2008	7/3/2016	0.6	P	0.55	8.687	1.037	12.24	3.07	5.11
11/7/2008	7/14/2016	0.6	W	0.45	10.526	1.516	14.13	2.54	4.23
11/13/2008	7/20/2016	0.6	NB	0	0	1.031	12.21	11.18	18.63
11/13/2008	7/20/2016	0.6	NB	0	0	0.519	5.45	4.93	8.22
11/15/2008	7/22/2016	0.6	NB	0	0	0.519	5.95	5.43	9.05
11/17/2008	7/24/2016	0.6	W	0.45	10.531	1.044	27.17	16.05	26.74
11/17/2008	7/24/2016	0.6	NB	0	0	0.523	7.03	6.51	10.85
11/23/2008	7/30/2016	0.6	SB	0.53	6.94	0.997	23.09	15.68	26.14
11/27/2008	8/3/2016	1	W	0.45	10.457	1.0503	18.15	7.09	7.09
11/27/2008	8/3/2016	1	W	0.45	10.559	1.0548	16.84	5.68	5.68
11/29/2008	8/5/2016	1	W	0.45	10.557	2.1037	19.38	7.17	7.17
11/29/2008	8/5/2016	1	SB	0.53	7.18	1.0323	10.99	3.31	3.31
12/1/2008	8/7/2016	1	W	0.45	10.357	0.9004	13.7	2.89	2.89
12/1/2008	8/7/2016	1	W	0.45	10.551	1.0514	13.11	1.96	1.96
12/3/2008	8/9/2016	1	NB	0	0	1.6878	4.388	2.70	2.70
12/3/2008	8/9/2016	1	W	0.45	10.554	1.047	20.11	8.96	8.96
12/4/2008	8/10/2016	1	W	0.45	10.523	1.045	17.76	6.64	6.64
12/4/2008	8/10/2016	1	SB	0.53	7.247	1.055	12.43	4.66	4.66
8/20/2016	8/20/2016	1	P	0.55	8.813	1.044	12.08	2.77	2.77
8/20/2016	8/20/2016	1	P	0.55	9.046	1.03	14.66	5.13	5.13
8/23/2016	8/23/2016	1	SB	0.53	6.97	1.04	11.82	4.34	4.34
8/23/2016	8/23/2016	1	NB	0	0	1.051	6.39	5.34	5.34
8/24/2016	8/24/2016	1	SB	0.53	7.37	1.036	9.33	1.45	1.45
8/24/2016	8/24/2016	1	SB	0.53	7.24	1.022	11.14	3.41	3.41
12/28/2008	9/3/2016	1	P	0.55	9.024	1.035	21.35	11.84	11.84
12/28/2008	9/3/2016	1	SB	0.53	7.22	1.03	14.38	6.66	6.66
12/29/2008	9/4/2016	1	SB	0.53	6.95	1.032	15.49	8.04	8.04
12/29/2008	9/4/2016	1	SB	0.53	6.94	1.024	17.58	10.15	10.15

9.6 Monthly model results

9.6.1 First calibration (Avg Qc: 0.20)

Runoff modelled with rMMF-HS model for all four plots with bunds. Runoff is modelled for situation with and without bunds and the % decrease of runoff by bunds is indicated as well.

plot1

	Q1	Qc:1	Q2	Qc:2	Sl.
	mm	-	mm	-	ton/ha
jan	2,0	0,050	1,35	0,034	0,00
feb	7,7	0,101	5,3	0,069	0,01
mar	12,6	0,089	8,7	0,061	0,03
apr	95,6	0,259	67,6	0,183	1,21
may	23,7	0,149	16,5	0,104	0,06
jun	24,6	0,144	17,1	0,100	0,06
jul	40,3	0,170	28,2	0,118	0,17
aug	29,1	0,160	20,3	0,111	0,09
sep	43,1	0,180	30,1	0,126	0,19
oct	13,1	0,103	9,0	0,071	0,03
nov	10,6	0,099	7,3	0,068	0,02
dec	4,0	0,113	2,7	0,078	0,00
Year	**306,4**	**0,13**	**214,0**	**0,09**	**1,9**

	Q	NBQ1	NBQ2	Bund-a	Bund-b
		mm	mm	% decreas	% decrease
jan		2,85	2,73	29,9	50,7
feb		10,95	10,61	29,9	50,2
mar		18,02	17,42	29,9	50,3
apr		136,27	133,89	29,8	49,5
may		33,75	32,89	29,9	50,0
jun		35,08	34,16	29,9	50,0
jul		57,53	56,18	29,9	49,9
aug		41,51	40,50	29,9	49,9
sep		61,46	60,08	29,9	49,8
oct		18,73	18,14	29,9	50,2
nov		15,05	14,57	29,9	50,2
dec		5,68	5,51	29,9	50,1
Total		**436,9**	**426,7**	**29,9**	**49,8**

plot 2

	Q1	Qc:1	Q2	Qc:2	Sl.
	mm	-	mm	-	ton/ha
jan	1,2	0,029	1,51	0,038	0,00
feb	5,1	0,067	5,70	0,075	0,01
mar	8,2	0,058	9,41	0,066	0,03
apr	76,4	0,207	69,44	0,188	1,13
may	17,0	0,107	17,41	0,110	0,06
jun	17,5	0,102	18,11	0,106	0,06
jul	29,7	0,125	29,59	0,124	0,16
aug	21,2	0,116	21,38	0,117	0,09
sep	32,1	0,134	31,58	0,132	0,19
oct	8,8	0,069	9,75	0,076	0,03
nov	7,0	0,066	7,84	0,074	0,02
dec	2,7	0,077	2,95	0,084	0,00
Year	**226,8**	**0,10**	**224,7**	**0,10**	**1,8**

	Q	NBQ1	NBQ2	Bund-a	Bund-b
		mm	mm	% decreas	% decrease
jan		1,70	2,42	31,8	37,7
feb		7,49	9,65	31,8	40,9
mar		12,02	15,58	31,8	39,6
apr		112,10	128,02	31,8	45,8
may		24,92	30,41	31,8	42,7
jun		25,71	31,54	31,8	42,6
jul		43,55	52,24	31,8	43,3
aug		31,07	37,56	31,8	43,1
sep		47,06	56,00	31,8	43,6
oct		12,86	16,52	31,8	41,0
nov		10,26	13,25	31,8	40,8
dec		3,97	5,04	31,8	41,5
Total		332,71	398,23	31,8	43,6

plot4

	Q1	Qc:1	Q2	Qc:2	Sl.
	mm	-	mm	-	ton/ha
jan	2,4	0,059	1,26	0,031	0,00
feb	8,8	0,116	4,8	0,063	0,01
mar	14,5	0,102	7,9	0,056	0,02
apr	105,2	0,285	59,8	0,162	0,69
may	26,6	0,168	14,8	0,094	0,03
jun	27,7	0,162	15,4	0,090	0,04
jul	45,2	0,190	25,3	0,106	0,10
aug	32,7	0,179	18,2	0,100	0,05
sep	48,2	0,201	27,0	0,112	0,11
oct	15,0	0,118	8,2	0,065	0,02
nov	12,1	0,114	6,6	0,062	0,01
dec	4,5	0,129	2,5	0,071	0,00
Year	**343,0**	**0,15**	**191,9**	**0,08**	**1,1**

	Q	NB Q1	NB Q2	Bund-a	Bund-b
		mm	mm	% decreas	% decreas
jan		3,18	3,03	25,9	58,5
feb		11,87	11,45	25,9	57,9
mar		19,63	18,90	25,9	58,0
apr		141,99	139,20	25,9	57,1
may		35,97	34,97	25,9	57,6
jun		37,45	36,38	25,9	57,6
jul		60,99	59,43	25,9	57,5
aug		44,12	42,95	25,9	57,5
sep		65,01	63,41	25,9	57,4
oct		20,27	19,58	25,9	57,9
nov		16,32	15,75	25,9	57,9
dec		6,13	5,93	25,9	57,8
Total		462,92	450,98	25,9	57,5

plot 6

	Q1	Qc:1	Q2	Qc:2	Sl.
	mm	-	mm	-	ton/ha
jan	2,3	0,057	1,40	0,035	0,00
feb	8,8	0,115	5,5	0,072	0,02
mar	14,4	0,101	9,0	0,063	0,04
apr	108,2	0,293	69,2	0,188	1,35
may	26,9	0,170	16,9	0,107	0,06
jun	28,0	0,164	17,6	0,103	0,07
jul	45,8	0,193	29,0	0,122	0,19
aug	33,1	0,182	20,9	0,115	0,10
sep	48,9	0,204	31,0	0,129	0,22
oct	15,0	0,117	9,3	0,073	0,03
nov	12,0	0,113	7,5	0,070	0,02
dec	4,5	0,129	2,8	0,081	0,00
Year	**348,0**	**0,15**	**220,1**	**0,10**	**2,1**

	Q	NB Q1	NB Q2	Bund-a	Bund-b
		mm	mm	% decreas	% decreas
jan		2,91	2,79	21,2	49,9
feb		11,12	10,79	21,2	49,4
mar		18,31	17,73	21,2	49,5
apr		137,30	135,17	21,2	48,8
may		34,14	33,33	21,2	49,2
jun		35,50	34,63	21,2	49,2
jul		58,14	56,87	21,2	49,1
aug		41,98	41,02	21,2	49,1
sep		62,09	60,79	21,2	49,0
oct		19,00	18,45	21,2	49,4
nov		15,28	14,82	21,2	49,4
dec		5,76	5,60	21,2	49,3
Total		441,52	431,98	21,2	49,1

Soil loss and runoff modelled with the rMMF model for all four plots with bunds and the runoff and soil loss scaled with the decrease from the rMMF-HS model.

P1		reduction by bund			P2		reduction by bund	
ST (t/ha)	Q (mm)	ST (t/ha)	Q (mm)		ST (t/ha)	Q (mm)	ST (t/ha)	Q (mm)
0,02	2,71	0,00	1,55	**jan**	0,02	2,56	0,01	1,51
0,26	10,55	0,08	6,03	**feb**	0,28	10,04	0,10	5,98
0,52	17,32	0,15	9,89	**mar**	0,56	16,45	0,19	9,78
21,99	133,66	6,42	76,18	**apr**	23,73	129,77	8,36	77,85
1,06	32,75	0,31	18,69	**may**	1,13	31,41	0,39	18,75
1,15	34,02	0,33	19,41	**jun**	1,22	32,61	0,42	19,46
3,11	55,96	0,90	31,93	**jul**	3,31	53,80	1,15	32,16
1,62	40,34	0,47	23,02	**aug**	1,72	38,75	0,60	23,15
3,56	59,86	1,03	34,14	**sep**	3,79	57,64	1,32	34,47
0,48	18,05	0,14	10,31	**oct**	0,52	17,19	0,18	10,23
0,36	14,50	0,11	8,28	**nov**	0,39	13,80	0,13	8,21
0,07	5,49	0,02	3,13	**dec**	0,08	5,23	0,03	3,11
Year	**Year**	**Year**	**Year**		**Year**	**Year**	**Year**	**Year**
34,2	425,2	9,9	242,6		36,7	409,2	12,9	244,7

P4		reduction by bund			P6		reduction by bund	
ST (t/ha)	Q (mm)	ST (t/ha)	Q (mm)		ST (t/ha)	Q (mm)	ST (t/ha)	Q (mm)
0,02	3,01	0,00	1,72	**jan**	0,02	2,78	0,01	1,72
0,24	11,39	0,07	6,51	**feb**	0,24	10,74	0,08	6,62
0,48	18,80	0,14	10,74	**mar**	0,47	17,65	0,16	10,89
19,26	139,04	5,26	78,99	**apr**	19,81	134,89	6,73	82,95
0,96	34,82	0,26	19,84	**may**	0,96	33,22	0,33	20,46
1,04	36,22	0,29	20,64	**jun**	1,03	34,52	0,35	21,26
2,78	59,20	0,76	33,71	**jul**	2,79	56,70	0,95	34,91
1,45	42,77	0,40	24,36	**aug**	1,45	40,89	0,50	25,18
3,16	63,18	0,87	35,96	**sep**	3,19	60,61	1,09	37,31
0,45	19,48	0,12	11,12	**oct**	0,44	18,37	0,15	11,33
0,34	15,67	0,09	8,94	**nov**	0,33	14,76	0,11	9,10
0,06	5,90	0,02	3,36	**dec**	0,06	5,58	0,02	3,44
Year	**Year**	**Year**	**Year**		**Year**	**Year**	**Year**	**Year**
30,2	449,5	8,3	255,9		30,8	430,7	10,5	265,2

9.6.2 Second calibration (Avg Qc: 0.25)

Runoff modelled with rMMF-HS model for all four plots with bunds. Runoff is modelled for situation with and without bunds and the % decrease of runoff by bunds is indicated as well.

plot 1

	Q1	Qc1	Q2	Qc2	Sl	Q	NB Q1	NB Q2	Bund-a	Bund-b
	mm	-	mm	-	ton/ha		mm	mm	% decrease	% decrease
jan	2,0	0,050	1,35	0,034	0,00	jan	2,85	2,73	29,9	50,7
feb	7,7	0,101	5,3	0,069	0,01	feb	10,95	10,61	29,9	50,2
mar	19,1	0,134	13,2	0,093	0,06	mar	27,25	26,51	29,9	50,0
apr	116,3	0,315	82,7	0,224	1,44	apr	165,81	163,48	29,9	49,4
may	31,8	0,201	22,3	0,141	0,08	may	45,36	44,42	29,9	49,8
jun	33,3	0,195	23,3	0,136	0,09	jun	47,49	46,48	29,9	49,8
jul	52,9	0,223	37,2	0,157	0,22	jul	75,46	74,02	29,9	49,7
aug	38,6	0,212	27,1	0,149	0,12	aug	55,07	53,98	29,9	49,7
sep	55,9	0,233	39,4	0,164	0,25	sep	79,74	78,28	29,9	49,7
oct	18,7	0,147	13,0	0,102	0,04	oct	26,69	26,00	29,9	50,0
nov	13,7	0,129	9,5	0,089	0,03	nov	19,54	19,00	29,9	50,1
dec	4,0	0,113	2,7	0,078	0,00	dec	5,68	5,51	29,9	50,1
Year	394,1	0,17	277,2	0,12	2,4	Total	561,9	551,0	29,9	49,7

plot 2

	Q1	Qc1	Q2	Qc2	Sl	Q	NB Q1	NB Q2	Bund-a	Bund-b
	mm	-	mm	-	ton/ha		mm	mm	% decrease	% decrease
jan	1,2	0,029	1,51	0,038	0,00	jan	1,70	2,42	31,8	37,7
feb	5,1	0,067	5,70	0,075	0,01	feb	7,49	9,65	31,8	40,9
mar	13,4	0,094	14,09	0,099	0,07	mar	19,71	24,17	31,8	41,7
apr	96,6	0,262	84,11	0,228	1,33	apr	141,75	157,57	31,8	46,6
may	24,2	0,153	23,24	0,147	0,08	may	35,49	41,61	31,8	44,1
jun	25,2	0,147	24,35	0,142	0,08	jun	36,94	43,49	31,8	44,0
jul	41,1	0,173	38,58	0,162	0,21	jul	60,25	69,68	31,8	44,6
aug	29,7	0,163	28,19	0,155	0,11	aug	43,56	50,70	31,8	44,4
sep	43,8	0,183	40,72	0,170	0,23	sep	64,25	73,85	31,8	44,9
oct	13,4	0,105	13,78	0,108	0,04	oct	19,64	24,03	31,8	42,7
nov	9,6	0,090	10,11	0,095	0,03	nov	14,01	17,45	31,8	42,1
dec	2,7	0,077	2,95	0,084	0,00	dec	3,97	5,04	31,8	41,5
Year	305,8	0,13	287,3	0,13	2,2	Total	448,77	519,67	31,8	44,7

plot 4

	Q1	Qc1	Q2	Qc2	Sl	Q	NB Q1	NB Q2	Bund-a	Bund-b
	mm	-	mm	-	ton/ha		mm	mm	% decrease	% decrease
jan	2,4	0,059	1,26	0,031	0,00	jan	3,18	3,03	25,9	58,5
feb	8,8	0,116	4,8	0,063	0,01	feb	11,87	11,45	25,9	57,9
mar	21,6	0,152	12,0	0,084	0,05	mar	29,17	28,31	25,9	57,7
apr	127,0	0,344	72,7	0,197	0,82	apr	171,37	168,66	25,9	56,9
may	35,4	0,223	19,9	0,126	0,05	may	47,76	46,68	25,9	57,3
jun	37,1	0,217	20,8	0,122	0,05	jun	50,07	48,91	25,9	57,4
jul	58,6	0,246	33,1	0,139	0,13	jul	79,11	77,47	25,9	57,3
aug	42,9	0,235	24,2	0,133	0,07	aug	57,86	56,60	25,9	57,3
sep	61,8	0,258	35,0	0,146	0,14	sep	83,44	81,77	25,9	57,2
oct	21,1	0,165	11,7	0,092	0,03	oct	28,47	27,67	25,9	57,6
nov	15,5	0,146	8,6	0,081	0,02	nov	20,95	20,32	25,9	57,7
dec	4,5	0,129	2,5	0,071	0,00	dec	6,13	5,93	25,9	57,8
Year	436,6	0,19	246,6	0,11	1,4	Total	589,37	576,79	25,9	57,3

plot 6

	Q1	Qc1	Q2	Qc2	Sl	Q	NB Q1	NB Q2	Bund-a	Bund-b
	mm	-	mm	-	ton/ha		mm	mm	% decrease	% decrease
jan	2,3	0,057	1,40	0,035	0,00	jan	2,91	2,79	21,2	49,9
feb	8,8	0,115	5,5	0,072	0,02	feb	11,12	10,79	21,2	49,4
mar	21,7	0,153	13,7	0,096	0,10	mar	27,59	26,89	21,2	49,2
apr	131,5	0,356	84,6	0,229	1,61	apr	166,81	164,74	21,2	48,7
may	36,1	0,228	22,9	0,145	0,09	may	45,78	44,90	21,2	49,0
jun	37,8	0,221	24,0	0,140	0,10	jun	47,95	47,00	21,2	49,0
jul	60,0	0,252	38,2	0,161	0,25	jul	76,11	74,76	21,2	48,9
aug	43,8	0,241	27,9	0,153	0,13	aug	55,57	54,54	21,2	48,9
sep	63,4	0,264	40,4	0,168	0,28	sep	80,40	79,03	21,2	48,9
oct	21,3	0,167	13,4	0,105	0,05	oct	27,01	26,36	21,2	49,2
nov	15,6	0,147	9,8	0,092	0,04	nov	19,79	19,27	21,2	49,3
dec	4,5	0,129	2,8	0,081	0,00	dec	5,76	5,60	21,2	49,3
Year	446,7	0,19	284,5	0,12	2,7	Total	566,80	556,66	21,2	48,9

Soil loss and runoff modelled with the rMMF model for all four plots with bunds and the runoff and soil loss scaled with the decrease from the rMMF-HS model.

P1		Reduction by bund			P2		Reduction by bund	
ST (t/ha)	Q (mm)	ST (t/ha)	Q (mm)		ST (t/ha)	Q (mm)	ST (t/ha)	Q (mm)
0,02	2,71	0,00	1,55	**jan**	0,02	2,56	0,01	1,49
0,26	10,55	0,08	6,04	**feb**	0,28	10,04	0,09	5,90
1,21	26,39	0,35	15,09	**mar**	1,29	25,25	0,43	14,86
25,77	163,25	7,70	93,16	**apr**	28,44	159,30	9,83	94,56
1,46	44,27	0,42	25,29	**may**	1,56	42,72	0,53	25,24
1,60	46,32	0,46	26,46	**jun**	1,70	44,68	0,58	26,40
4,07	73,79	1,18	42,14	**jul**	4,33	71,37	1,48	42,22
2,16	53,81	0,63	30,73	**aug**	2,30	52,00	0,78	30,75
4,56	78,05	1,32	44,57	**sep**	4,85	75,59	1,66	44,74
0,83	25,89	0,24	14,80	**oct**	0,88	24,82	0,30	14,62
0,62	18,91	0,18	10,81	**nov**	0,66	18,08	0,22	10,64
0,07	5,49	0,02	3,14	**dec**	0,08	5,23	0,03	3,07
Year	**Year**	**Year**	**Year**		**Year**	**Year**	**Year**	**Year**
42,6	549,4	12,6	313,8		46,4	531,62	15,9	314,48

P4		Reduction by bund			P6		Reduction by bund	
ST (t/ha)	Q (mm)	ST (t/ha)	Q (mm)		ST (t/ha)	Q (mm)	ST (t/ha)	Q (mm)
0,02	3,01	0,00	1,73	**jan**	0,02	2,78	0,01	1,72
0,24	11,39	0,07	6,52	**feb**	0,24	10,74	0,08	6,64
1,10	28,18	0,30	16,09	**mar**	1,09	26,80	0,37	16,54
22,70	168,51	6,20	95,81	**apr**	23,60	164,46	8,03	101,24
1,29	46,52	0,36	26,51	**may**	1,31	44,78	0,45	27,60
1,41	48,74	0,39	27,78	**jun**	1,43	46,87	0,49	28,90
3,56	77,23	0,98	43,99	**jul**	3,63	74,58	1,24	45,96
1,90	56,42	0,52	32,15	**aug**	1,93	54,40	0,66	33,53
3,97	81,53	1,09	46,43	**sep**	4,06	78,84	1,39	48,58
0,75	27,55	0,21	15,73	**oct**	0,75	26,27	0,26	16,21
0,56	20,22	0,16	11,55	**nov**	0,56	19,20	0,19	11,85
0,06	5,90	0,02	3,37	**dec**	0,06	5,58	0,02	3,44
Year	**Year**	**Year**	**Year**		**Year**	**Year**	**Year**	**Year**
37,6	575,19	10,3	327,66		38,7	555,30	13,2	262,13